

NI-47
181603

Design of a Global Soil Moisture Initialization Procedure for the Simple Biosphere Model

G. E. Liston, Y. C. Sud, and G. K. Walker

August 1993

(NASA-TM-104590) DESIGN OF A
GLOBAL SOIL MOISTURE INITIALIZATION
PROCEDURE FOR THE SIMPLE BIOSPHERE
MODEL (NASA) 130 p

N94-10940

Unclass

G3/47 0181603



Design of a Global Soil Moisture Initialization Procedure for the Simple Biosphere Model

G. E. Liston
Universities Space Research Association
Columbia, Maryland

Y. C. Sud
Goddard Space Flight Center
Greenbelt, Maryland

G. K. Walker
General Sciences Corporation
Laurel, Maryland



National Aeronautics and
Space Administration

**Scientific and Technical
Information Branch**

1993

ABSTRACT

Global soil moisture and land-surface evapotranspiration fields are computed using an analysis scheme based on the Simple Biosphere (SiB) soil-vegetation-atmosphere interaction model. The scheme is driven with observed precipitation, and potential evapotranspiration, where the potential evapotranspiration is computed following the surface air temperature-potential evapotranspiration regression of Thornthwaite (1948). The observed surface air temperature is corrected to reflect potential (zero soil moisture stress) conditions by letting the ratio of actual transpiration to potential transpiration be a function of normalized difference vegetation index (NDVI), based on advanced very high resolution radiometer (AVHRR) data. The land-surface hydrology model features the integration of soil moisture equations and simplified evaporation routines patterned after SiB. Soil moisture, evapotranspiration, and runoff data are generated on a daily basis for a 10-year period, January 1979 through December 1988, using observed average monthly precipitation scaled by the frequency of observed 1979 daily precipitation events, and gridded at a 4° by 5° resolution. The data set provides model-compatible soil moisture initial conditions for general circulation models (GCMs) using the SiB land-surface parameterization. In addition, the methodology described can be readily adapted to compute similarly compatible soil moisture initialization fields for other land-surface schemes.

TABLE OF CONTENTS

Section	Page
1. Introduction	1
2. Land-surface hydrology model	5
a. Soil moisture	5
b. Evapotranspiration	9
c. Atmospheric forcing	9
3. Presentation of data	14
4. Concluding summary	17
NUMERICAL DATA	20
ACKNOWLEDGEMENTS	20
REFERENCES	21
Table 1	24
HYDROLOGIC FIELDS: 10-Year Average of Monthly Means, and Standard Deviations	25
PRECIPITATION (January - December)	27
EVAPOTRANSPIRATION (January - December)	53
ROOT ZONE SOIL WETNESS (January - December)	79
RUNOFF (January - December)	105

1. Introduction

Several numerical studies have shown that large-scale atmospheric circulation and precipitation are sensitive to land-surface evapotranspiration (e.g., Shukla and Mintz, 1982; Rowntree, 1983; Yeh et al., 1984; Sud and Smith, 1985; and others reviewed by Mintz, 1984). In addition, it is now generally recognized that land-surface evapotranspiration is one of the more important physical processes of the global weather and climate system – and that soil moisture, which strongly influences evapotranspiration, is an important physical state variable of the system. Soil moisture and land-surface evapotranspiration can be determined by employing a moisture budget model and knowledge of the potential evapotranspiration (the evapotranspiration in the absence of water stress) obtained by applying the conservation of energy equation at the Earth's surface.

Penman (1948), Budyko (1956), and Priestley and Taylor (1972) showed that the potential evapotranspiration is most strongly dependent upon the net all-wavelength downward radiation flux, R_n , at the surface of the Earth. This radiation flux is a function of cloud structure, surface albedo, and the vertical distribution of temperature and water vapor in the atmosphere. The vertical distributions of atmospheric temperature and moisture can be estimated from satellite retrievals and radiosonde measurements. Unfortunately, however, the rapidly varying cloud structure and land-surface temperature introduce complexities that make an accurate determination of the surface radiation balance difficult. In an effort to circumvent some of these radiation-related difficulties, Thornthwaite (1948) introduced a method to determine potential

evapotranspiration using surface air temperature. This method invokes an empirical regression between the potential evapotranspiration, the observed daily mean surface air temperature over well-watered vegetation, and the length of daylight; employing the hypothesis that the air temperature under potential conditions and the daylight length serve as a proxy measurement for R_n (Thornthwaite and Hare, 1965). Willmott et al. (1985) showed that the Thornthwaite procedure produces monthly potential evapotranspiration estimates with root mean square errors that are comparable to those produced by several other commonly applied radiation-based and combination methods (Jensen, 1973; Willmott, 1984). In a recent paper, Mintz and Walker (1993) compared the potential evapotranspiration computed using Thornthwaite's methodology with the energy balance schemes of Penman, Budyko, and Priestly-Taylor at locations where net radiation flux measurements were available. They concluded that potential evapotranspiration computed using the Thornthwaite equation closely agrees with that computed by the net radiation schemes (to within $\pm 0.5 \text{ mm day}^{-1}$). They also confirmed that Thornthwaite's method provides a reasonable representation of evapotranspiration under potential conditions. In view of these findings, we use the Thornthwaite (1948) regression analysis to determine global fields of potential evapotranspiration.

In the Simple Biosphere Model (SiB) of Sellers et al. (1986) and several other land-surface hydrology parameterizations (e.g., Abramopoulos et al., 1988; Wood et al., 1992), computed evapotranspiration, and subsequently all other components of the surface energy balance, are strongly dependent upon

soil moisture. Consequently, the initialization of soil moisture plays a key role in the evolution of simulated fields during the early phases of a general circulation model (GCM) integration (e.g., Sato et al., 1989a). Serafini and Sud (1987) show soil moisture time scales ranging from weeks to several months (5 - 90 days), depending upon the season and geographic region. Global soil moisture fields used for initialization of GCMs are generally produced by simple water budget calculations (e.g., Willmott, 1977). In these schemes, the actual evapotranspiration is typically defined to be proportional to the potential evapotranspiration, where the proportionality factor, or β function, is dependent upon soil moisture. Fennessy and Sud (1983), for example, defined β to be the soil moisture function based on Nappo (1975). In their study and several others (e.g., Willmott et al., 1985; Schemm et al., 1992; Mintz and Walker, 1993), the potential evapotranspiration is computed based on Thornthwaite (1948).

The complexities of biophysical control over moisture exchanges between the soil and atmosphere in the Simple Biosphere Model suggests that an internally consistent soil moisture initialization procedure will include much of the same control over these processes as the actual model. Sato et al. (1989b) described a method to develop SiB-compatible soil moisture that transforms soil moisture fields, such as those produced by Willmott et al. (1985) and Gordon (1986), into SiB-compatible fields by preserving some of the SiB vegetation control over evapotranspiration; however, they did not take into consideration the influence of the moisture transport within the modeled soil column. Thus, a global soil moisture analysis scheme that is fully consistent

with the soil hydrology of SiB is still needed to produce SiB-compatible soil moisture initialization fields. Such a scheme would, at a minimum, feature the integration of SiB soil moisture and evapotranspiration equations with observed precipitation and estimated potential evapotranspiration.

Measured surface air temperature is frequently obtained under 'non-potential' surface conditions. To compute potential evapotranspiration using Thornthwaite (1948), the observed surface air temperature requires correction to reflect potential (zero soil moisture stress) conditions; if such a correction is not made, and observed surface air temperatures are used directly in the Thornthwaite equation, it can lead to a misrepresentation of the potential evapotranspiration, in part because the reduction in evaporation leads to increased sensible heat and, consequently, higher air temperatures than those found under potential conditions. In our formulation, this temperature correction is accomplished by letting the ratio of actual transpiration to potential transpiration be a function of normalized difference vegetation index (NDVI), determined from satellite measurements. This eliminates the need to consider root zone soil moisture and the soil moisture storage capacity when performing the temperature correction, as was done, for example, by Mintz and Walker (1993). Daily, 4° by 5° gridded, global evapotranspiration, runoff, and soil moisture for each of the three SiB soil layers, are generated for the 10-year period January 1979 through December 1988, using observed fields of surface air temperature, precipitation, and NDVI.

2. Land-surface hydrology model

A simple local water budget for the land surface can be written as

$$\frac{\partial S}{\partial t} = P + I - E - Q \quad (1)$$

where S is the storage of surface and groundwater, P is the precipitation rate, E is the evapotranspiration rate, I is the inflow rate from adjacent regions, Q is the runoff rate or discharge from surface and groundwater, and t is time. For modeling purposes, the storage term in (1) can be cast in the form

$$S = W \theta_s D \quad (2)$$

where W is the fractional soil wetness, $0 \leq W \leq 1$, θ_s is the porosity (or the volumetric soil moisture at saturation), and D is the hydrologically active soil column depth.

a. Soil moisture

The foundation of the soil moisture computations performed in this study is the discretization of (1) and (2) into the three-layer soil moisture equations used in SiB. The land area contained within each GCM grid box is considered horizontally uniform, but the soil–vegetation types vary globally. In this application, the SiB governing soil moisture equations have been cast in the form

$$\frac{\partial W_1}{\partial t} = \frac{1}{\theta_s D_1} [P_1 - Q_{1,2} - E_1] \quad (3a)$$

$$\frac{\partial W_2}{\partial t} = \frac{1}{\theta_s D_2} [Q_{1,2} - Q_{2,3} - E_2] \quad (3b)$$

$$\frac{\partial W_3}{\partial t} = \frac{1}{\theta_s D_3} [Q_{2,3} - Q_3 - Q_b] \quad (3c)$$

where the subscripts 1, 2, and 3 indicate the three soil layers; $Q_{i,i+1}$ is the moisture transfer rate between layers i and $i+1$, for $i = 1, 2$; Q_3 is the gravitational drainage rate from layer three; E_1 is the soil evaporation rate; E_2 is the rate of root zone moisture loss due to transpiration; and Q_b is baseflow drainage rate produced by a linear reservoir model. These equations are similar to those presented by Sellers et al. (1986) except that they contain fewer evaporation terms in layers one and two and have an additional moisture drainage term, Q_b , in layer three.

The general flux-moisture gradient structure of this three-layer soil hydrology model is similar to several other state-of-the-art land-surface hydrology parameterizations used in GCMs, including the Biosphere-Atmosphere Transfer Scheme (BATS) (Dickinson et al., 1986), the Goddard Institute for Space Studies model (Abramopoulos et al., 1988), and the Canadian Land Surface Scheme (CLASS) (Verseghy, 1991). The moisture exchange between soil layers is determined by the steady-state, unsaturated, one-dimensional solution of Darcy's law (Freeze and Cherry, 1979),

$$Q = -K \left(\frac{d\psi}{dz} + 1 \right) \quad (4)$$

where Q is the downward transport of water, K is the hydraulic conductivity of the soil, ψ is the soil moisture potential, and z is the vertical coordinate. To solve for the soil moisture transport, (4) is discretized, and the soil moisture potential, ψ_i , of layer i , is given by

$$\psi_i = \psi_s W_i^{-B} \quad (5)$$

where ψ_s is the soil moisture potential at saturation, and the coefficient B is a

function of soil type (Clapp and Hornberger, 1978). The hydraulic conductivity, K_i , of layer i , is given by (Campbell, 1974) as

$$K_i = K_s W_i^{(2B+3)} \quad (6)$$

where the saturated hydraulic conductivity, K_s , varies with soil characteristics as listed by Clapp and Hornberger (1978). Gravitational drainage transports moisture out of the lowest layer, such that

$$Q_3 = -K_3 \sin(\mu) \quad (7)$$

where μ is the mean slope angle.

In addition to the gravitational drainage from the third soil layer, baseflow runoff from layer three is produced by a linear reservoir model. In this formulation, subgrid-scale spatial variability of soil moisture has been included in the runoff formulation by assuming that the grid box contains a saturated areal fraction that is equal to the soil wetness of the third soil layer (Liston et al., 1993). This saturated region then drains as a linear reservoir, thus producing a term, Q_b , in the governing equation for the third soil moisture store,

$$Q_b = k_b W_3 \quad (8)$$

where k_b is the discharge rate from the third layer at saturation. In SiB, there are twelve soil-vegetation categories corresponding to the indices 1 through 12 (Dorman and Sellers, 1989). Based on off-line simulations over the Mississippi River Basin, for 'grassland' (soil-vegetation type 7), k_b^7 was shown to be 0.6 mm day^{-1} (Liston et al., 1993), where the number superscript indicates vegetation type index. To allow extrapolation to other soil-vegetation types, k_b is scaled by

the depth of layer three, D_3^j , for the j^{th} soil-vegetation type, according to

$$k_b^j = k_b^7 \frac{D_3^j}{D_3^7} \quad (9)$$

where $1 \leq j \leq 12$.

In this implementation, all precipitation reaching the ground enters the soil matrix. In the original SiB model, the precipitation was given only one time step to infiltrate the soil. Any moisture that did not infiltrate during that time step, called precipitation excess, was identified as surface runoff. This was found to produce unrealistically large runoff events during periods of low hydraulic conductivity, such as late summer, when the precipitation could not infiltrate the soil. Using a runoff routing model designed to generate river discharge hydrographs from gridded runoff data produced by a land-surface hydrology model or GCM (Liston et al., 1993), these Hortonian-like runoff events, occurring at the 4° by 5° GCM scale, were so significant that they produced an anomalous autumn peak in the Mississippi River Basin discharge hydrograph.

In summary, the significant changes made to the original SiB soil hydrology formulation are first, addition of linear reservoir drainage, through the inclusion of the drainage term Q_b in (3c), and its description given by (8) and (9); and second, the practice of forcing all precipitation to enter the upper soil matrix in one time step. These modifications to the SiB soil hydrology are currently being tested in on-line simulations using the Goddard Laboratory for Atmospheres (GLA) SiB-GCM.

b. Evapotranspiration

Soil moisture dependent evapotranspiration is computed by scaling the potential evapotranspiration, E_p , by a factor β_i ,

$$E_i = \beta_i E_p \quad (10)$$

where the subscript $i = 1, 2$ identifies the soil layer of interest, and E is the actual evaporation rate. For the case of vegetated land, β_2 is defined to be the soil water stress factor for the second soil layer, $f(\psi_2)$, given by Xue et al. (1991),

$$f(\psi_2) = 1 - \exp(-c_2 (c_1 - \ln(-\psi_2))) \quad 0 \leq f(\psi_2) \leq 1 \quad (11)$$

where c_1 and c_2 are empirical constants representing the progression of closing stomata. Values of c_1 and c_2 for the different vegetation types are given in Table 1, where the swapping of c_1 and c_2 in the table presented by Xue et al. (1991) has been corrected. For the case of soil-vegetation type 11 (bare soil), $\beta_1 \equiv W_1$, the soil wetness of the uppermost soil layer.

c. Atmospheric forcing

In its reduced form described above, the SiB land-surface hydrology parameterization was forced using daily values of potential evaporation and surface station precipitation climatology. Potential evapotranspiration, E_p , was computed following Thornthwaite (1948), which requires a surface air temperature representative of potential conditions. To account for measured surface air temperatures, that may not have been collected under conditions of zero soil moisture stress, we let the ratio of actual transpiration to potential transpiration be a function of normalized difference vegetation index (NDVI),

available from satellite measurements. This has eliminated the need to consider root zone soil moisture and the soil water storage capacity when computing the temperature correction, and has also prevented errors in measured precipitation from affecting the computations (Mintz and Walker, 1993).

In Thornthwaite's empirical formulation, the daily potential evapotranspiration is a function of the number of daylight hours, h , and the mean daily air temperature, T_a^* , obtained under conditions of no water stress,

$$E_p = \begin{cases} 0, & T_a^* < 0^\circ\text{C} \\ 0.533 \left(10 T_a^* / I \right)^\alpha (h/12), & 0 < T_a^* < 26.5^\circ\text{C} \\ (-13.86 + 1.075 T_a^* - 0.0144 T_a^{*2}) (h/12), & 26.5^\circ\text{C} < T_a^* \end{cases} \quad (12)$$

with

$$I = \sum_{i=1}^{12} i ; \quad i = \left(T_m / 5 \right)^{1.514}, \quad T_m \geq 0^\circ\text{C} \quad (13)$$

and

$$\alpha = (6.75 \times 10^{-7} I^3) - (7.71 \times 10^{-5} I^2) + (1.79 \times 10^{-2} I) + 0.492 \quad (14)$$

where T_m is the monthly mean surface air temperature; and I is the annual heat index, or sum of the 12 monthly heat indices, i . The daylight duration, in hours, is calculated from

$$h = (24/180) \arccos(-\tan \phi \tan \delta) \quad (15)$$

where ϕ is latitude, and δ is the Sun's declination, given by

$$\delta = \phi_T \cos \left(2\pi \left(\frac{d - d_r}{d_y} \right) \right) \quad (16)$$

where ϕ_T is the latitude of the Tropic of Cancer (23.45°), d is the Gregorian Day, d_r is the day of the summer solstice (173), and d_y is the average number of days in a year (365.25). Poleward of 50° latitude, Thornthwaite defined h to be the same as h at 50° .

The measured surface air temperature T_a , is related to the air temperature under potential conditions according to

$$T_a^* = (0.83 + 0.17 \beta_e) T_a \quad (17)$$

where β_e is a soil moisture dependent evapotranspiration coefficient. This relationship was derived from a comparison of the measured daily mean surface air temperatures in moist humid regions, and in dry desert regions at the same latitude and the same season of the year (Mintz and Walker, 1993).

In describing the evapotranspiration coefficient, β_e , Mintz and Walker considered the evaporative balance,

$$E_T + E_S = \beta_e (E_p - E_I) \quad (18)$$

where E_T , E_S , and E_I are the transpiration, soil evaporation, and interception losses, respectively. They defined β_e to be a function of soil wetness,

$$\beta_e = 1 - \exp(-6.8 (W/W^*)) \quad (19)$$

where W is the root zone soil moisture, and W^* is the root zone water storage capacity (Davies and Allen, 1973; Nappo, 1975).

In our application we follow Mintz (unpublished manuscript) and combine the interception loss (precipitation accumulated on the vegetative canopy and evaporated) and the soil evaporation into a single component, E_{IS} ,

assuming that they behave in a roughly complementary fashion. When precipitation is greater than the potential evapotranspiration, increasing (decreasing) leaf area index will increase (decrease) the amount of precipitation intercepted by, and evaporated from, the leaves, and there will be a corresponding reduction (increase) in the amount of insolation reaching the soil for soil evaporation. Thus, we let

$$\beta_e = E_T / (E_p - E_{I,S}) \quad (20)$$

where $E_{I,S}$ is considered to be the lesser of the daily precipitation, P , and daily potential evapotranspiration.

To derive an equation for the evapotranspiration coefficient, assume that $E_T / (E_p - E_{I,S})$ is proportional to the area average stomatal conductance, $1/r_s$, or the reciprocal of the stomatal resistance, r_s ,

$$E_T / (E_p - E_{I,S}) \propto 1/r_s \quad (21)$$

Adopting the findings of Sellers (1985), we let the area average stomatal conductance be proportional to the simple ratio, $I\eta_{(NIR)} / I\eta_{(VIS)}$,

$$1/r_s \propto \frac{I\eta_{(NIR)}}{I\eta_{(VIS)}} \quad (22)$$

where $I\eta_{(NIR)}$ and $I\eta_{(VIS)}$ are the nadir or near-nadir surface reflectance in the near infrared (0.7-3.0 μm) and visible wavelength (0.4-0.7 μm) intervals, respectively. This simple ratio is related to the normalized difference vegetation index, NDVI (Tucker et al., 1985), according to

$$\frac{I\eta_{(NIR)}}{I\eta_{(VIS)}} = \frac{(1 + \text{NDVI})}{(1 - \text{NDVI})} ; \quad \text{NDVI} = \frac{(I\eta_{(NIR)} - I\eta_{(VIS)})}{(I\eta_{(NIR)} + I\eta_{(VIS)})} \quad (23)$$

Combining (20) - (23) leads to a formulation for the evapotranspiration coefficient β_e , which is a function of NDVI,

$$\beta_e = \gamma + \lambda \frac{(1 + \text{NDVI})}{(1 - \text{NDVI})} \quad (24)$$

where the coefficients γ and λ can be obtained by letting $\beta_e = 0$ and 1 when NDVI equals the lower and upper limits of photosynthetically active transpiring vegetation, respectively. For example, values of $\gamma = -0.157$ and $\lambda = 0.129$ result if a lower NDVI limit of 0.10 and an upper limit of 0.80 are assumed.

It would be desirable to use daily precipitation observations in the model integrations. Unfortunately, the unavailability of global daily precipitation data for the 10-year period of interest precludes such an implementation. An alternative is to use the available daily global precipitation record from the 1979 First GARP Global Experiment (FGGE) year as a stencil for the other years of the period. Monthly station precipitation climatology (Spangler and Jenne, 1990) for the 10-year period, 1979 through 1988, were reduced to a 4° latitude by 5° longitude grid. A surrogate temporal record of daily precipitation was produced by scaling the gridded monthly precipitation climatology, by the magnitudes of the 1979 FGGE daily precipitation data, using the formula

$$P_d^C = P_d^F \left(\frac{P_m^C}{P_m^F} \right) \quad (25)$$

where P_d^C is the daily precipitation, P_d^F is the observed daily precipitation in the FGGE year, P_m^F is the observed monthly precipitation in the FGGE year, and P_m^C is the observed monthly precipitation climatology. Thus, the daily

precipitation forcing preserves measured monthly magnitudes and occurs at the frequency of the observed 1979 precipitation events. Admittedly, in the natural system, the frequency of precipitation events will vary from one year to the next. In this application, we have assumed that when the daily computed soil moisture, evapotranspiration, and runoff are compiled to produce monthly means, the resulting values will be representative of the period in question. The availability of daily precipitation data over the United States is currently being used to test this assumption. In the integrations, all precipitation data were treated as rainfall. Station monthly mean surface air temperature data were gridded and linearly interpolated to provide mean daily air temperatures.

3. Presentation of data

By aggregating the daily data produced by the model integrations, global monthly mean precipitation, evapotranspiration, runoff, and soil moisture for each of SiB's three soil layers have been produced for each month of the 10-year period, 1979 through 1988. In this technical memorandum, global distribution maps illustrating 10-year (1979 - 1988) monthly averages of the monthly mean precipitation, evapotranspiration, root zone soil moisture, and runoff fields have been plotted. In addition, the standard deviations of the monthly mean precipitation, evapotranspiration, root zone soil moisture, and runoff for the 10-year period are also included. These are found in the section titled: "HYDROLOGIC FIELDS: 10-Year Average of Monthly Means, and Standard Deviations" under the subheadings, PRECIPITATION (January - December), EVAPOTRANSPIRATION (January - December), ROOT ZONE SOIL

WETNESS (January - December), and RUNOFF (January - December).

Referring to the precipitation figures, in January, maximum precipitation values of over 8 mm day^{-1} occur in the tropical regions south of the equator in South America, Africa, the Pacific Islands, and Australia. In addition, a January precipitation maximum is found in the mountainous regions surrounding the Gulf of Alaska. In January, regions of precipitation less than 0.5 mm day^{-1} include Arctic North America, the central United States, central Africa, and central Asia. By July, the tropical precipitation peak has shifted north of the equator to include South and Central America, Africa, and India. The precipitation minimum in central Africa has shifted north. A minimum of less than 0.5 mm day^{-1} in July also exists in southern Africa, central South America, and central Australia. In general, the precipitation standard deviation patterns correspond to the precipitation patterns, with the highest standard deviations occurring in the regions of highest precipitation.

Evapotranspiration is minimal, less than 0.5 mm day^{-1} , in the Northern Hemisphere in January, while south of the equator, evapotranspiration is typically greater than 2 mm day^{-1} . In May, regions north of 30° N latitude show a significant increase in evapotranspiration. By July, Northern Hemisphere evapotranspiration has increased sharply, typically being between 2 and 4 mm day^{-1} , with the exception of the regions of northern Africa and Arabia, where values less than 0.5 mm day^{-1} are typical. In general, the evapotranspiration standard deviation patterns correspond to the

evapotranspiration patterns, with the highest standard deviations occurring in the regions of highest evapotranspiration. Typically the evapotranspiration standard deviation displays more structure than the relatively smooth evapotranspiration patterns. In the Southern Hemisphere winter, South America has minimal evapotranspiration standard deviation.

Referring to the soil wetness figures, the lowest January root zone soil wetness values are found in the southwest United States, Mexico, southern South America and Africa, the Sahara, Arabia, and central Asia. These minimum soil moisture fractions are typically between 0.15 and 0.2. Maximum values, between 0.6 and 0.8, are found in the tropics, in the middle latitude storm belt regions such as the northwest coastal regions of the United States and Canada, and in Europe. In July, subtle changes in the soil moisture patterns are evident over the globe, but nothing as dramatic as the differences found in the precipitation and evapotranspiration patterns. In general, the soil wetness standard deviations vary considerably. Note that in the SiB evapotranspiration formulation, although it does depend on soil-vegetation type, evapotranspiration occurs at the potential rate for soil wetness values around 0.60 and evapotranspiration becomes zero at a soil wetness value of near 0.30. As a consequence, a 0.10 change in soil wetness is able to have a significant influence on evapotranspiration. Typically the soil wetness standard deviations are greatest in the tropics and decrease with increasing latitude.

Peak January runoff occurs in the region surrounding the Gulf of Alaska and in the tropics of South America, Africa, the Pacific Islands, and

central Australia. In July, the tropical runoff maximum has shifted north, and India and regions to the north and east are producing runoff values greater than 8 mm day^{-1} . Since runoff is strongly a function of soil moisture, the relatively subtle seasonal changes in soil moisture are reflected in the subtle seasonal changes in runoff. The one significant exception to this is the dramatic seasonal change in runoff produced by the increased precipitation during the Indian monsoon. In general, the runoff standard deviation patterns correspond to the runoff patterns, with the highest standard deviations occurring in the regions of highest runoff. Compared to the minimal runoff standard deviations occurring in the Northern Hemisphere during the Northern Hemisphere summer, the tropics contain relatively high standard deviations during this period.

As part of the model integrations, global monthly mean soil moisture for each of SiB's three soil layers were produced for each month of the 10-year period. These soil moisture fields are currently being used as soil moisture initial conditions during climate simulations using the version of the GLA GCM that employs the SiB land-surface parameterization.

4. Concluding summary

An analysis scheme to generate global evapotranspiration and soil moisture fields, using key components of the Simple Biosphere Model, has been developed. Two modifications have been made to the original SiB soil hydrology formulation: a linear reservoir drainage term has been added to the third soil layer, and all precipitation is forced to enter the upper soil matrix

during each time step. The influence of these modifications is being tested in the Goddard Laboratory for Atmospheres SiB-GCM. In addition, the analysis scheme incorporates a simplified computation of evapotranspiration based on SiB evapotranspiration functions.

The method requires atmospheric forcing of precipitation and potential evapotranspiration. Potential evapotranspiration is computed using the method of Thornthwaite, where the observed air temperatures have been adjusted to represent potential conditions by using normalized difference vegetation index (NDVI) data determined from satellite observations. The analysis was run for 10 years, 1979 through 1988. In performing the model integrations, it would be desirable to use global observed daily precipitation. To circumvent the unavailability of global daily precipitation data for the period 1979 through 1988, we use the daily global precipitation record from the 1979 FGGE year as a stencil for the other years of the period. Thus, by using observed monthly mean precipitation data, we produce a 10-year, daily precipitation record which preserves measured monthly magnitudes, and occurs at the frequency of the observed 1979 FGGE year precipitation events.

The scheme represents an efficient methodology for generating soil moisture initialization fields for GCMs; it can also be applied to other land-surface hydrology parameterizations being used in GCMs, through a substitution of the parameterizations' soil hydrology and evapotranspiration functions. The resulting soil moisture fields are compatible with the atmospheric forcing of observed precipitation and surface air temperature climatology. In addition, these fields are computed in a manner consistent with

the soil hydrology and evapotranspiration representations found in the specific GCM land-surface hydrology parameterization of interest.

Validation of data sets such as the ones described here is an important and necessary step in the development and refinement of information used in climate simulations using GCMs. At seasonal and continental scales, terrestrial precipitation inputs are considered relatively well known, despite the scarcity of data in some regions of the world. In addition, river discharge measurements are readily available and are being used for model validation over large areas (Liston et al., 1993). This river discharge is an important integrator of the hydrologic cycle, and is able to provide much needed insight into whether or not the models produce realistic terrestrial water balances. Evapotranspiration comprises a significant fraction of the moisture transport within the hydrologic cycle; unfortunately, direct validation of land-surface evapotranspiration is difficult, and it is generally approximated using indirect methods that utilize air temperature or radiation observations. Soil moisture data from remote sensing measurements are now becoming available for comparison with modeled fields. A useful feature of these observations is the measurement of subgrid-scale soil moisture variability. These data and other satellite-derived products are expected to assist in the formulation of next generation runoff and evapotranspiration schemes, and thus provide a valuable contribution to future land-surface modeling efforts. The resulting improved understanding and description of terrestrial hydrology will add to the quality of global climate simulations.

NUMERICAL DATA. Input and derived fields described in this technical memorandum are available for all months of the 10-year period, 1979 through 1988, in the form of grid-area numerical values. They are available in printed tables, on magnetic tape, and via Internet using standard file transfer protocol (ftp). Contact the authors, Climate and Radiation Branch, Code 913, Laboratory for Atmospheres, NASA/Goddard Space Flight Center, Greenbelt, Maryland 20771.

ACKNOWLEDGEMENTS. Unpublished algorithms and empirical relationships developed by Professor Y. Mintz have been invaluable in the development of this method for estimating global soil moisture fields. We also thank J. Schemm for providing the gridded precipitation data sets. Support for this research was provided by the NASA Land and Climate program offices.

REFERENCES

- Abramopoulos, F., C. Rosenzweig and B. Choudhury, 1988: Improved ground hydrology calculations for global climate models (GCMs): Soil water movement and evapotranspiration. *J. Climate*, **1**, 921-941.
- Budyko, M.I., 1956: *Teplovoi Balans Zemnoi Poverkhnosti*. Gidrometeoizdat, Leningrad; Heat Balance of the Earth's Surface, translated by N.A. Sepanova, U.S. Weather Bur., Washington, D.C., 1958. MGA 8.5-20, 13E-286, IIB-25, 259 pp.
- Campbell, G.S., 1974: A simple method for determining unsaturated conductivity from moisture retention data. *Soil Sci.*, **117**, 311-314.
- Clapp, R.B., and G.M. Hornberger, 1978: Empirical equations for some soil hydraulic properties. *Water Resour. Res.*, **14**, 601-604.
- Davies, J.A., and C.D. Allen, 1973: Equilibrium, potential and actual evaporation from cropped surfaces in Southern Ontario. *J. Appl. Meteor.*, **12**, 649-657.
- Dickinson, T.L., A. Henderson-Sellers, P.J. Kennedy and M.F. Wilson, 1986: Biosphere-atmosphere transfer scheme (BATS) for the NCAR community climate model. NCAR Tech. Note, NCAR/TN-275+STR, 69 pp.
- Dorman, J.L., and P.J. Sellers, 1989: A global climatology of albedo, roughness length and stomatal resistance for atmospheric general circulation models as represented by the simple biosphere model (SiB). *J. Appl. Met.*, **28**, 833-855.
- Fennessy, M.J., and Y.C. Sud, 1983: A study of the influence of soil moisture on future precipitation. NASA Technical Memorandum 85042, Washington DC, 123 pp.
- Freeze, R.A., and J.A. Cherry, 1979: *Groundwater*. Prentice-Hall, Englewood Cliffs, New Jersey.
- Gordon, C.T., 1986: Boundary layer parameterizations and land surface processes in GFDL GCMs. ISLSCP, Proceedings of an International Conference, ESA SP-248, ESA, Paris, France, 23-37.
- Jensen, M.E., 1973: *Consumptive Use on Water and Irrigation Water Requirements*. American Society of Civil Engineers, New York.
- Liston, G.E., Y.C. Sud and E.F. Wood, 1993: Evaluating GCM land-surface hydrology parameterizations by computing river discharges using a

runoff routing model: Application to the Mississippi Basin. *J. Appl. Meteor.*, (submitted.)

Mintz, Y., 1984: The sensitivity of numerically simulated climates to land-surface conditions. In: *The Global Climate*, J. Houghton (ed.), Cambridge University Press, 79-105.

Mintz, Y., and G.K. Walker, 1993: Global fields of soil moisture and land-surface evapotranspiration, derived from observed precipitation and surface air temperature. *J. Appl. Meteor.*, (in press.)

Nappo, C.J., 1975: Parameterization of surface moisture and evaporation rate in a planetary boundary layer model. *J. Appl. Meteor.*, **14**, 289-296.

Penman, H.L., 1948: Natural evaporation from open water, bare soil and grass. *Proc. Roy. Soc., (A)*, **193**, 120-145.

Priestley, C.H.B., and R.J. Taylor, 1972: On the assessment of surface heat flux and evaporation using large-scale parameters. *Mon. Wea. Rev.*, **100**, 81-92.

Rowntree, P.R., 1983: Sensitivity of general circulation models to land surface processes. Proceedings of the Workshop on Intercomparison of Large Scale Models Used for Extended Range Forecasts, European Center for Medium Range Weather Forecasts, Shinfield Park, Reading, United Kingdom, 225-261.

Sato, N., P.J. Sellers, D.A. Randall, E.K. Schneider, J. Shukla, J.L. Kinter III, Y.-T. Hou and E. Albertazzi, 1989a: Effects of implementing the simple biosphere model (SiB) in a general circulation model. *J. Atmos. Sci.*, **46**, 2757-2782.

Sato, N., P.J. Sellers, D.A. Randall, E.K. Schneider, J. Shukla, J.L. Kinter III, Y.-T. Hou and E. Albertazzi, 1989b: Implementing the simple biosphere model (SiB) in a general circulation model: Methodologies and results. NASA Contractor Report 185509, Washington DC, 76 pp.

Schemm, J., S. Schubert, J. Terry and S. Bloom, 1992: Estimates of monthly mean soil moisture for 1979-1989. NASA Technical Memorandum 104571, Washington DC, 260 pp.

Sellers, P.J., 1985: Canopy reflectance, photosynthesis and transpiration. *Int. J. Rem. Sens.*, **6**, 1335-1372.

Sellers, P.J., Y. Mintz, Y.C. Sud and A. Dalcher, 1986: A simple biosphere model (SiB) for use within general circulation models. *J. Atmos. Sci.*, **43**, 505-531.

- Serafini, Y.V., and Y.C. Sud, 1987: The time scale of the soil hydrology using a simple water budget model. *J. Climatology*, **7**, 585-591.
- Shukla, J., and Y. Mintz, 1982: Influence of land surface evapotranspiration on the Earth's climate. *Science*, **215**, 1498-1501.
- Spangler, W.M.L., and R.L. Jenne, 1990: World monthly surface station climatology. National Center for Atmospheric Research, Boulder, CO.
- Sud, Y.C., and W.E. Smith, 1985: Influence of local land-surface processes on the Indian Monsoon: a numerical study. *J. Clim. and Appl. Meteor.*, **24**, 1015-1036.
- Thornthwaite, C.W., 1948: An approach toward a rational classification of climate. *Geographical Rev.*, **38**, 55-94.
- Thornthwaite, C.W., and F.K. Hare, 1965: The loss of water to the air. *Meteorological Monographs*, **28**, 163.
- Tucker, C.J., J.R.G. Townshend and T.E. Goff, 1985: African land-cover classification using satellite data. *Science*, **227**, 369-375.
- Versegny, D.L., 1991: CLASS-A Canadian land surface scheme for GCMs. I. Soil model. *Int. J. Climatology*, **11**, 111-133.
- Willmott, C.J., 1977: WATBUG: A FORTRAN IV algorithm for calculating the climatic water budget. *Publications in Climatology*, **30**, (2).
- Willmott, C.J., 1984: On the evaluation of model performance in physical geography. In: *Spatial Statistics and Models*, Gaile, G.L. and C.J. Willmott (eds.), D. Reidel, Dordrecht, Holland.
- Willmott, C.J., C.M. Rowe and Y. Mintz, 1985: Climatology of the terrestrial seasonal water cycle. *J. Climatology*, **5**, 589-606.
- Wood, E.F., D.P. Lettenmaier and V.G. Zartarian, 1992: A land-surface parameterization with subgrid variability for general circulation models. *J. Geophys. Res.*, **97**, 2717-2728.
- Xue, Y., P.J. Sellers, J.L. Kinter and J. Shulka, 1991: A simplified biosphere model for global climate studies. *J. Climate*, **4**, 345-364.
- Yeh, T.-C., R.T. Wetherald and S. Manabe, 1984: The effect of soil moisture on the short-term climate and hydrology change—a numerical experiment. *Mon. Wea. Rev.*, **112**, 474-490.

Table 1. Values of the Evapotranspiration Coefficients c_1 and c_2 for the Twelve SiB Vegetation Types*

Type	SiB Biome	c_1	c_2
1	Broadleaf-evergreen trees (tropical forest)	6.25	1.2
2	Broadleaf-deciduous trees	5.57	5.35
3	Broadleaf and needleleaf trees (mixed forest)	5.73	1.92
4	Needleleaf-evergreen trees	5.53	3.7
5	Needleleaf-deciduous trees (larch)	5.66	7.8
6	Broadleaf trees with grass and shrubs (savanna)	5.67	1.8
7	Grassland (perennial)	5.80	1.73
8	Broadleaf shrubs with perennial groundcover	5.98	3.0
9	Broadleaf shrubs with bare soil (semi-desert)	6.37	1.39
10	Dwarf trees and shrubs with groundcover (tundra)	5.37	0.96
11	Bare soil (desert)	—	—
12	Cultivated land idealized to grow wheat	4.36	0.58

* from Xue et al. (1991)

HYDROLOGIC FIELDS: 10-Year Average of Monthly Means, and Standard Deviations

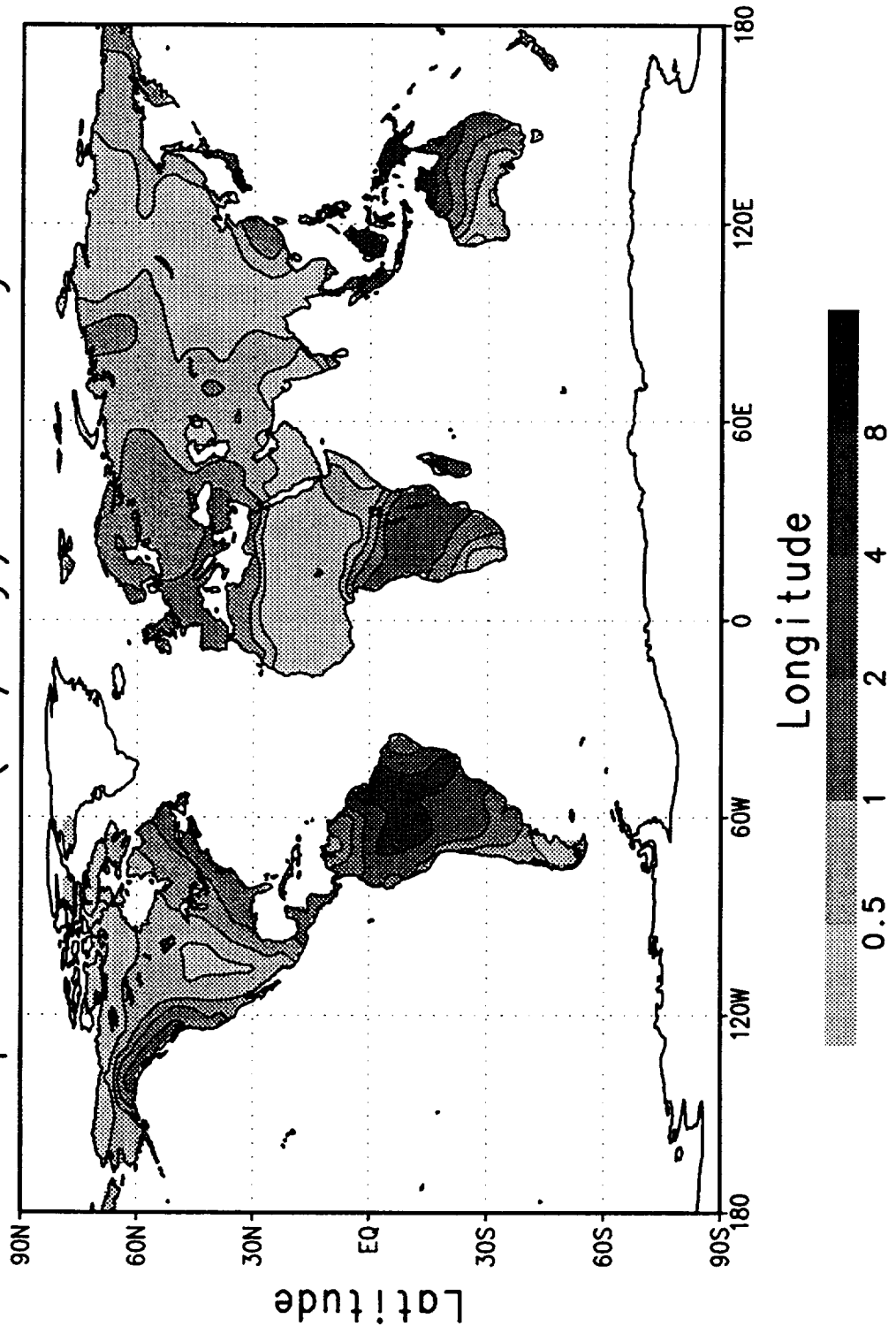
Global distribution maps of key hydrologic fields are included in this report. Ten-year (1979 - 1988) averages of the monthly mean precipitation, evapotranspiration, root zone soil moisture, and runoff fields are plotted. In addition, the standard deviations of the monthly mean precipitation, evapotranspiration, root zone soil moisture, and runoff for the 10-year period have been included.

PRECIPITATION

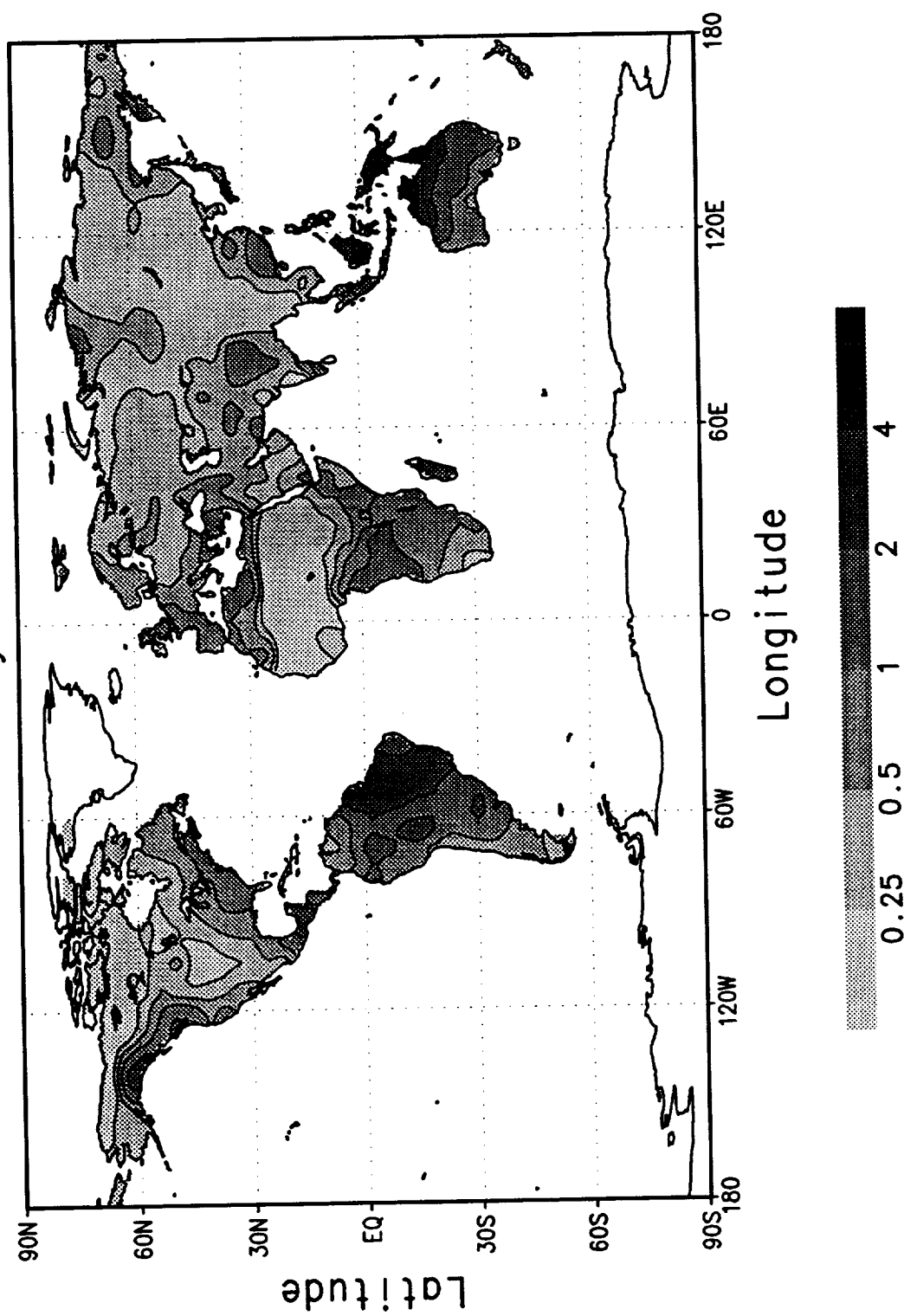
(January - December)

Ten-year average (1979 - 1988) of the monthly mean precipitation (mm day^{-1}), obtained from rain gage observations (Spangler and Jenne, 1990). Also plotted are the standard deviations of the monthly mean fields as determined from the 10-year data set.

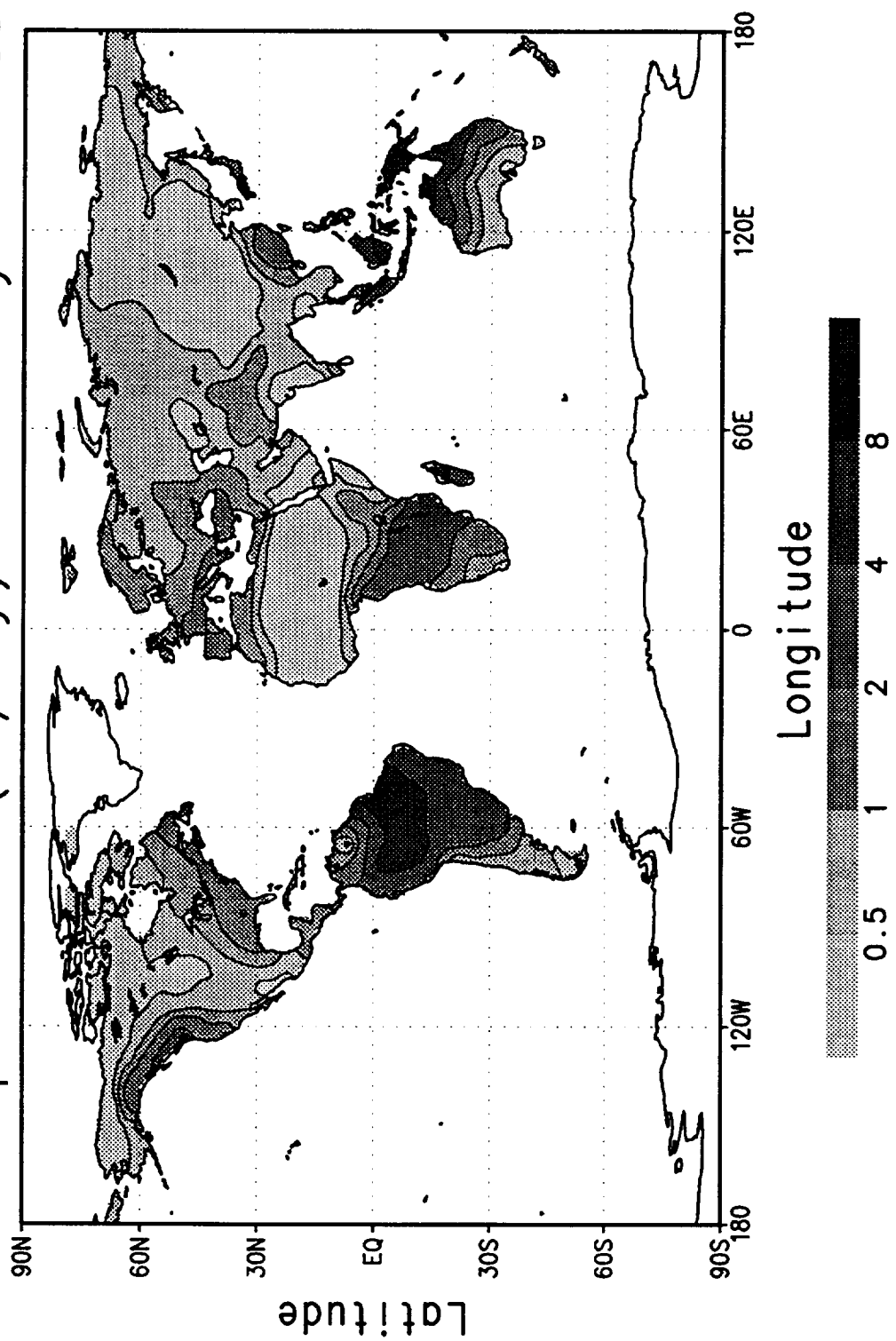
Precipitation (mm/day) January 1979–88



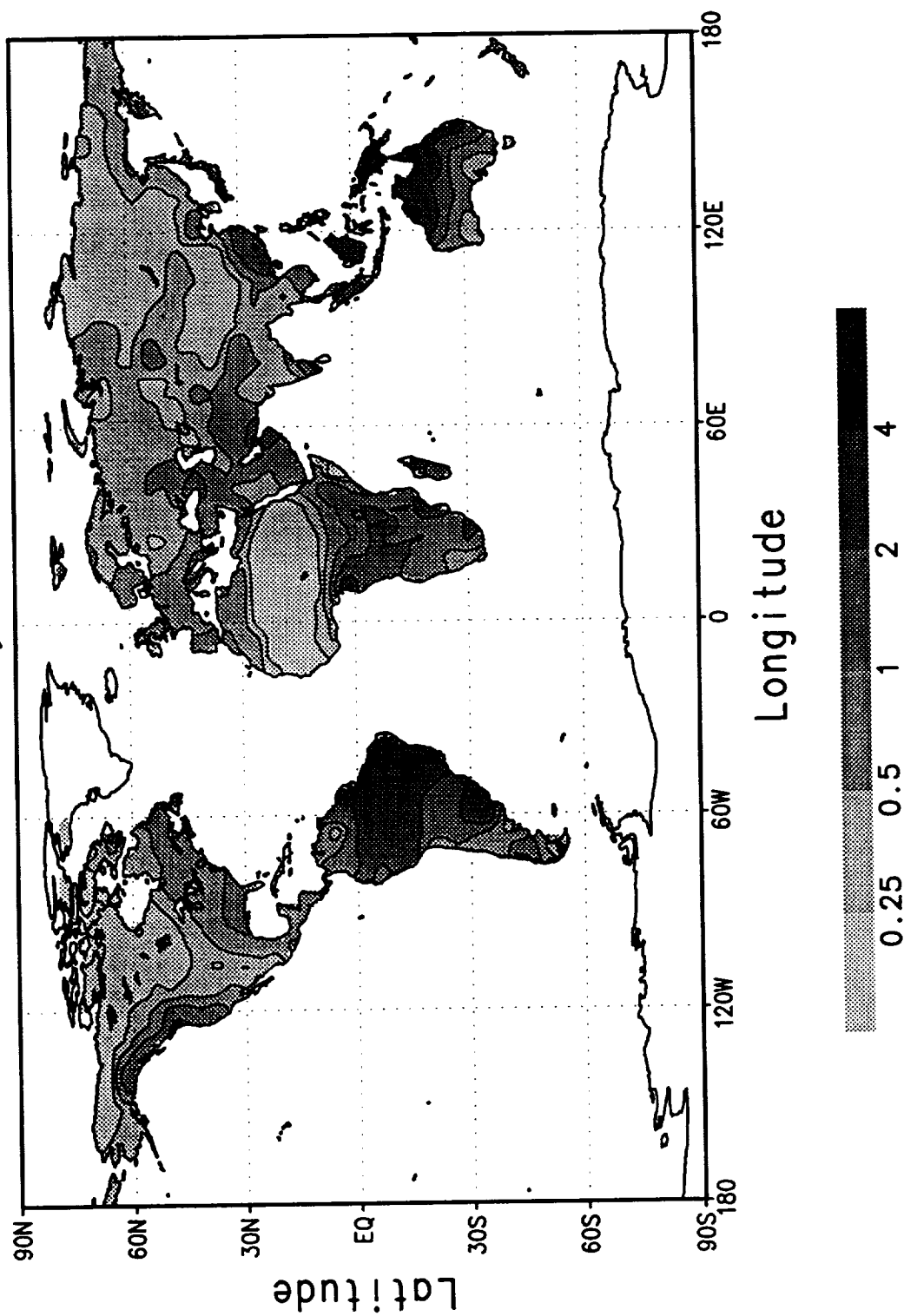
Precipitation Standard Deviation (mm/day)
January 1979-88



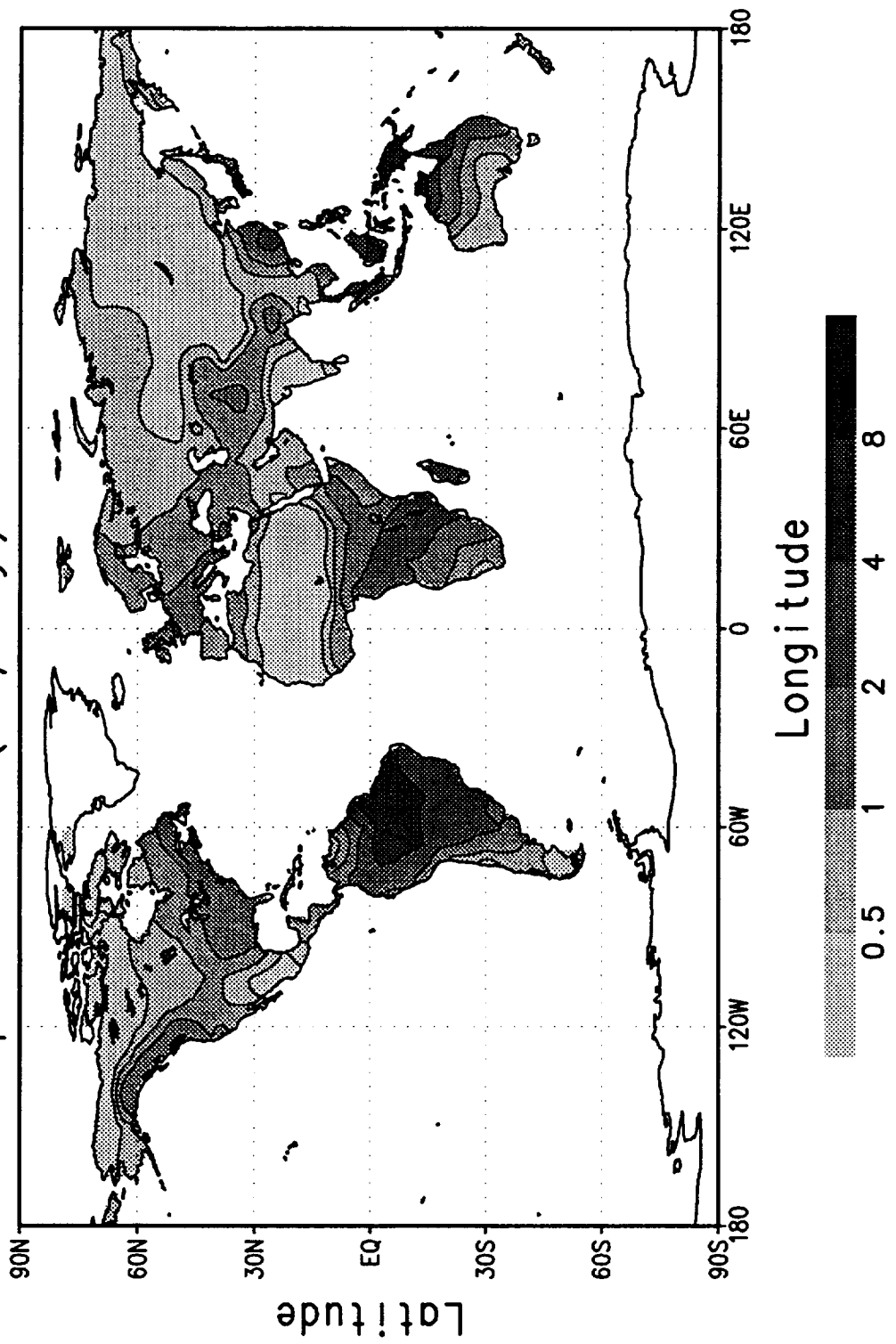
Precipitation (mm/day) February 1979–88



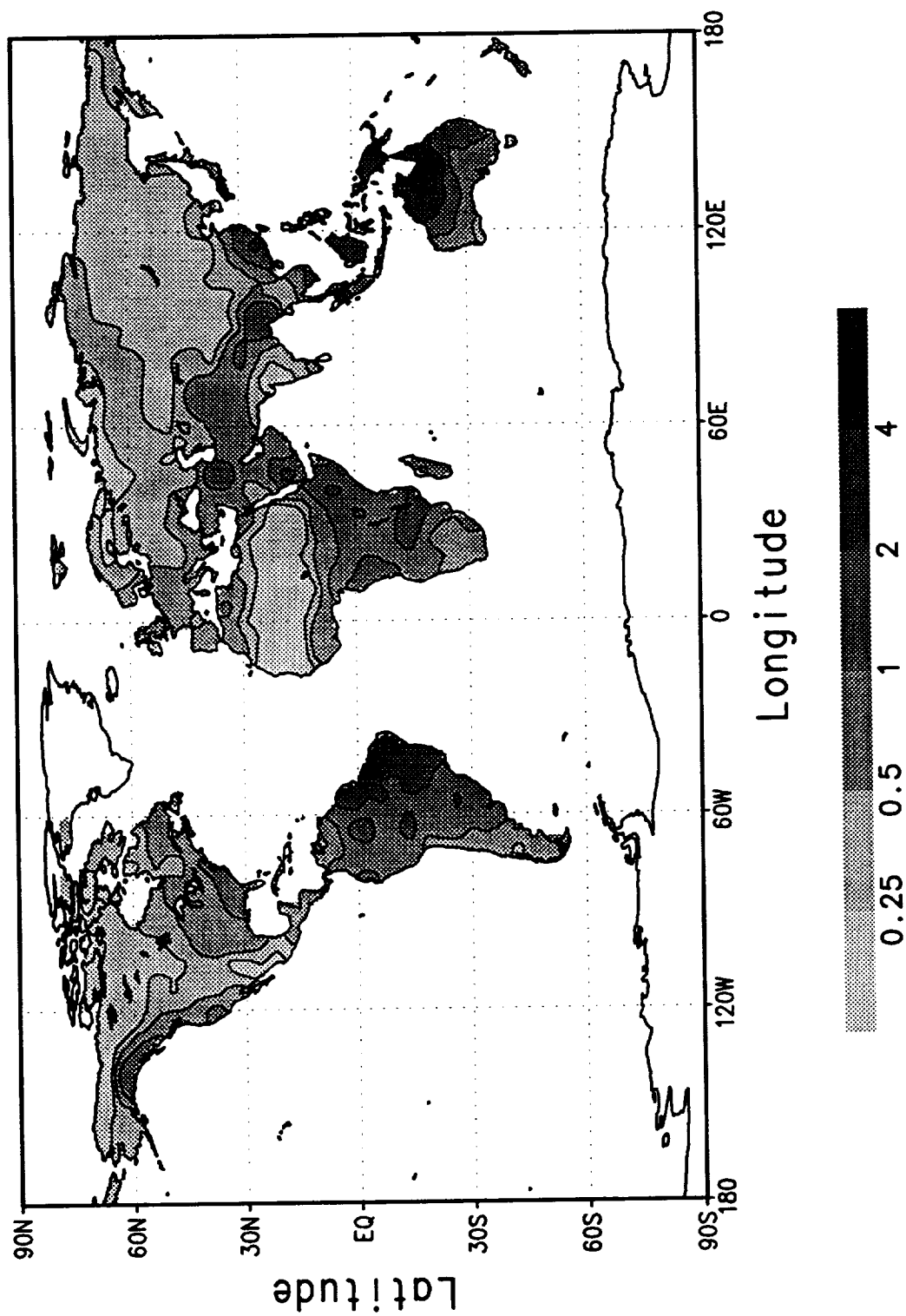
Precipitation Standard Deviation (mm/day)
February 1979-88



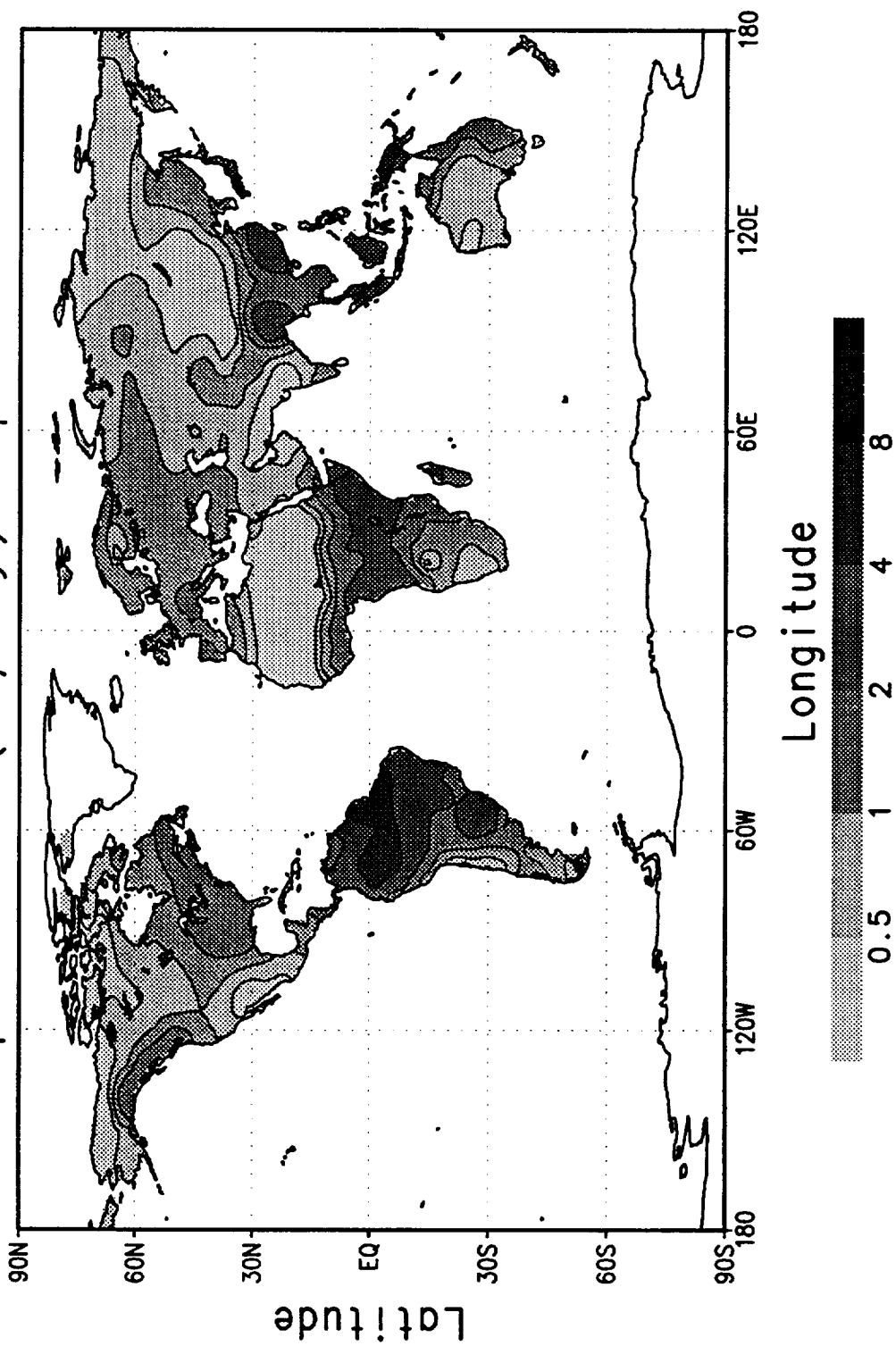
Precipitation (mm/day) March 1979-88



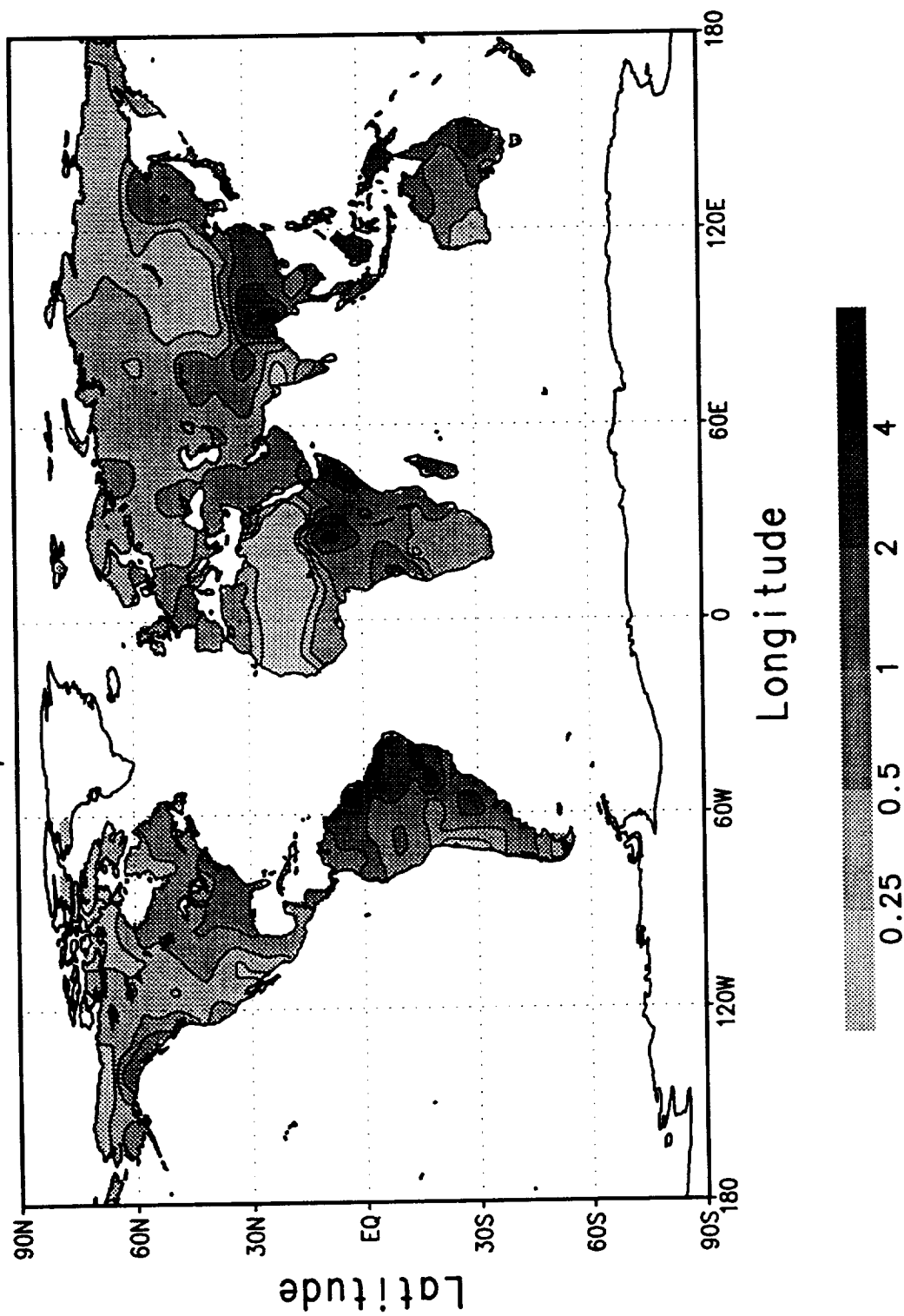
Precipitation Standard Deviation (mm/day)
March 1979-88

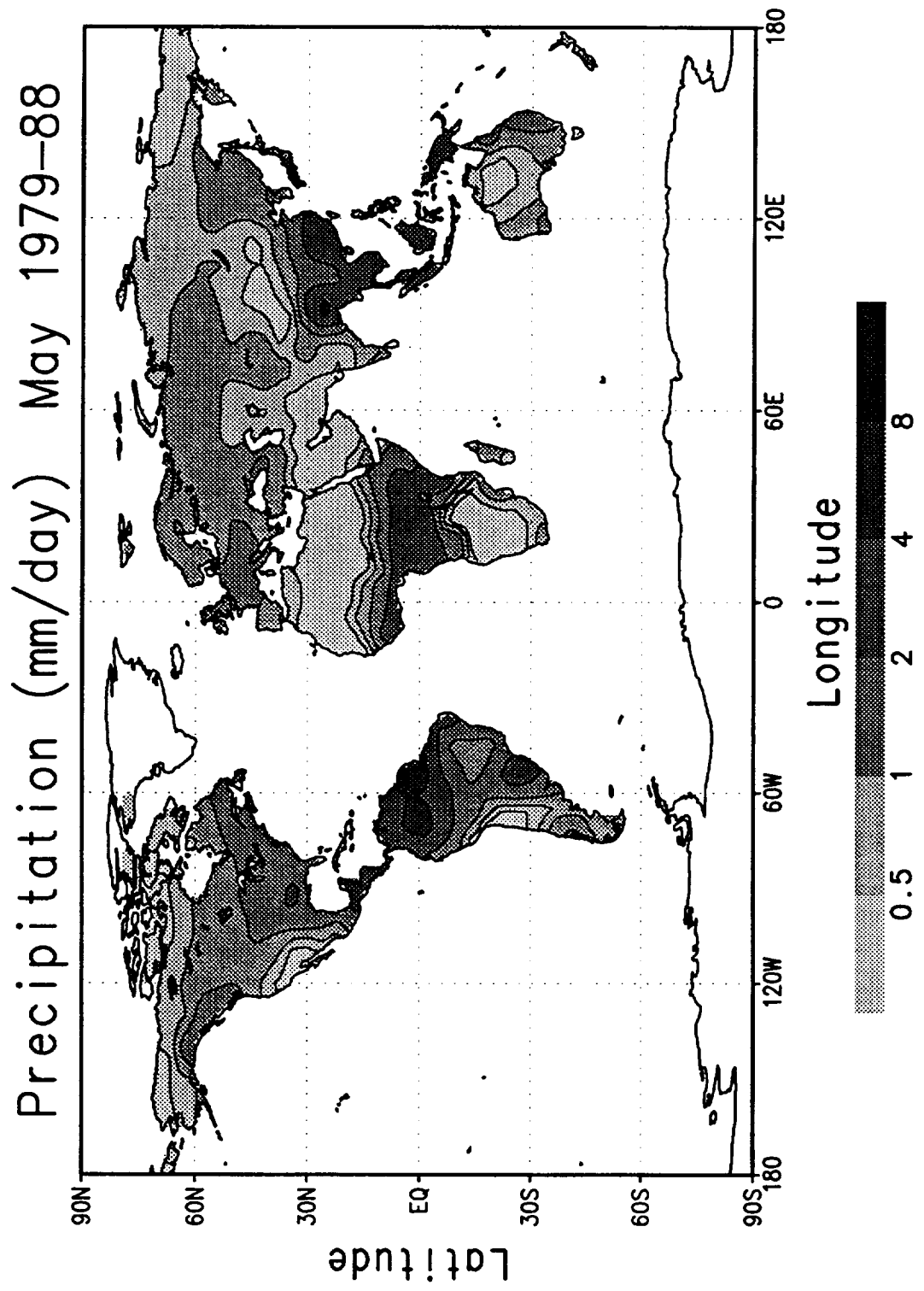


Precipitation (mm/day) April 1979-88

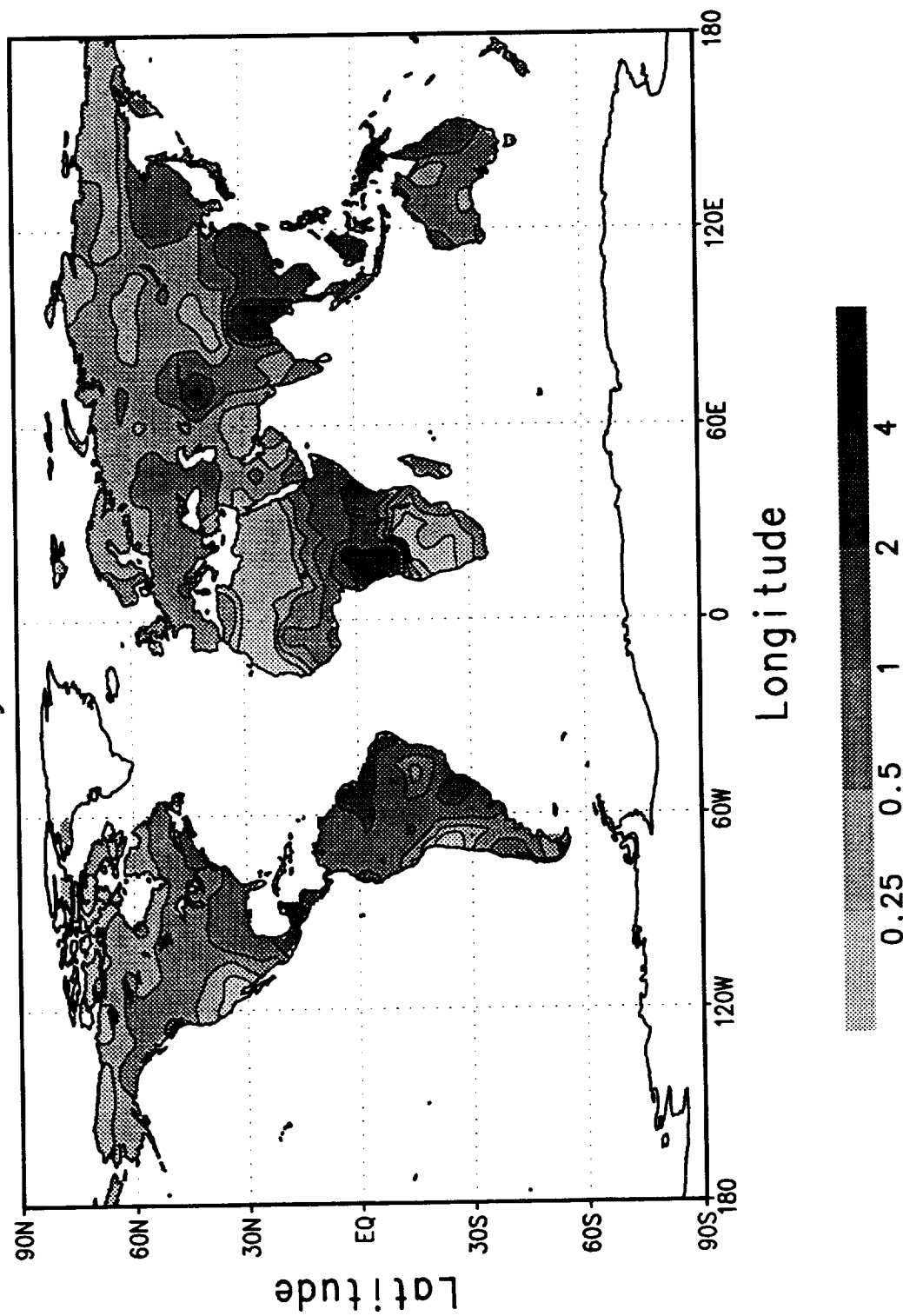


Precipitation Standard Deviation (mm/day)
April 1979-88

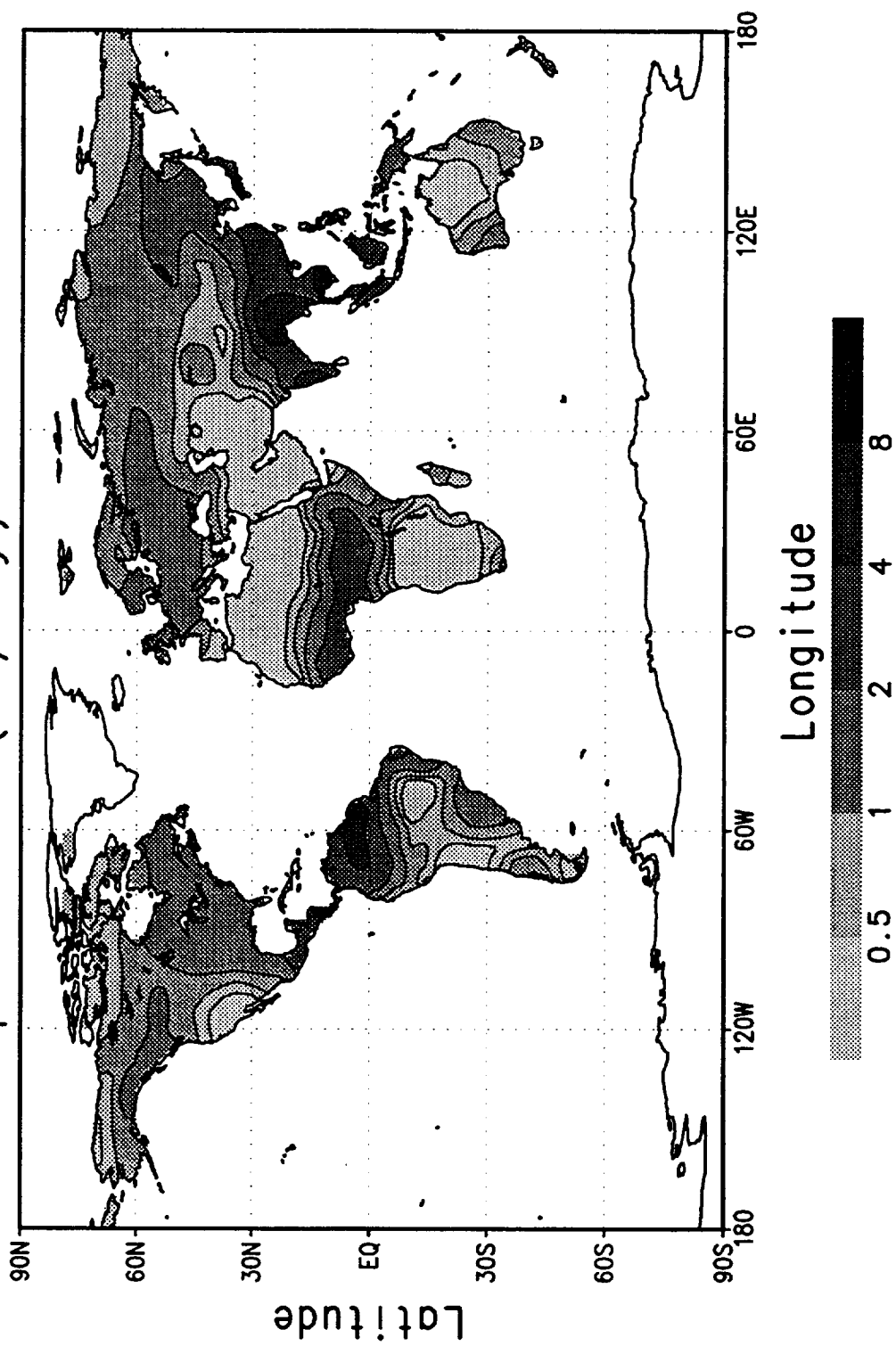




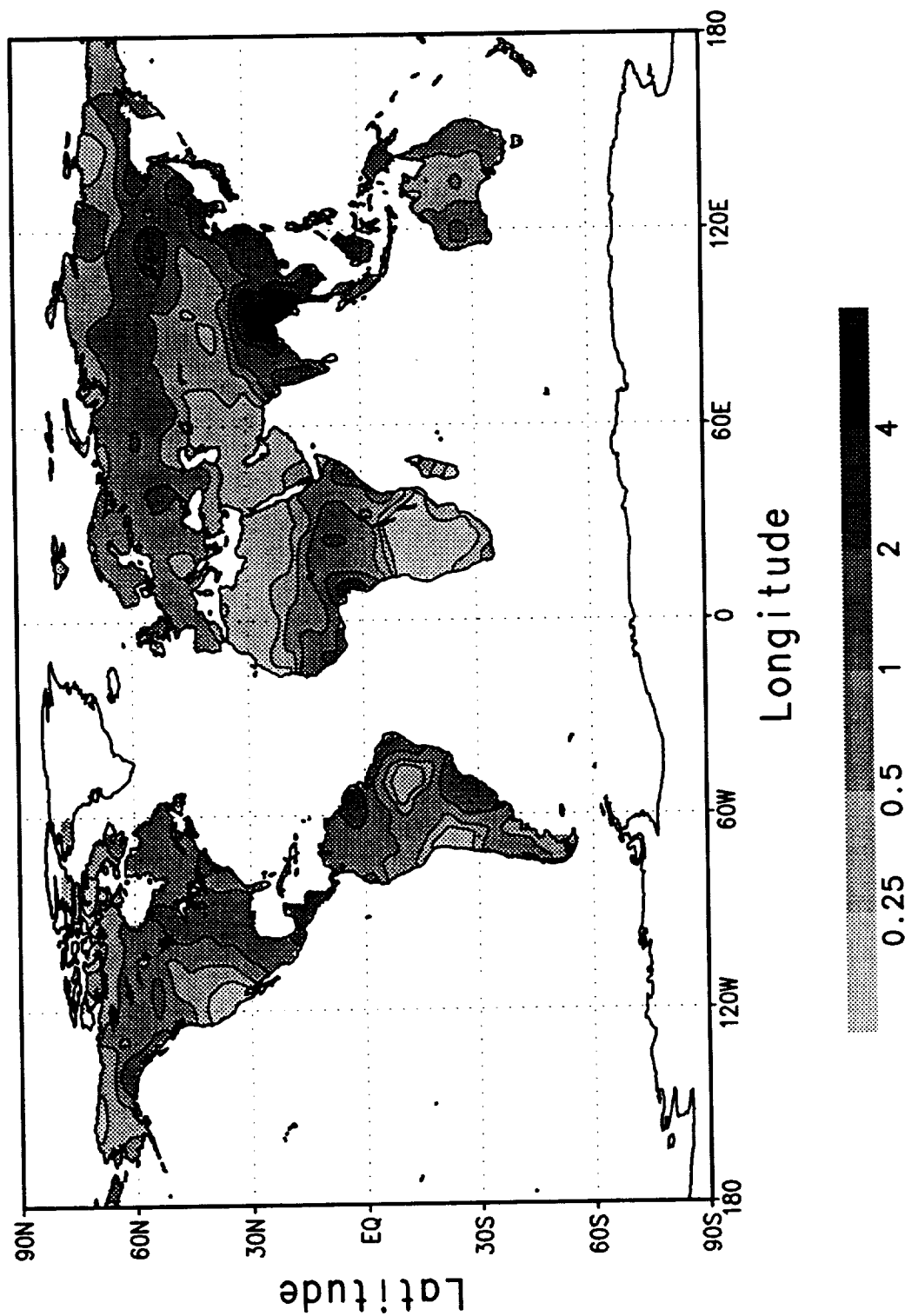
Precipitation Standard Deviation (mm/day)
May 1979-88

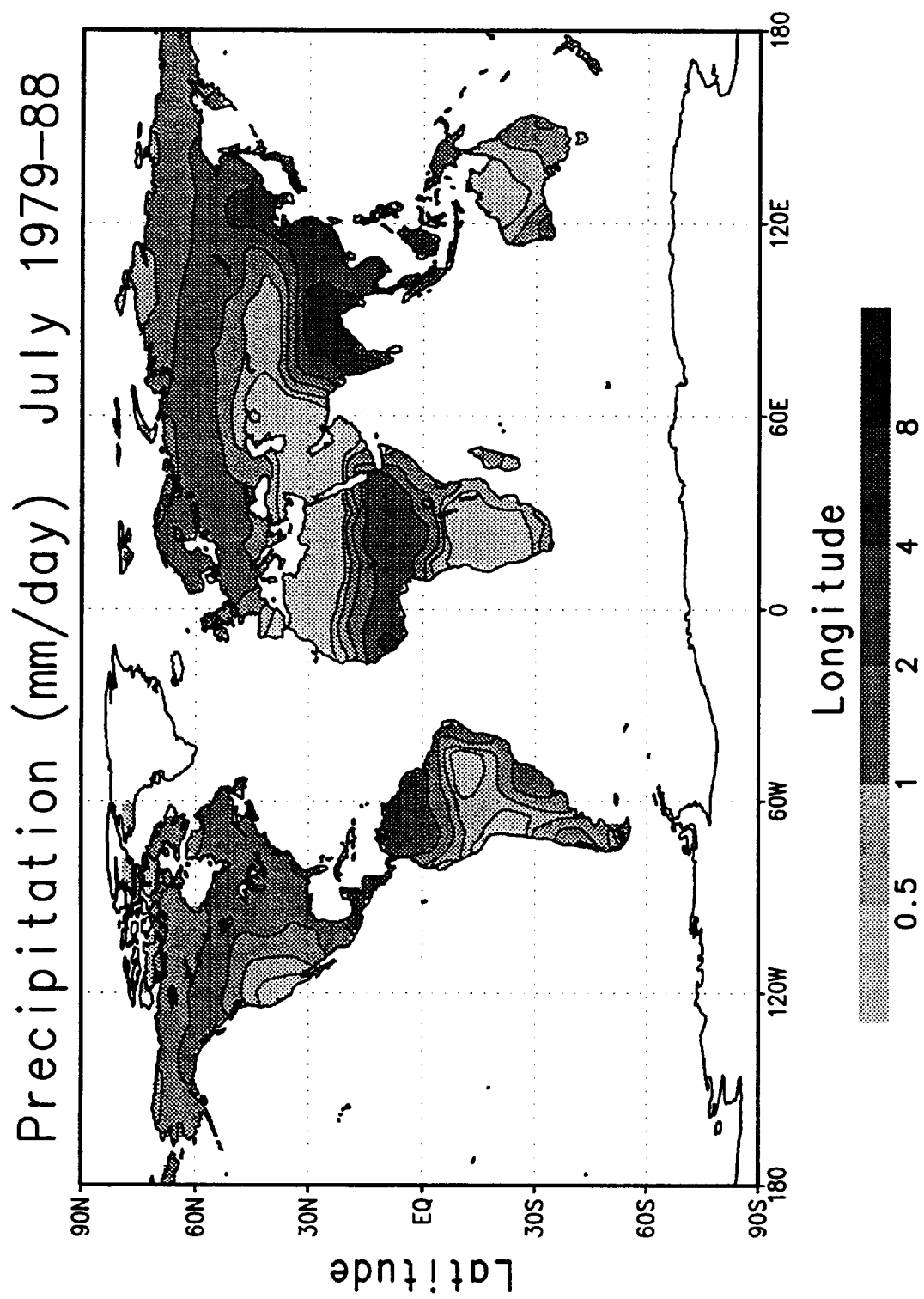


Precipitation (mm/day) June 1979-88

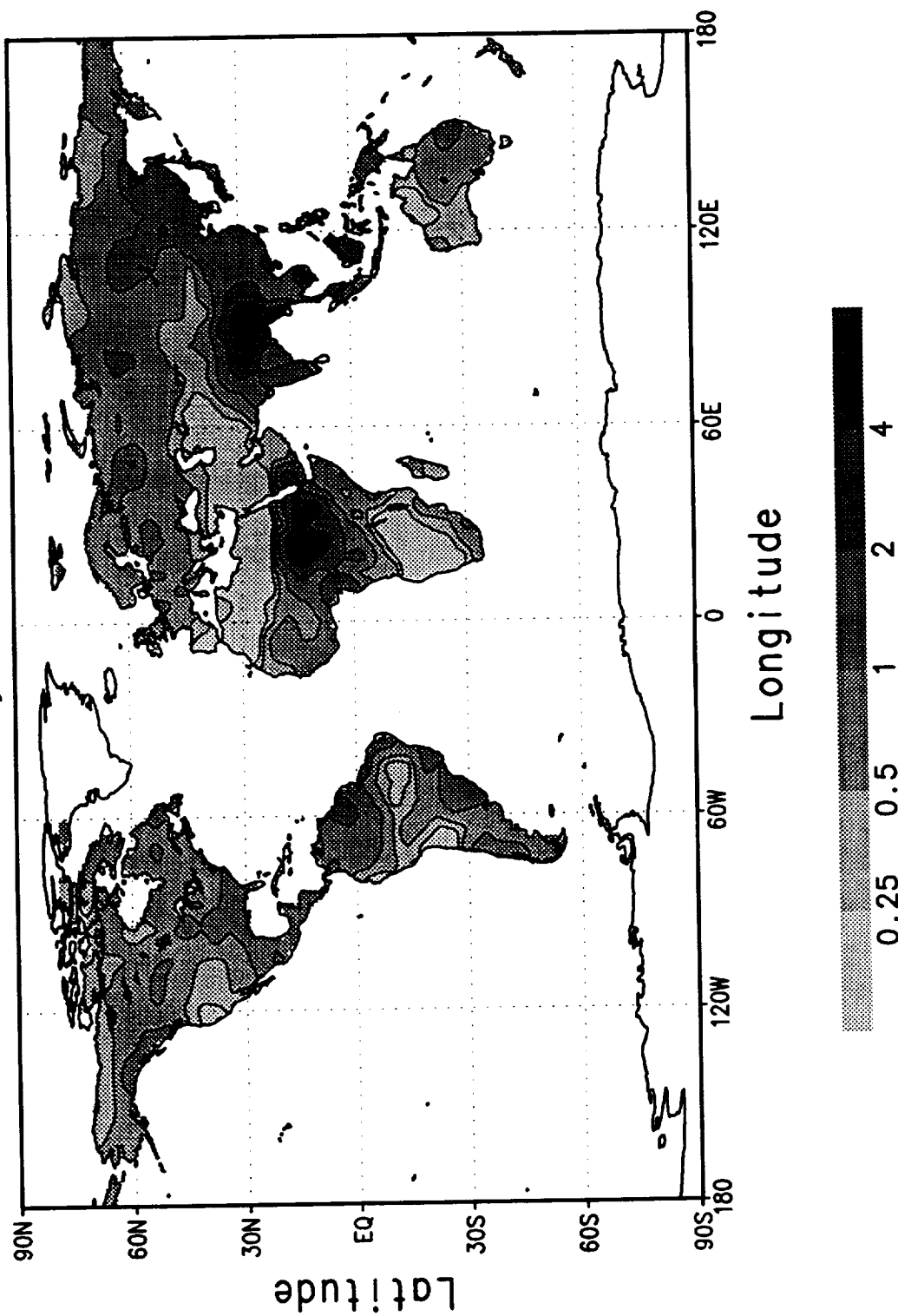


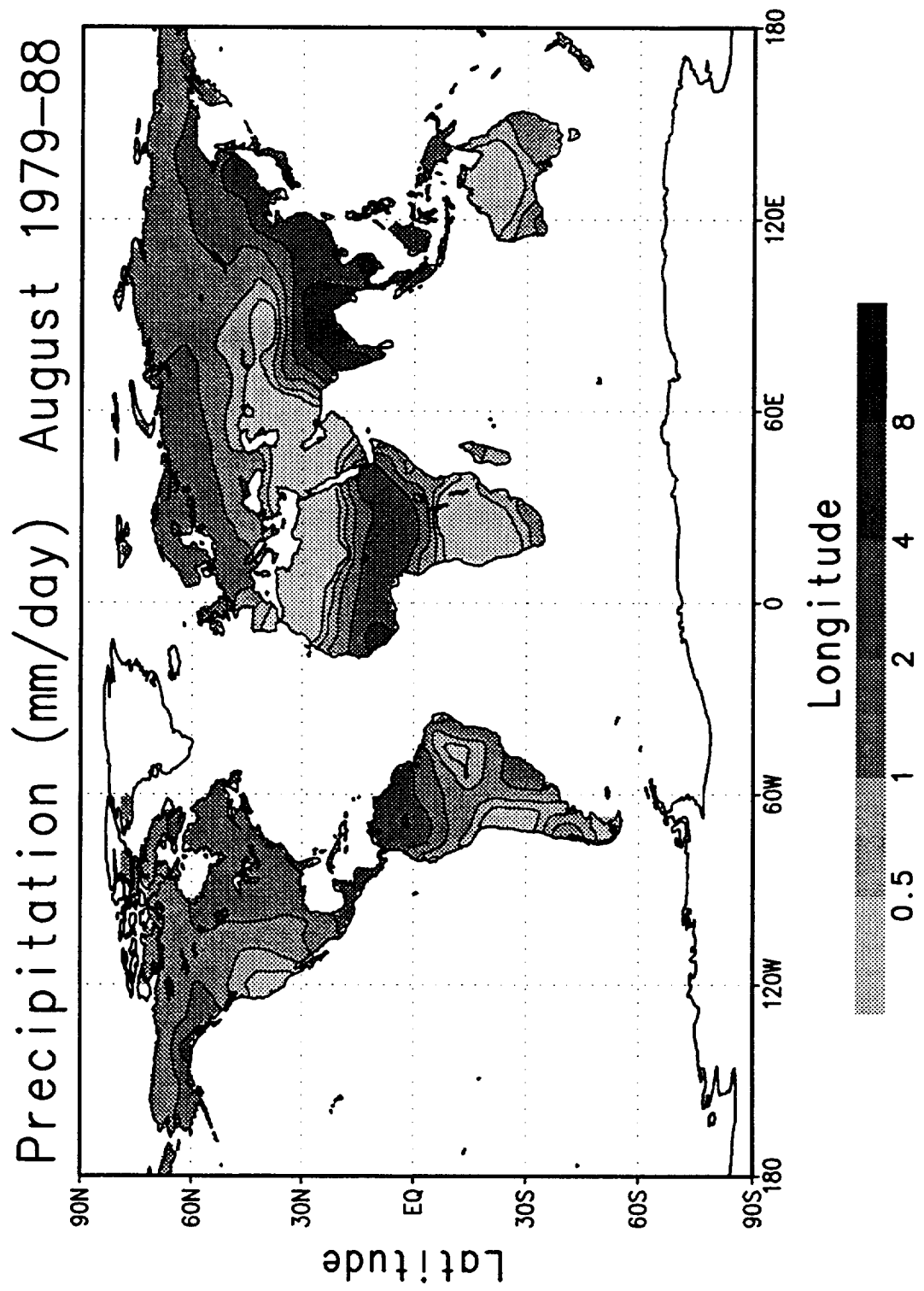
Precipitation Standard Deviation (mm/day)
June 1979-88



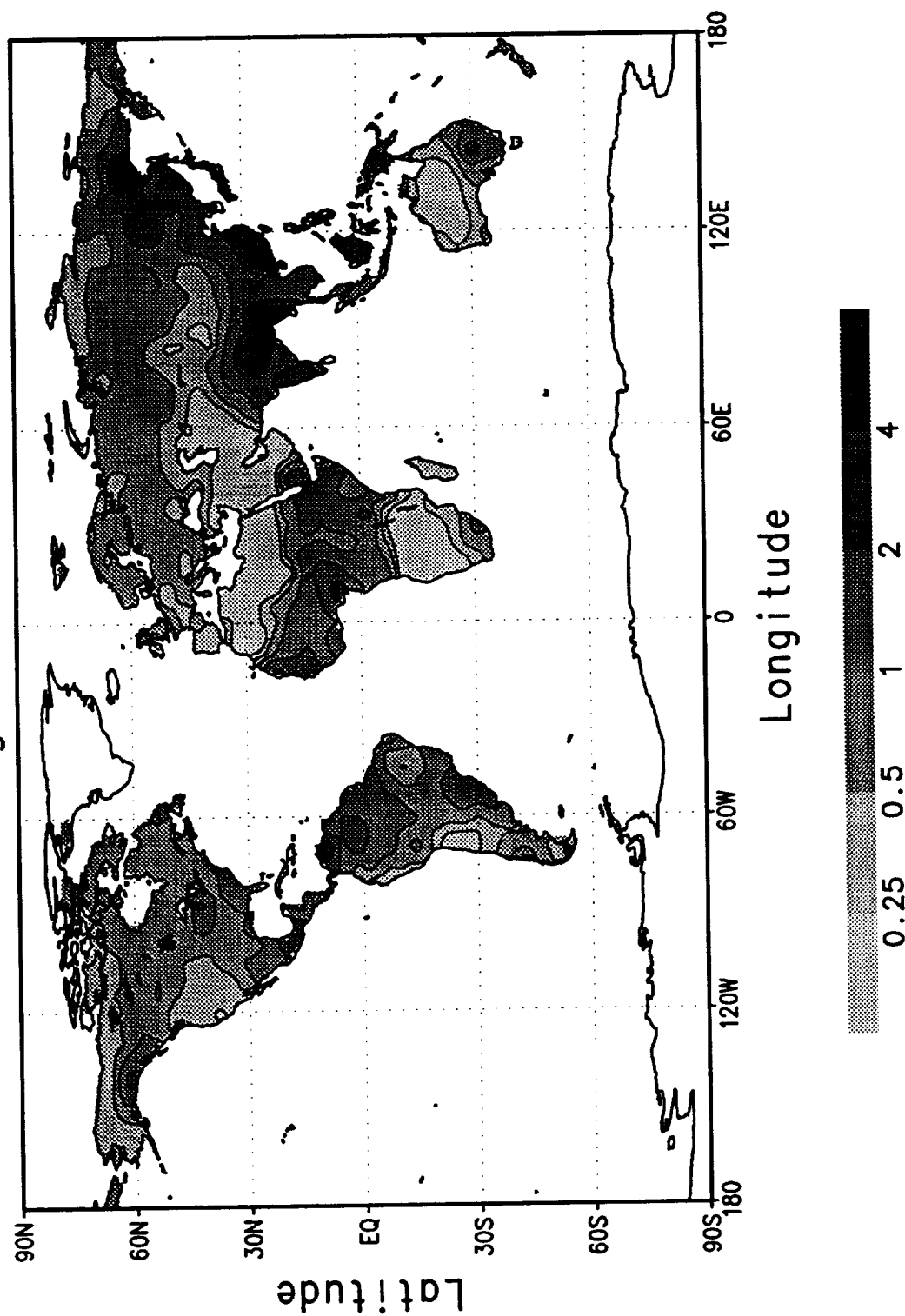


Precipitation Standard Deviation (mm/day)
July 1979-88

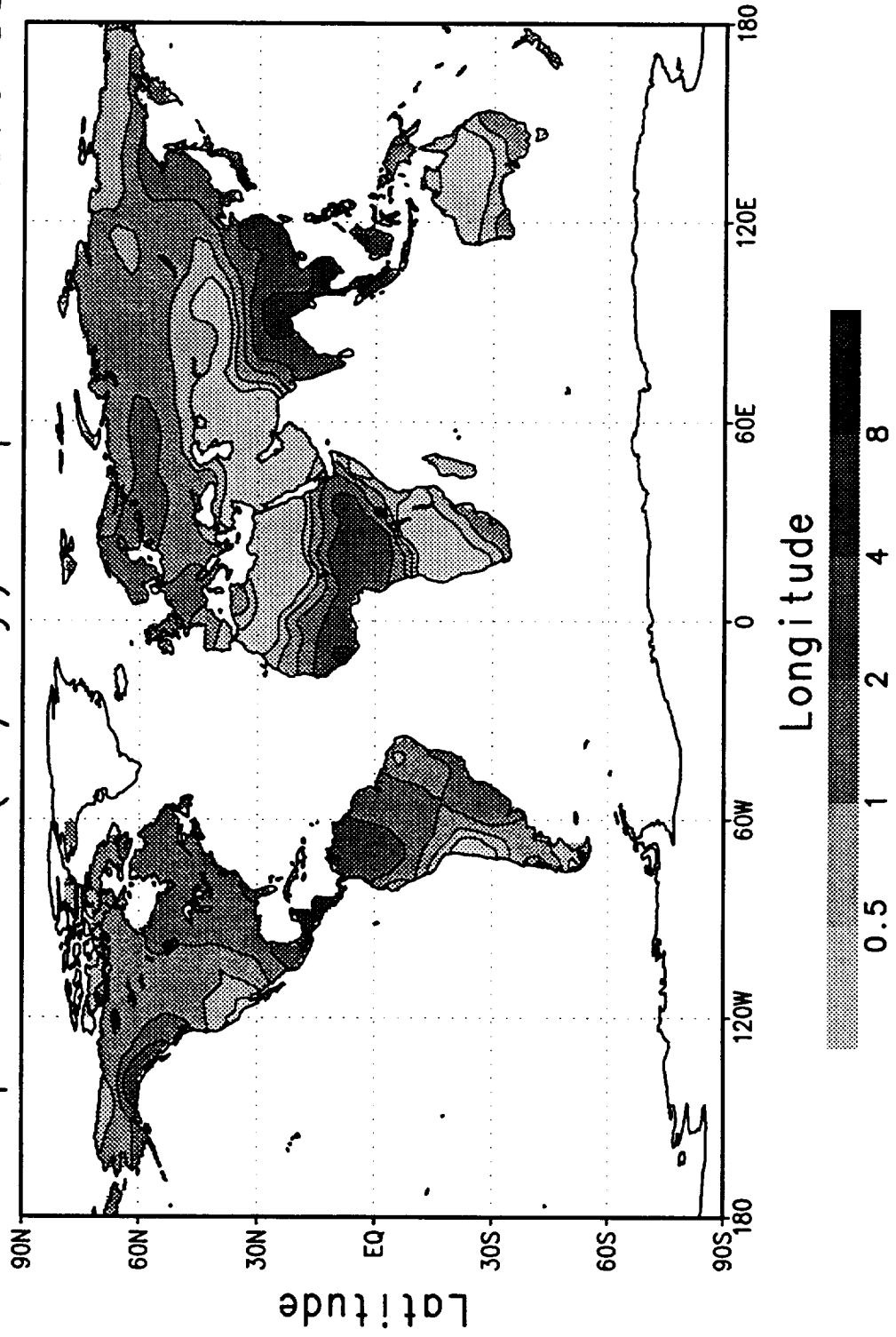




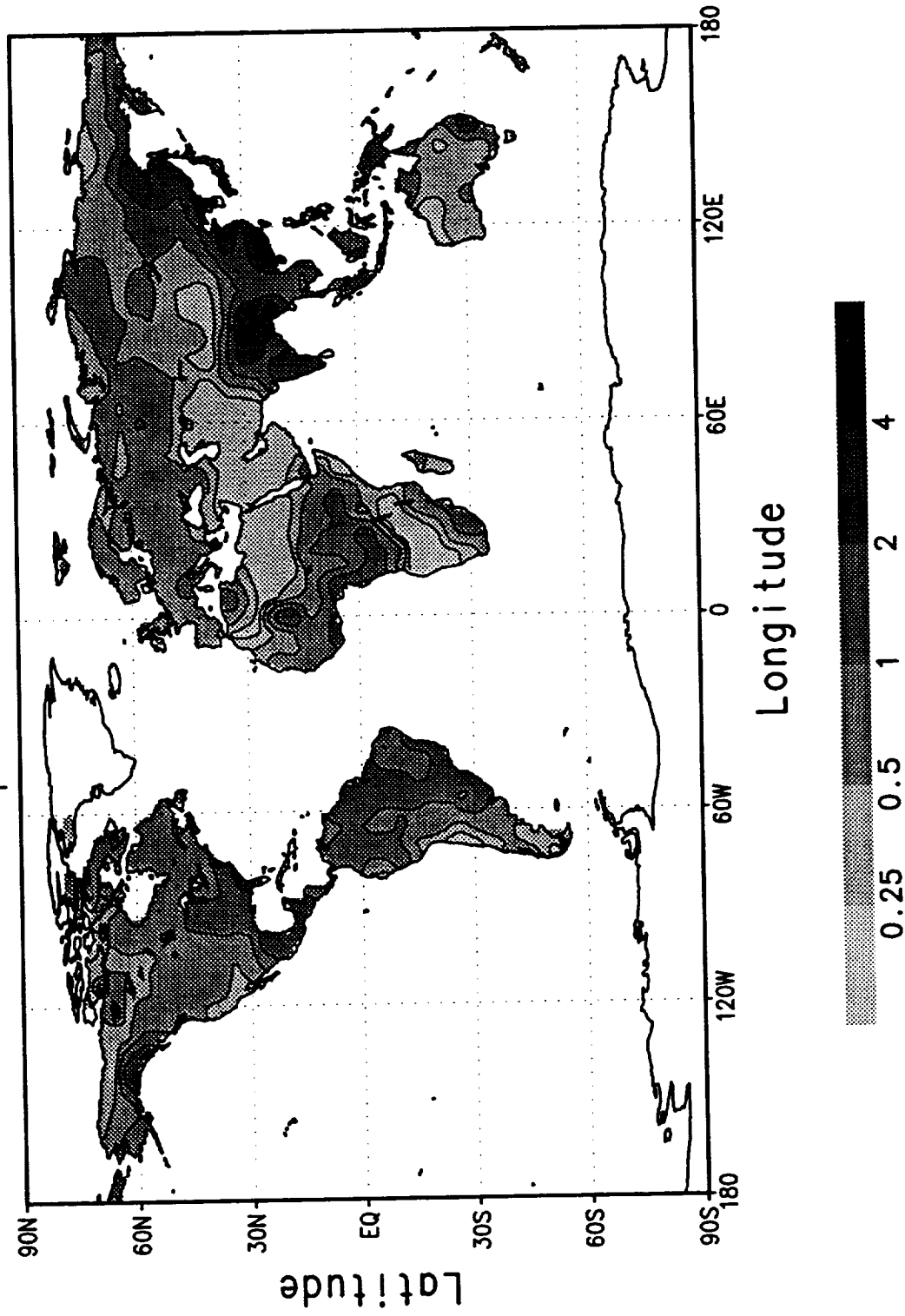
Precipitation Standard Deviation (mm/day)
August 1979-88



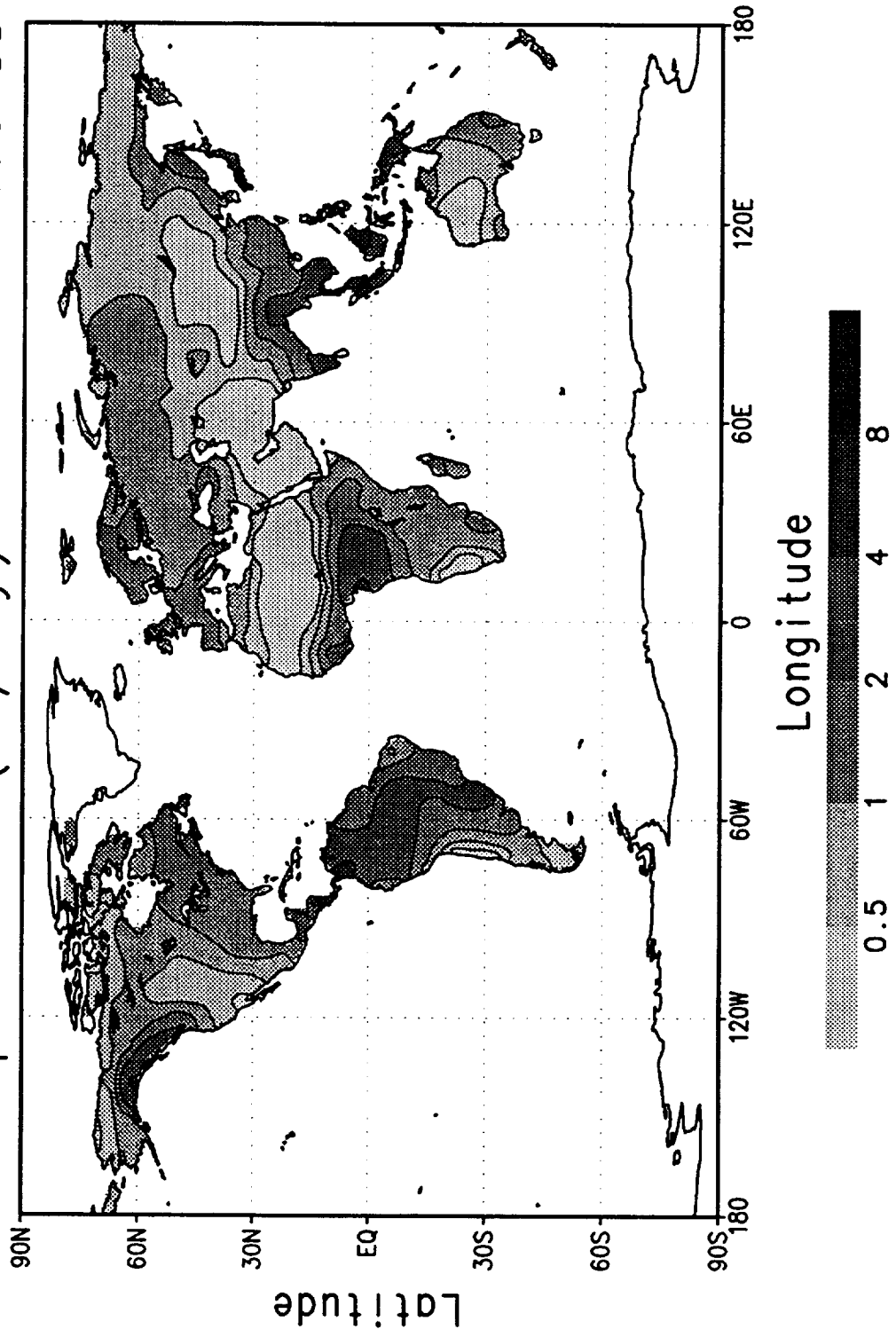
Precipitation (mm/day) September 1979-88



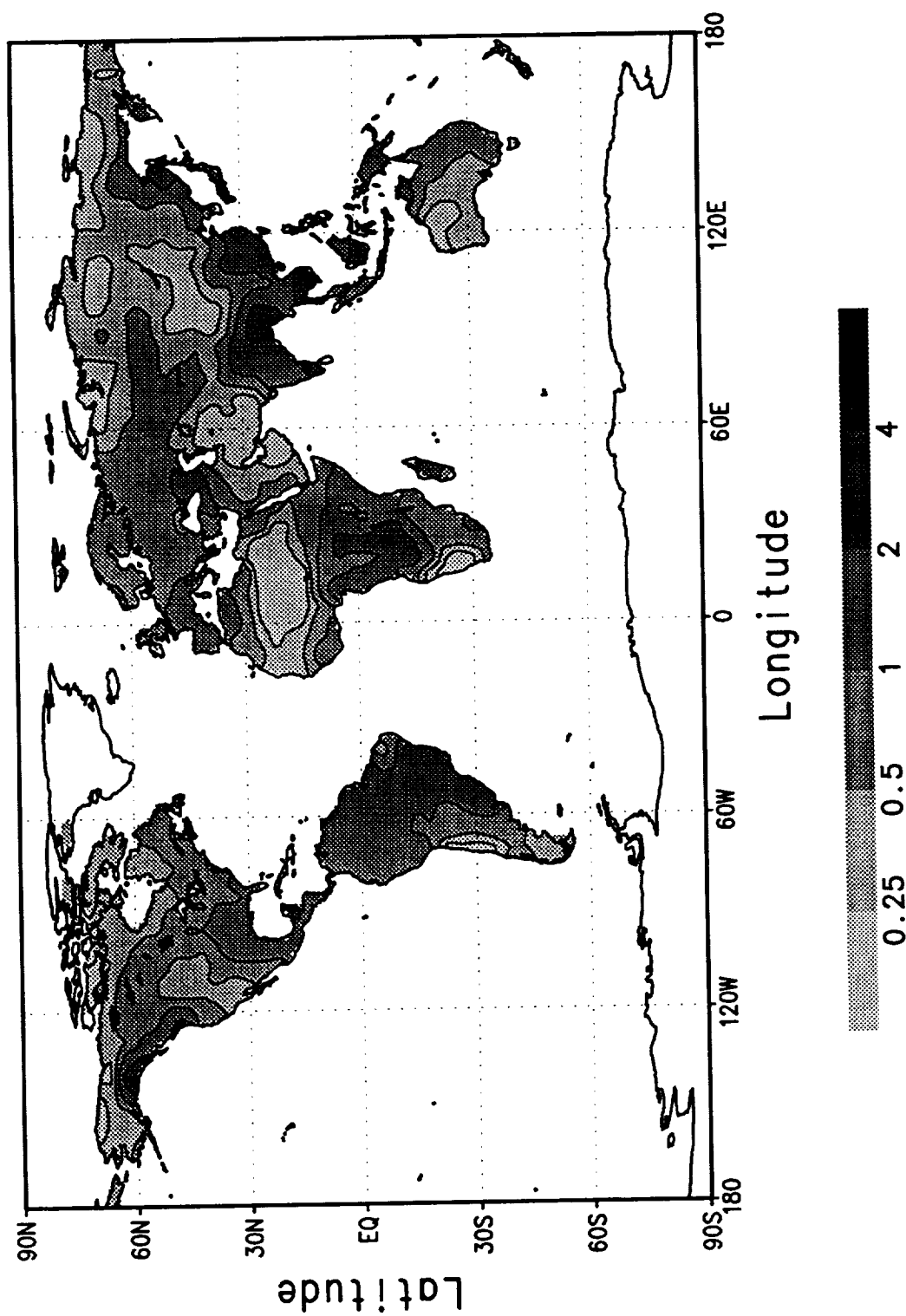
Precipitation Standard Deviation (mm/day)
September 1979-88



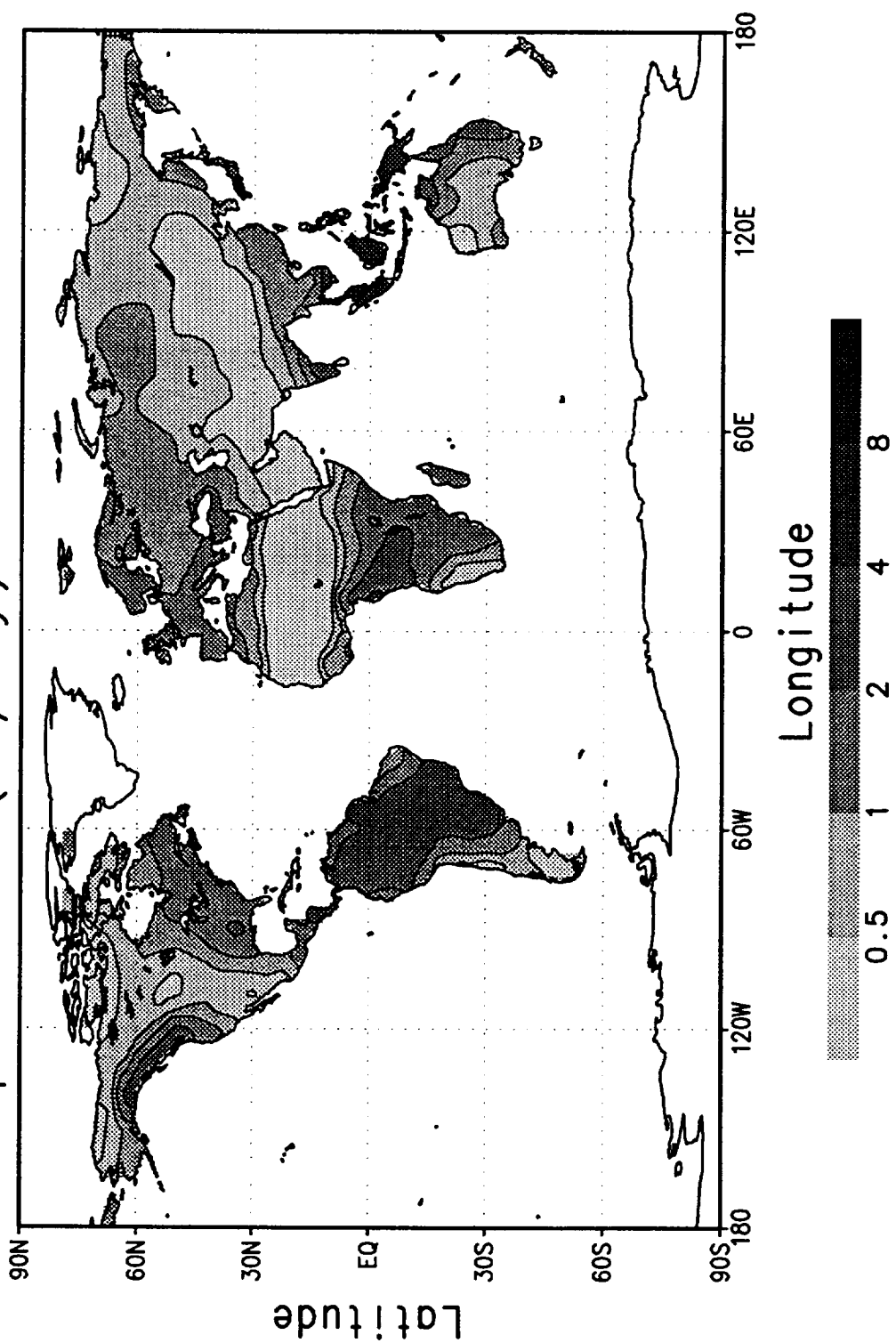
Precipitation (mm/day) October 1979–88



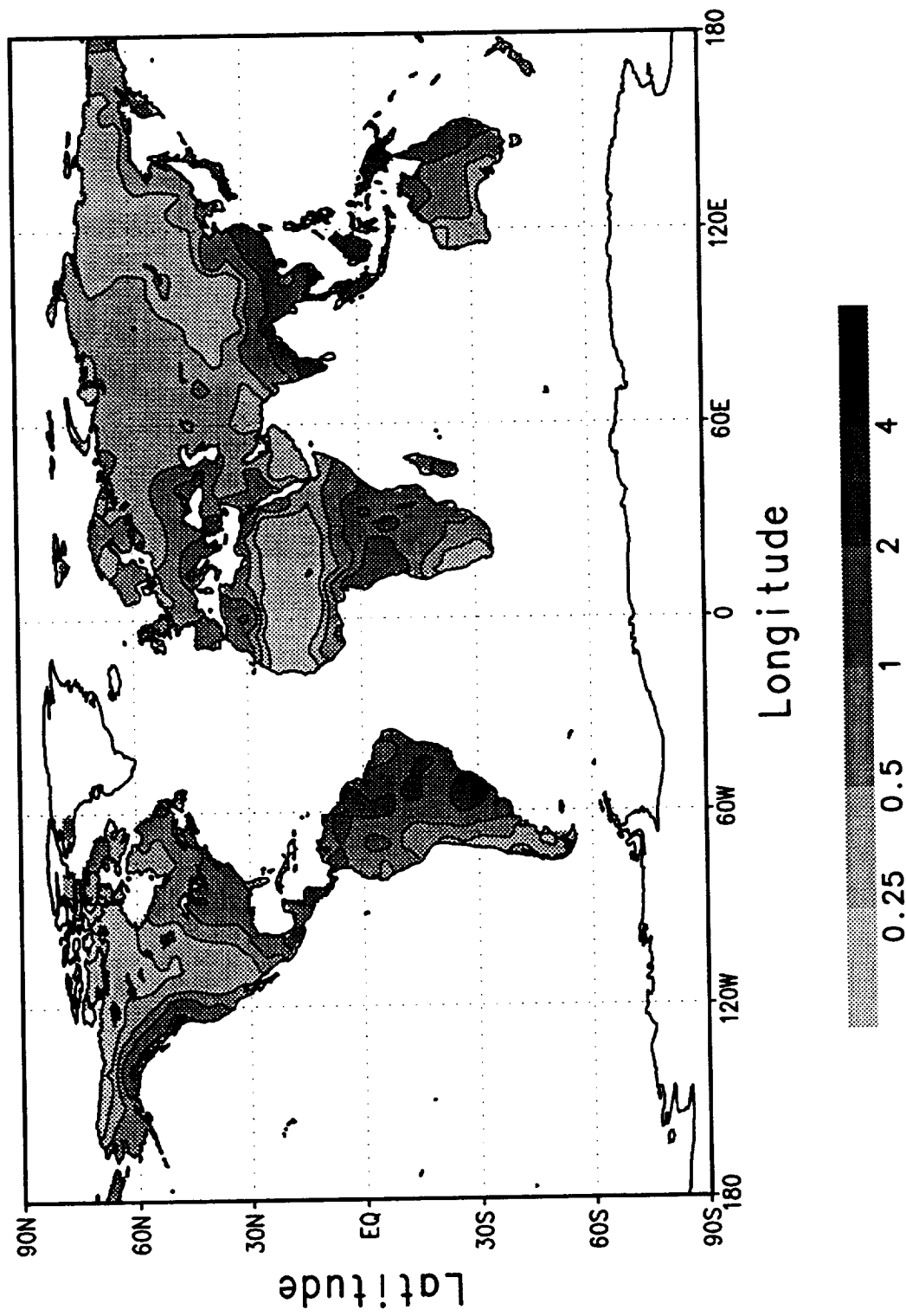
Precipitation Standard Deviation (mm/day)
October 1979-88



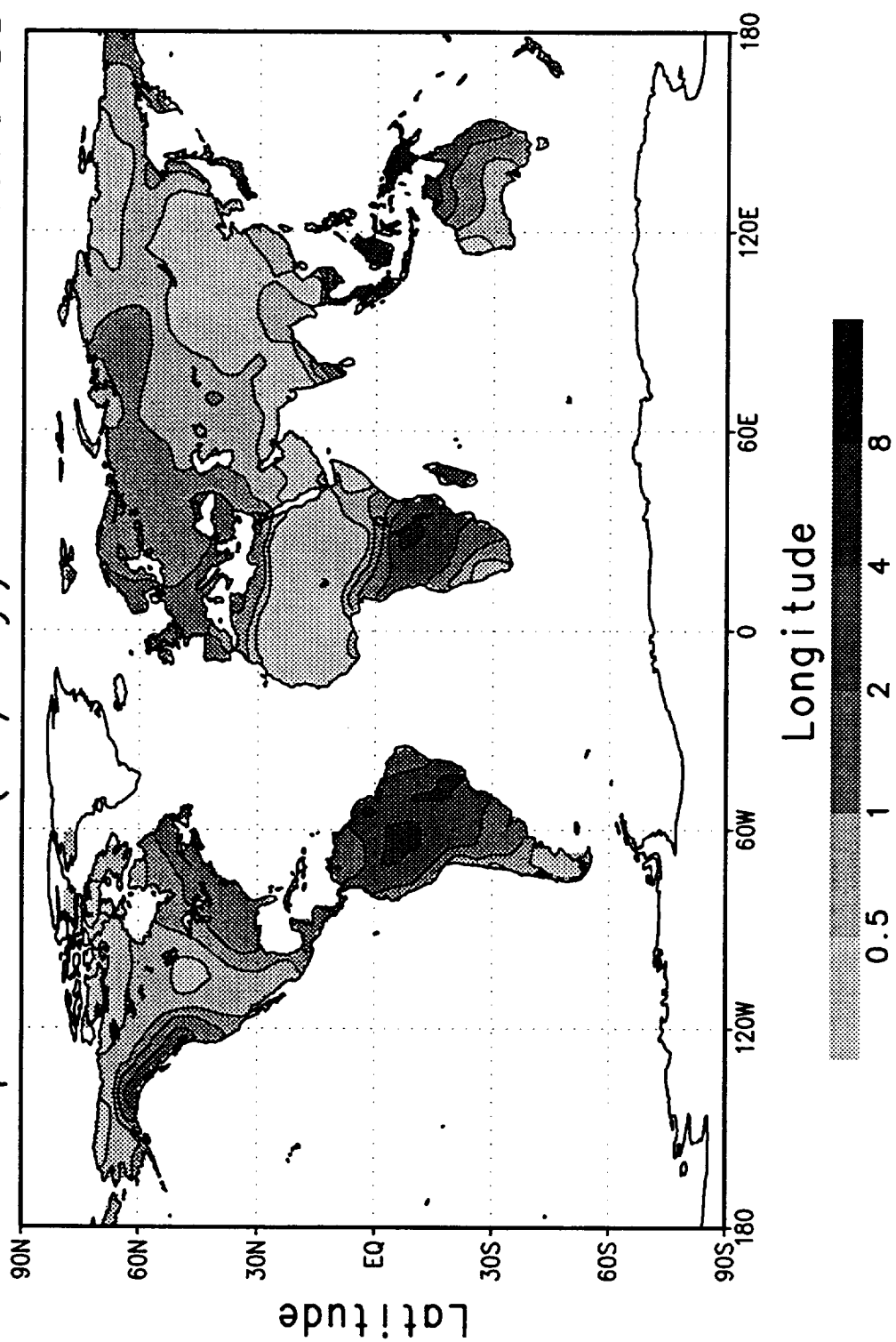
Precipitation (mm/day) November 1979–88



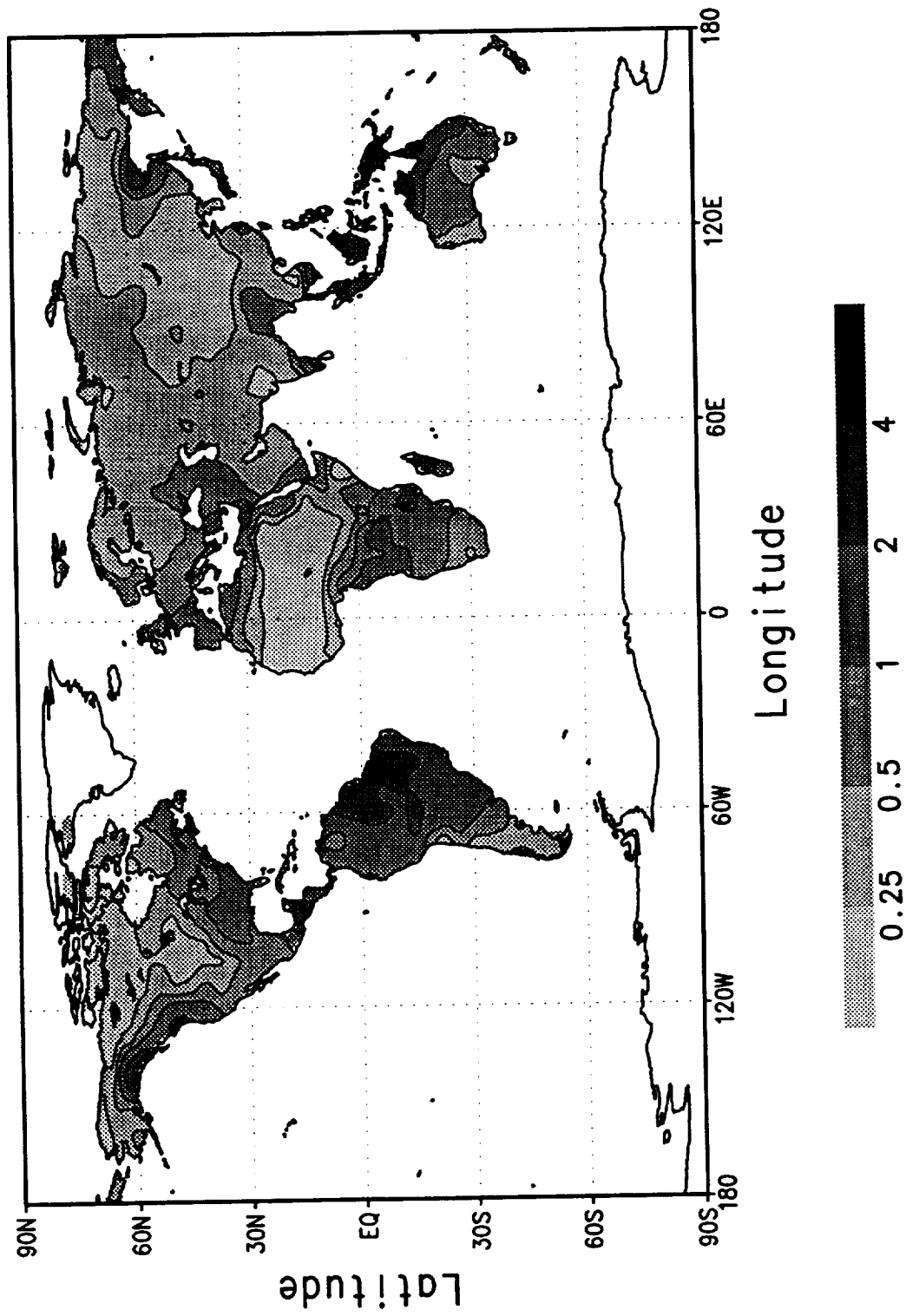
Precipitation Standard Deviation (mm/day)
November 1979-88



Precipitation (mm/day) December 1979–88



Precipitation Standard Deviation (mm/day)
December 1979-88

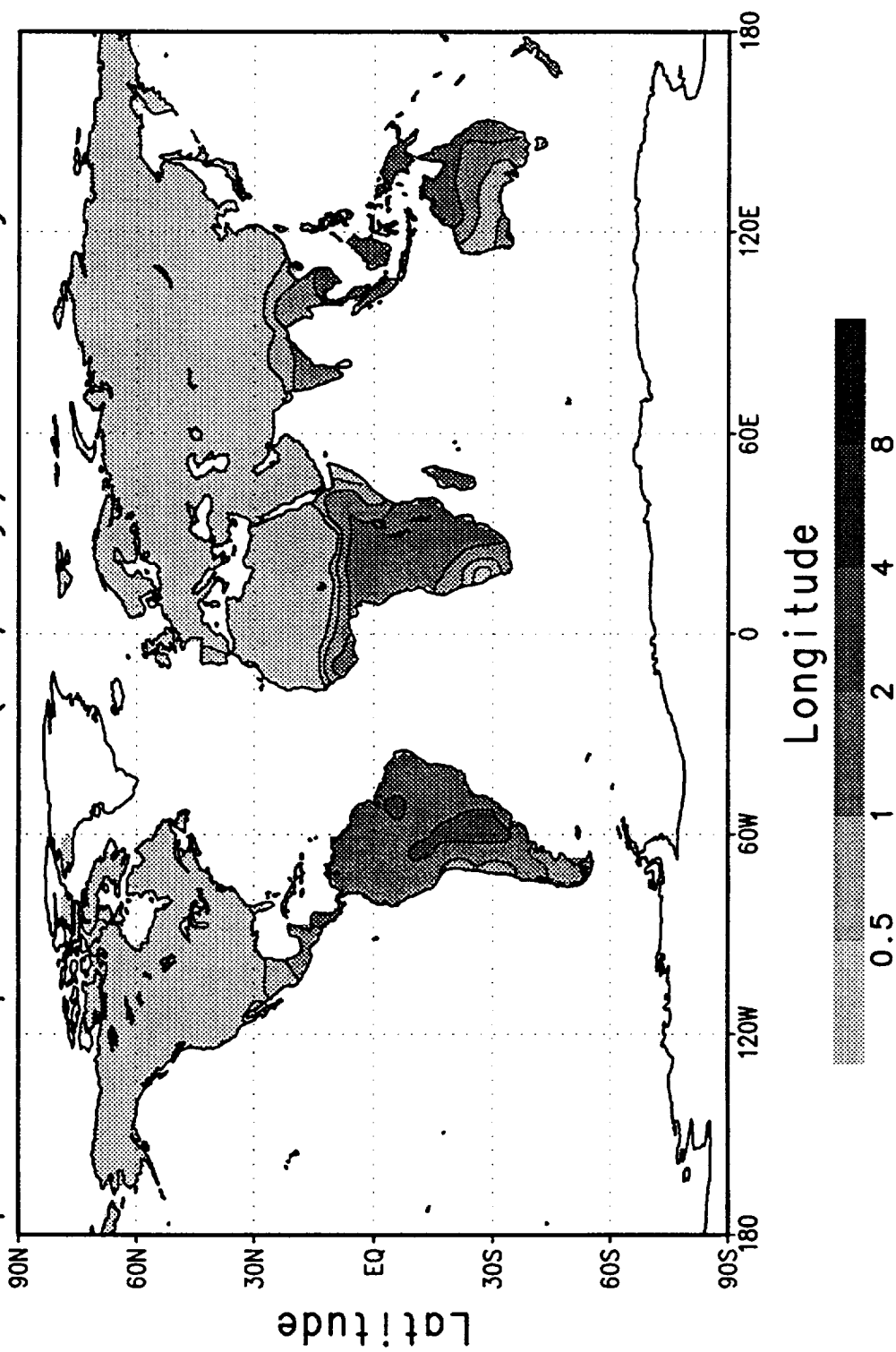


EVAPOTRANSPIRATION

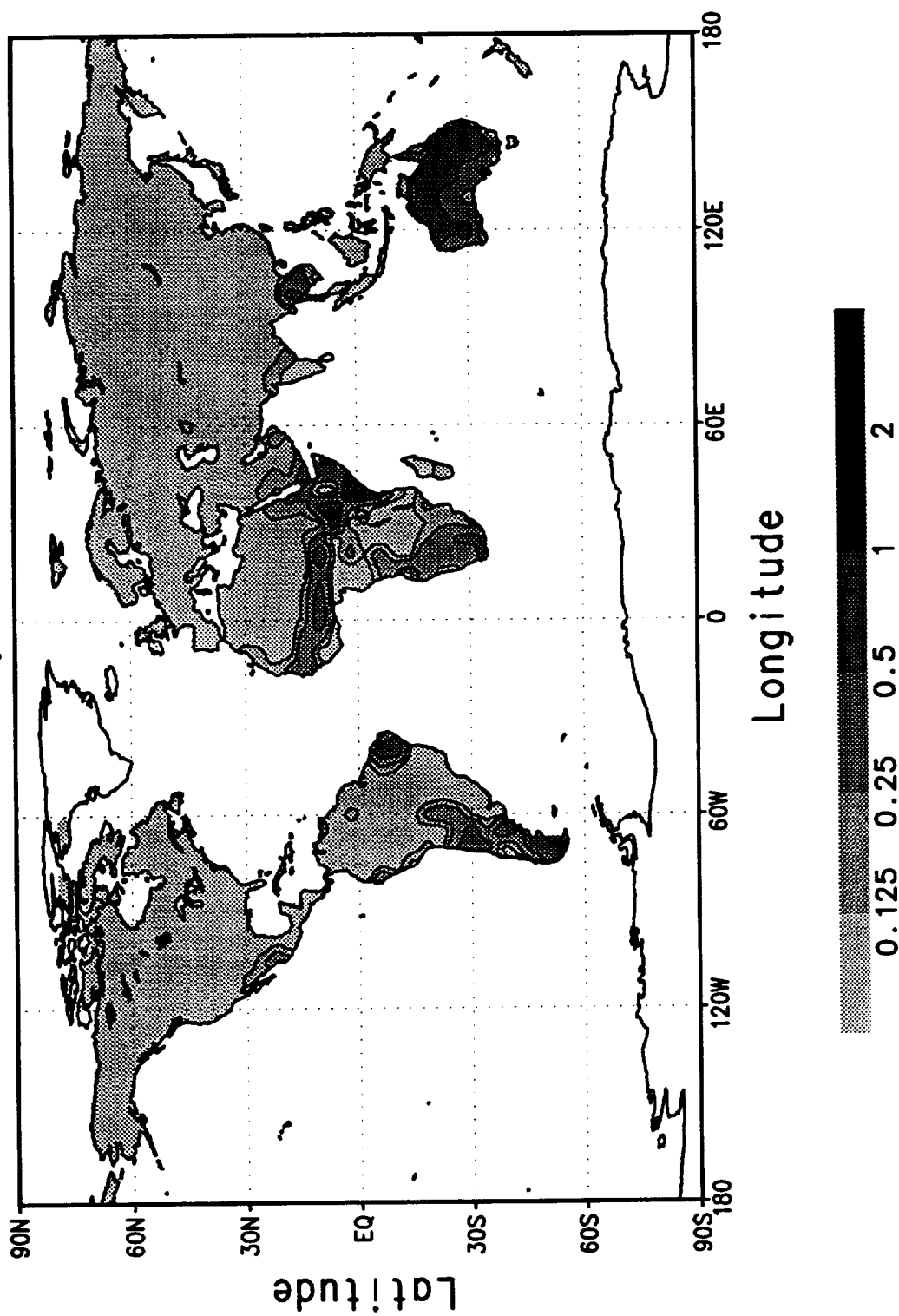
(January - December)

Ten-year average (1979 - 1988) of the monthly mean evapotranspiration (mm day^{-1}), computed from soil moisture initialization scheme. Also plotted are the standard deviations of the monthly mean fields as determined from the 10-year data set.

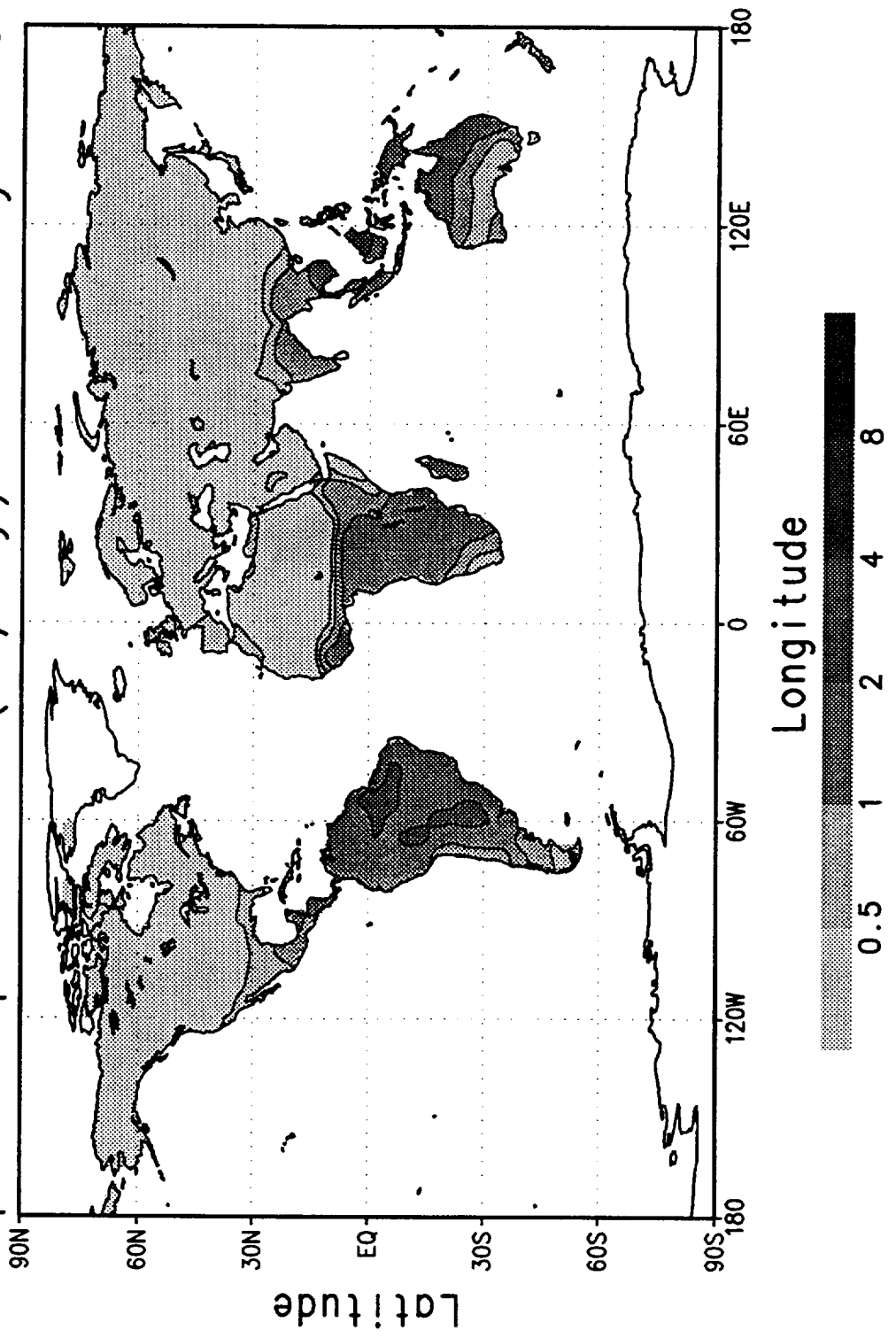
Evapotranspiration (mm/day) January 1979-88



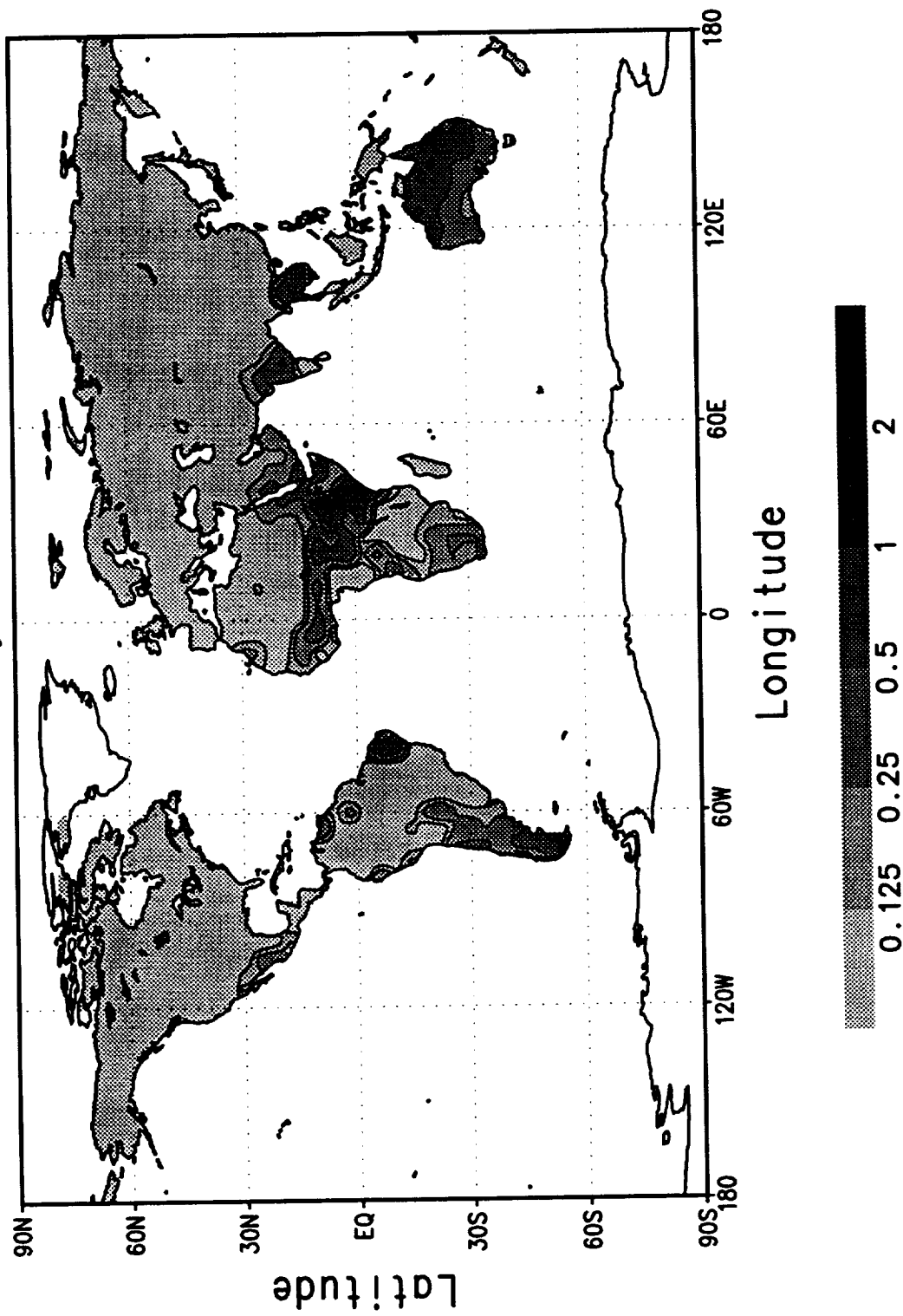
Evapotranspiration Standard Deviation (mm/day)
January 1979-88



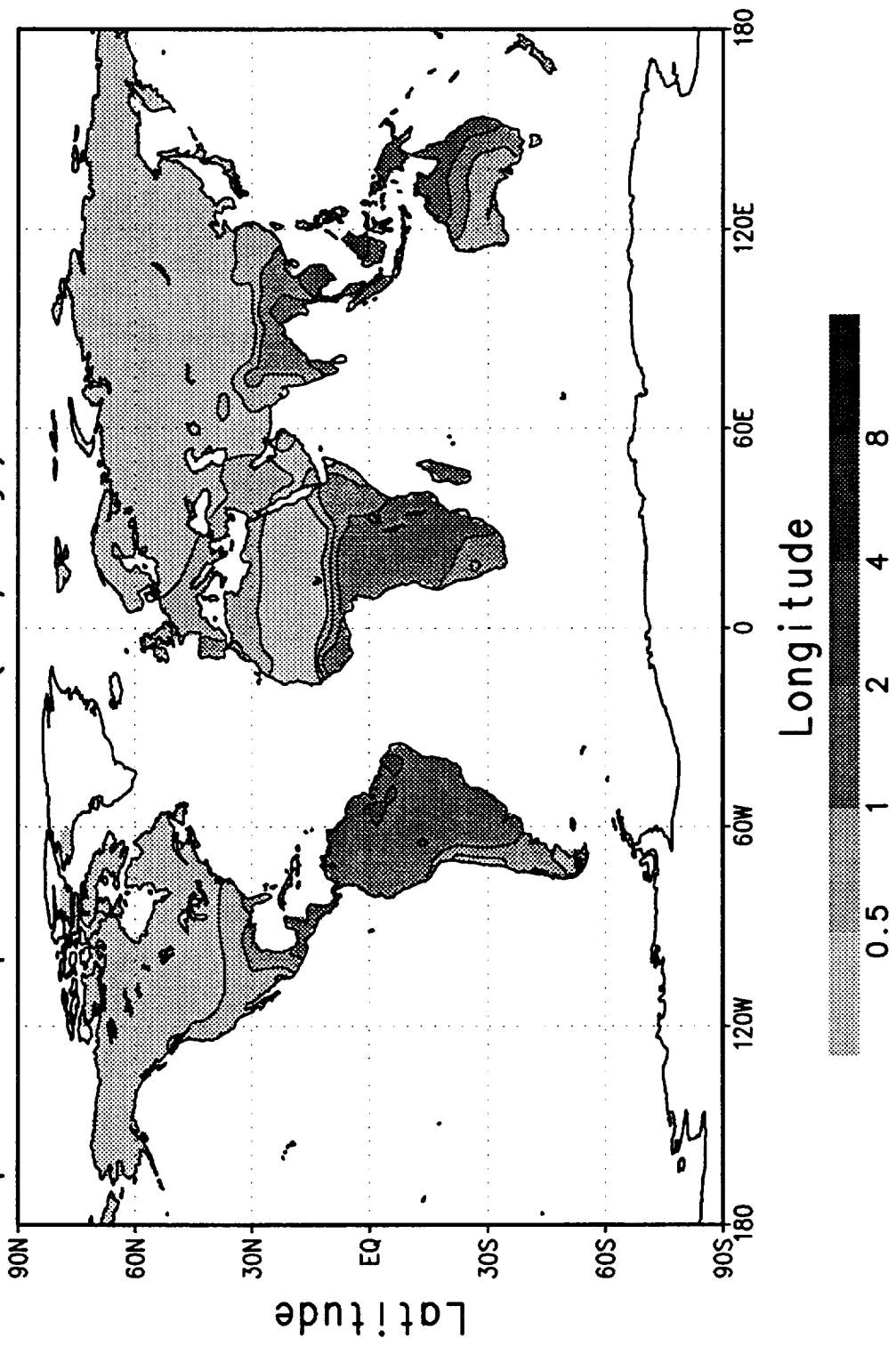
Evapotranspiration (mm/day) February 1979-88



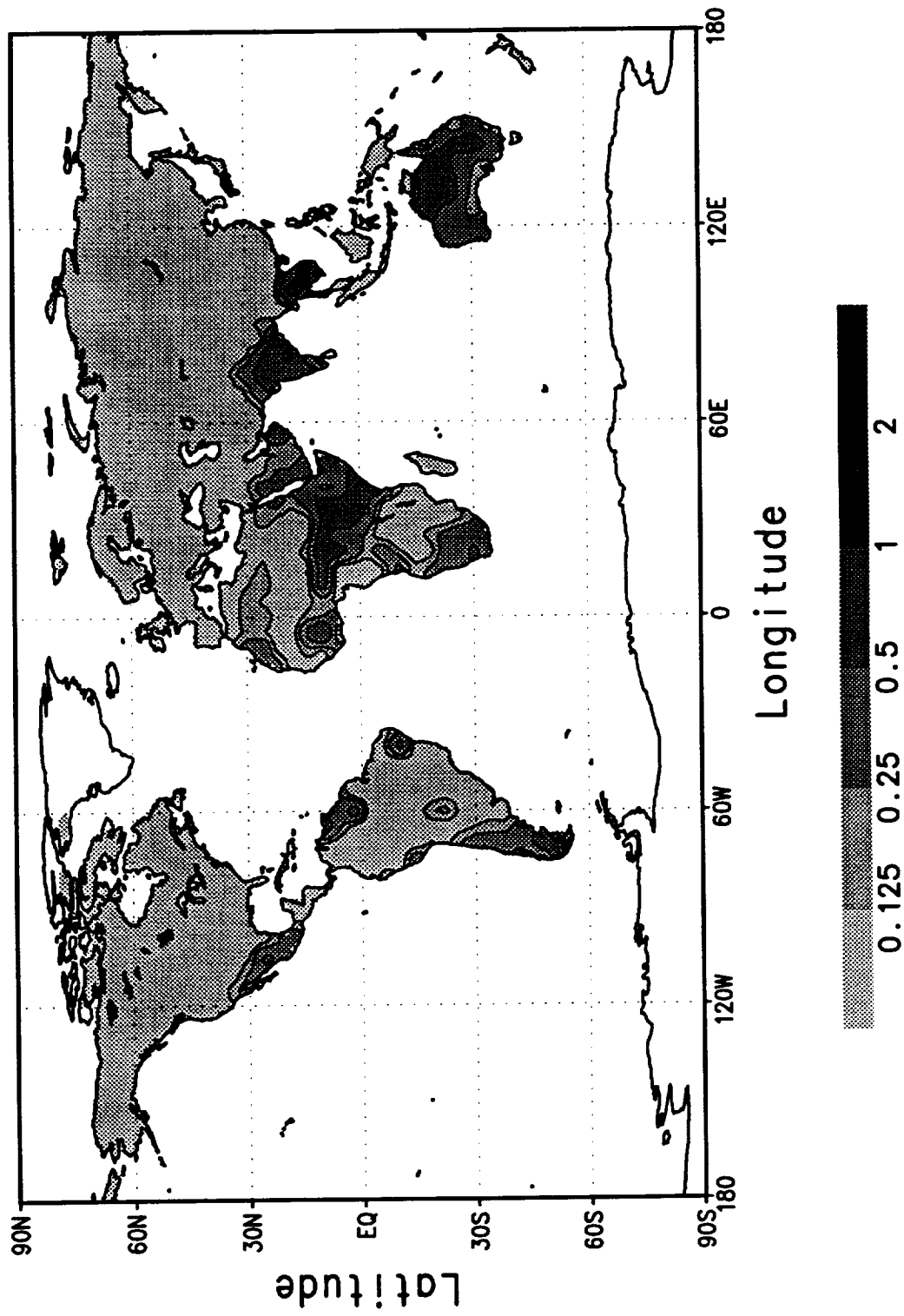
Evapotranspiration Standard Deviation (mm/day)
February 1979-88



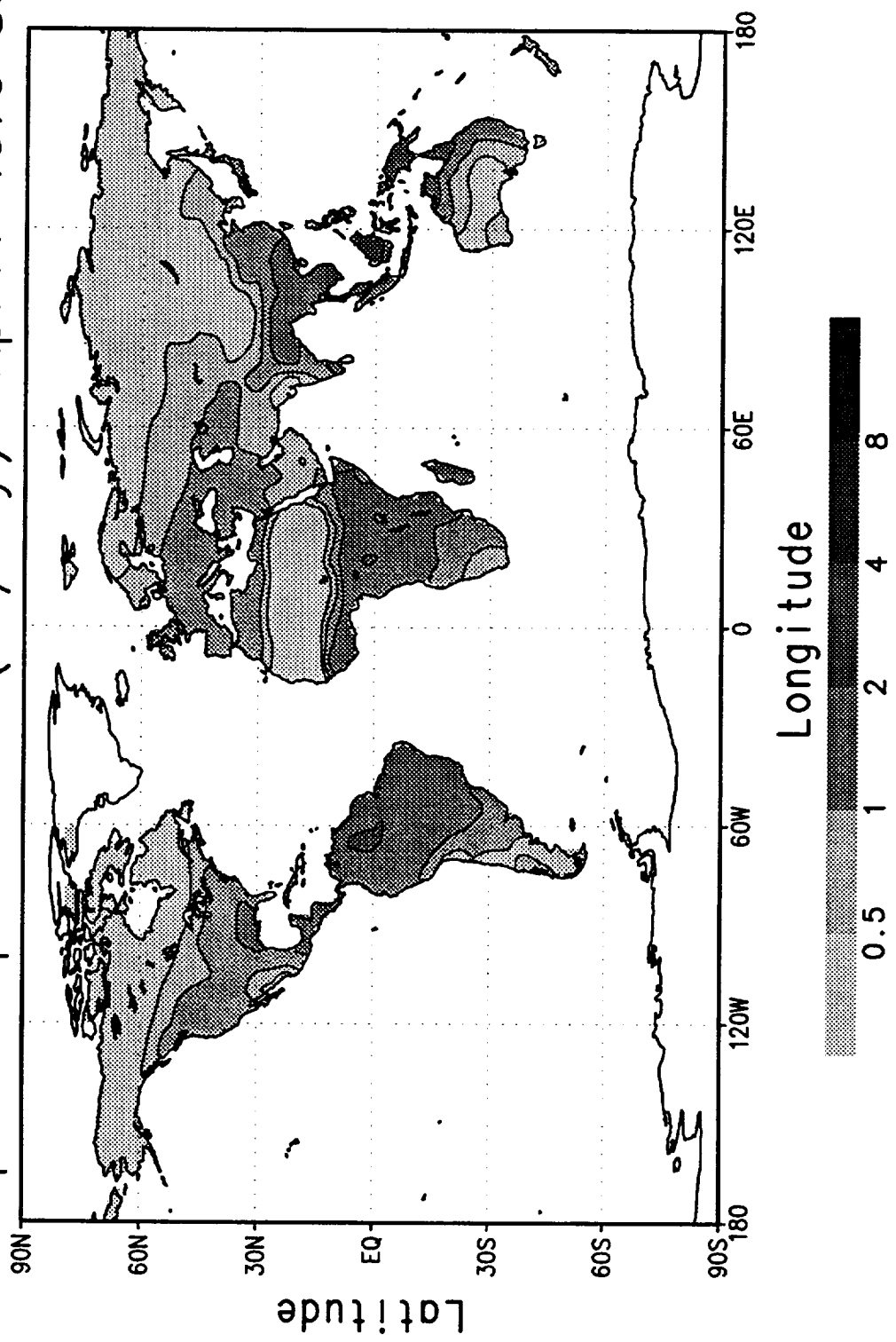
Evapotranspiration (mm/day) March 1979–88



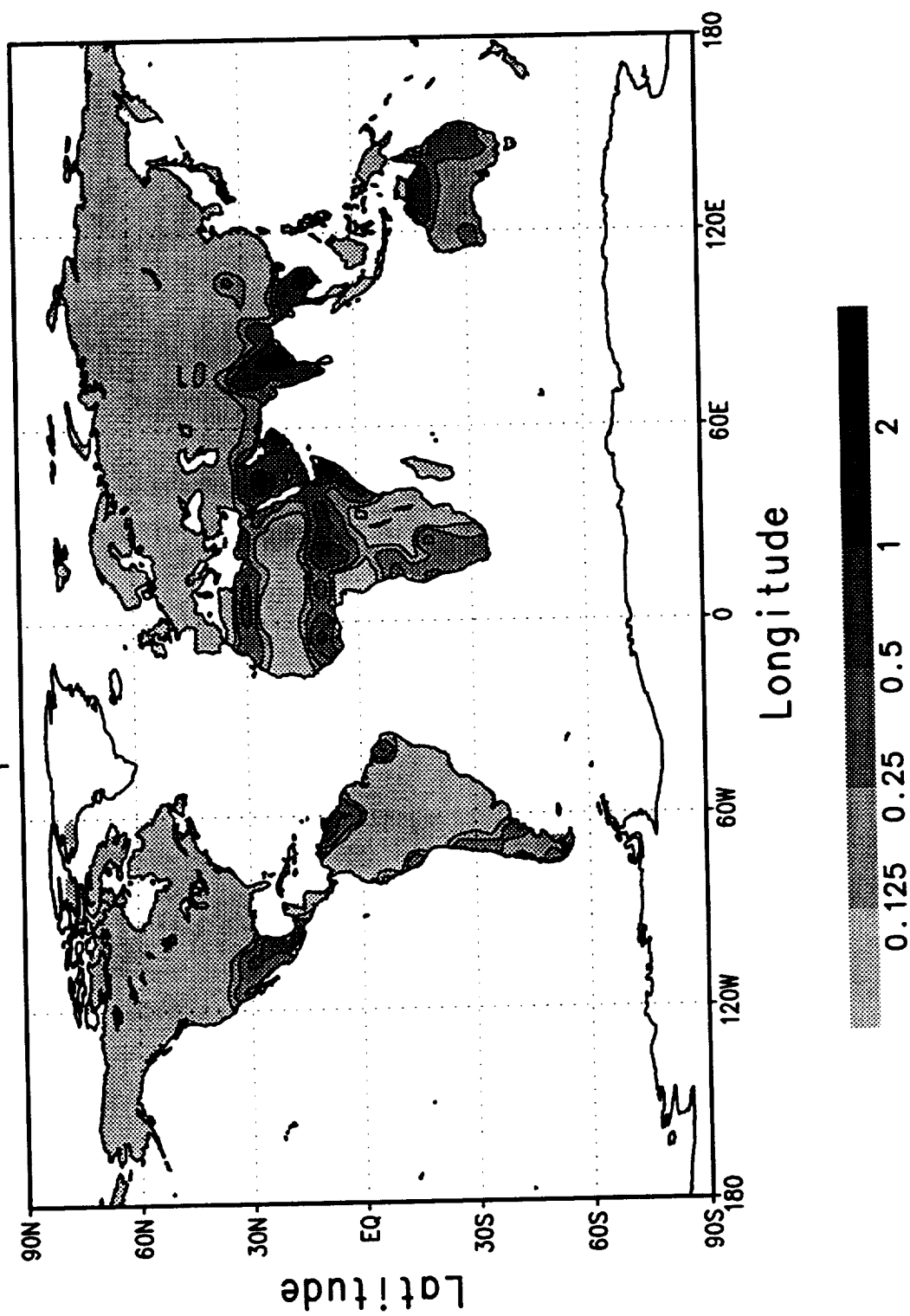
Evapotranspiration Standard Deviation (mm/day)
March 1979-88



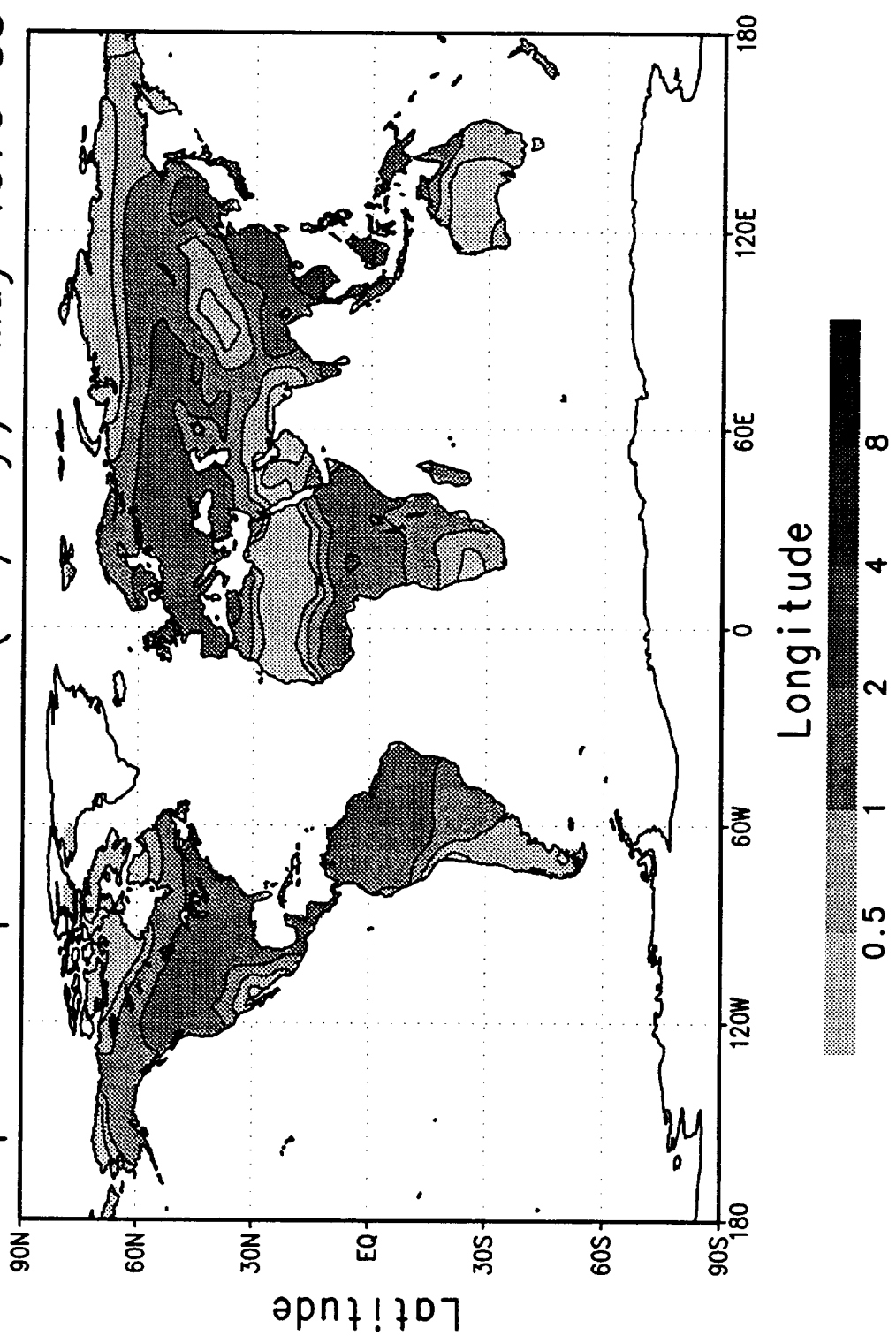
Evapotranspiration (mm/day) April 1979-88



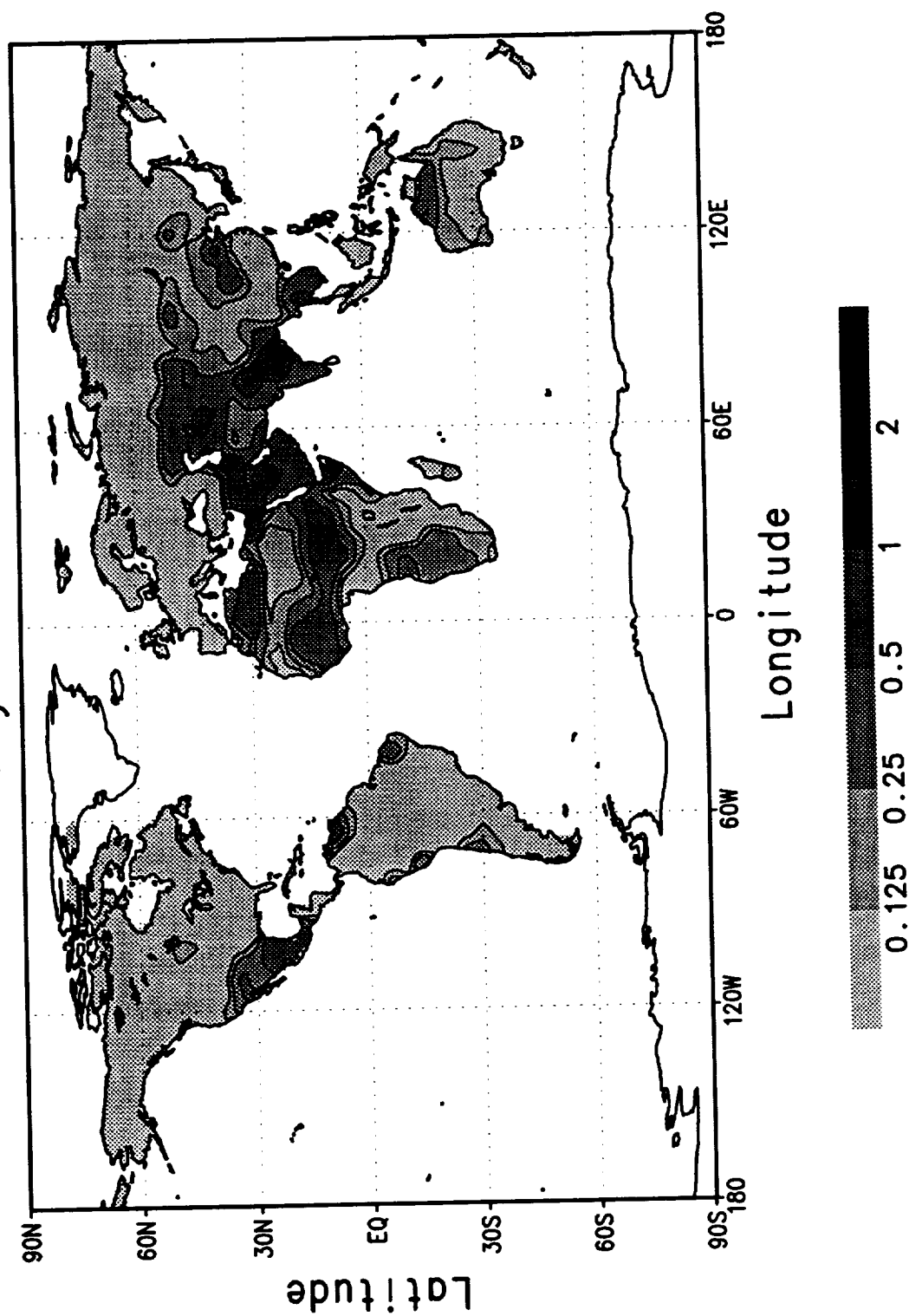
Evapotranspiration Standard Deviation (mm/day)
April 1979-88



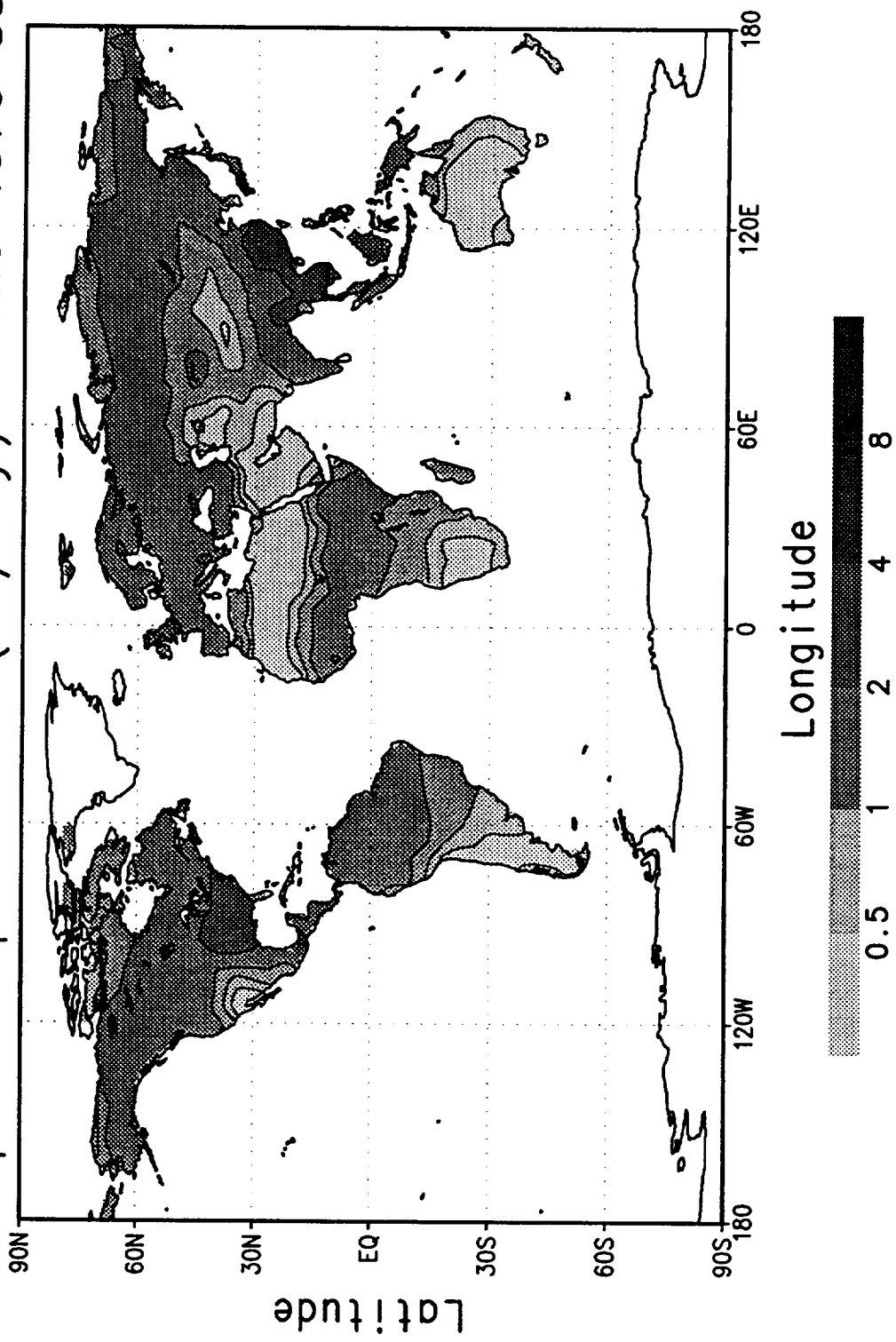
Evapotranspiration (mm/day) May 1979-88



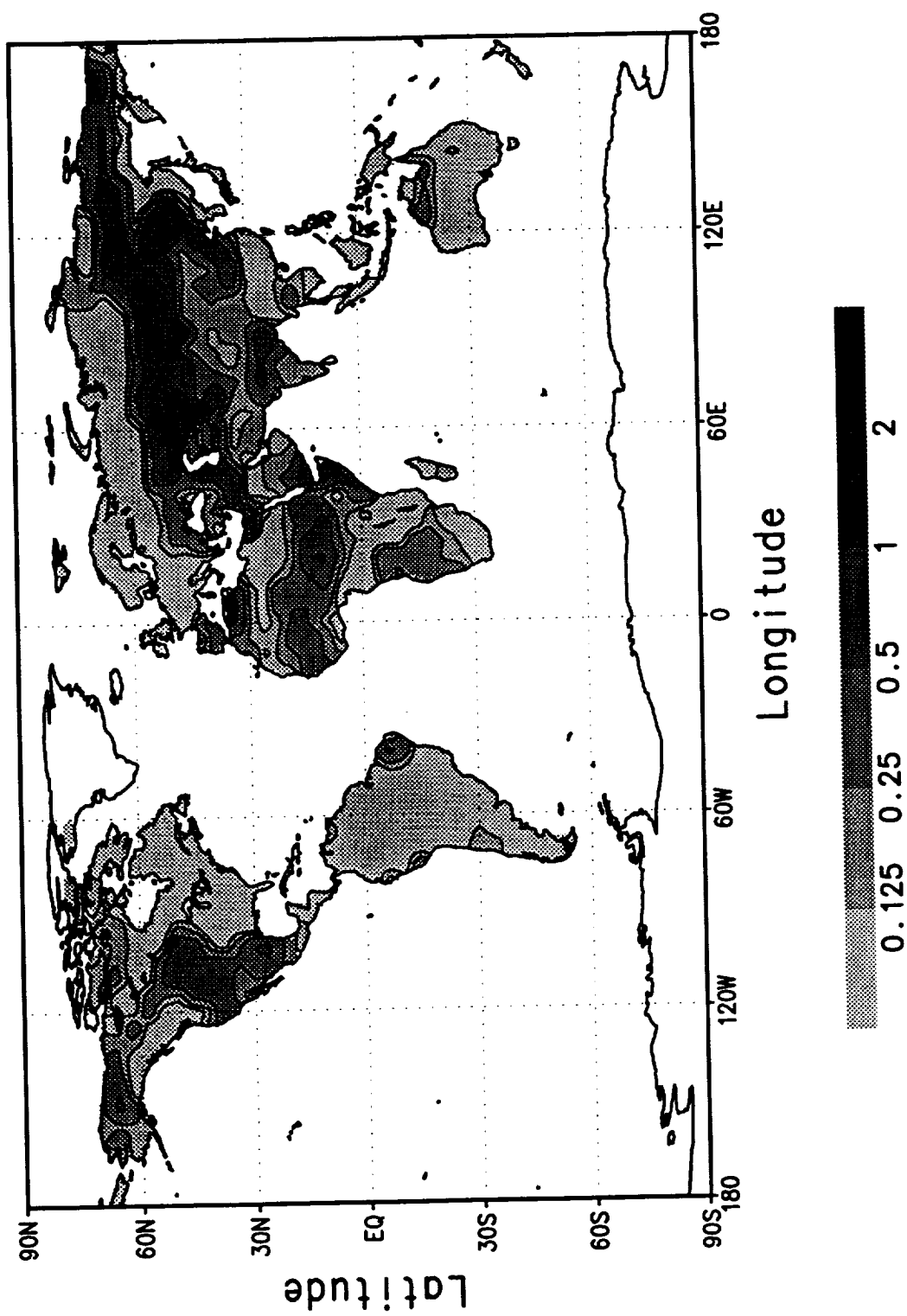
Evapotranspiration Standard Deviation (mm/day)
May 1979-88



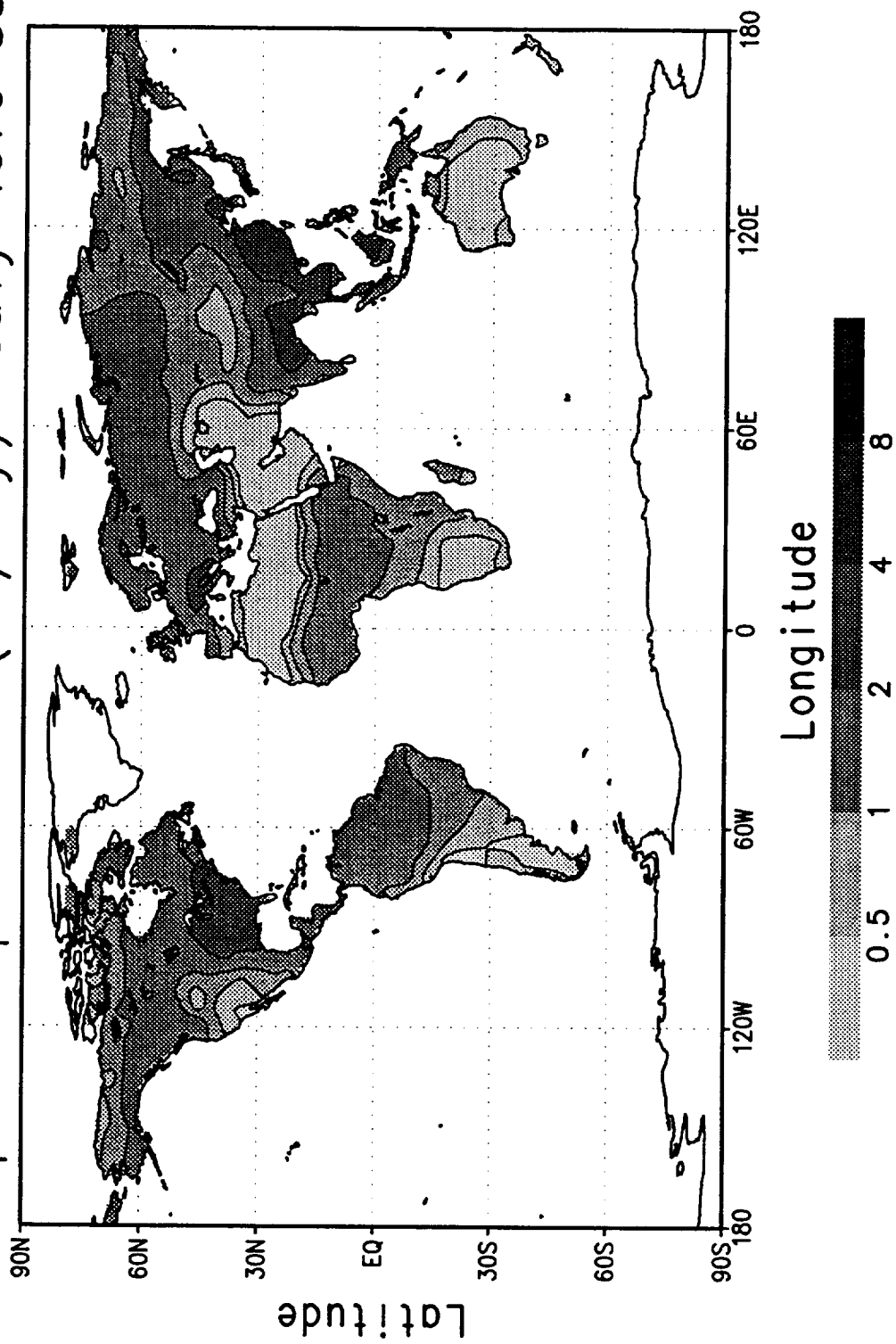
Evapotranspiration (mm/day) June 1979-88



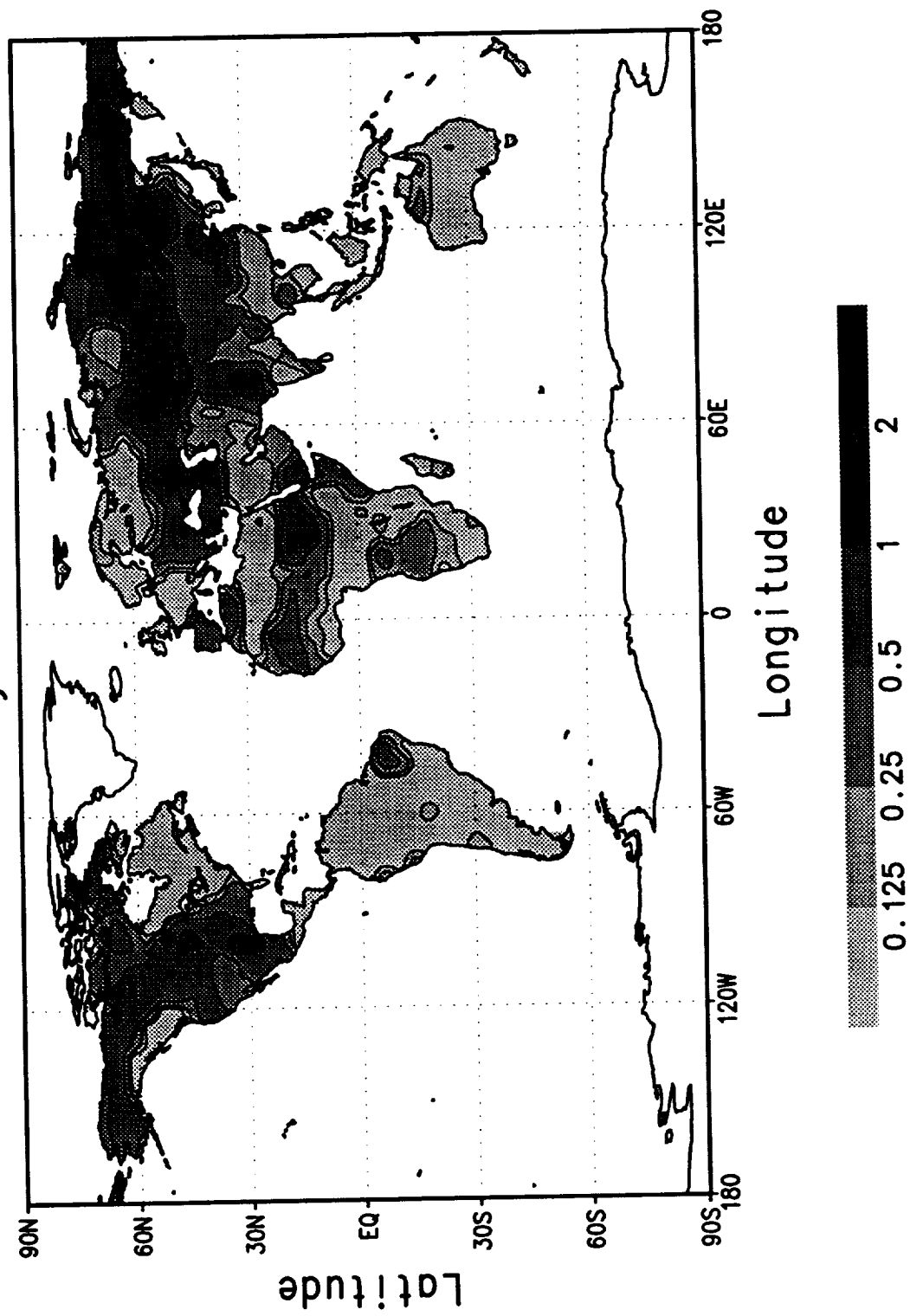
Evapotranspiration Standard Deviation (mm/day)
June 1979-88



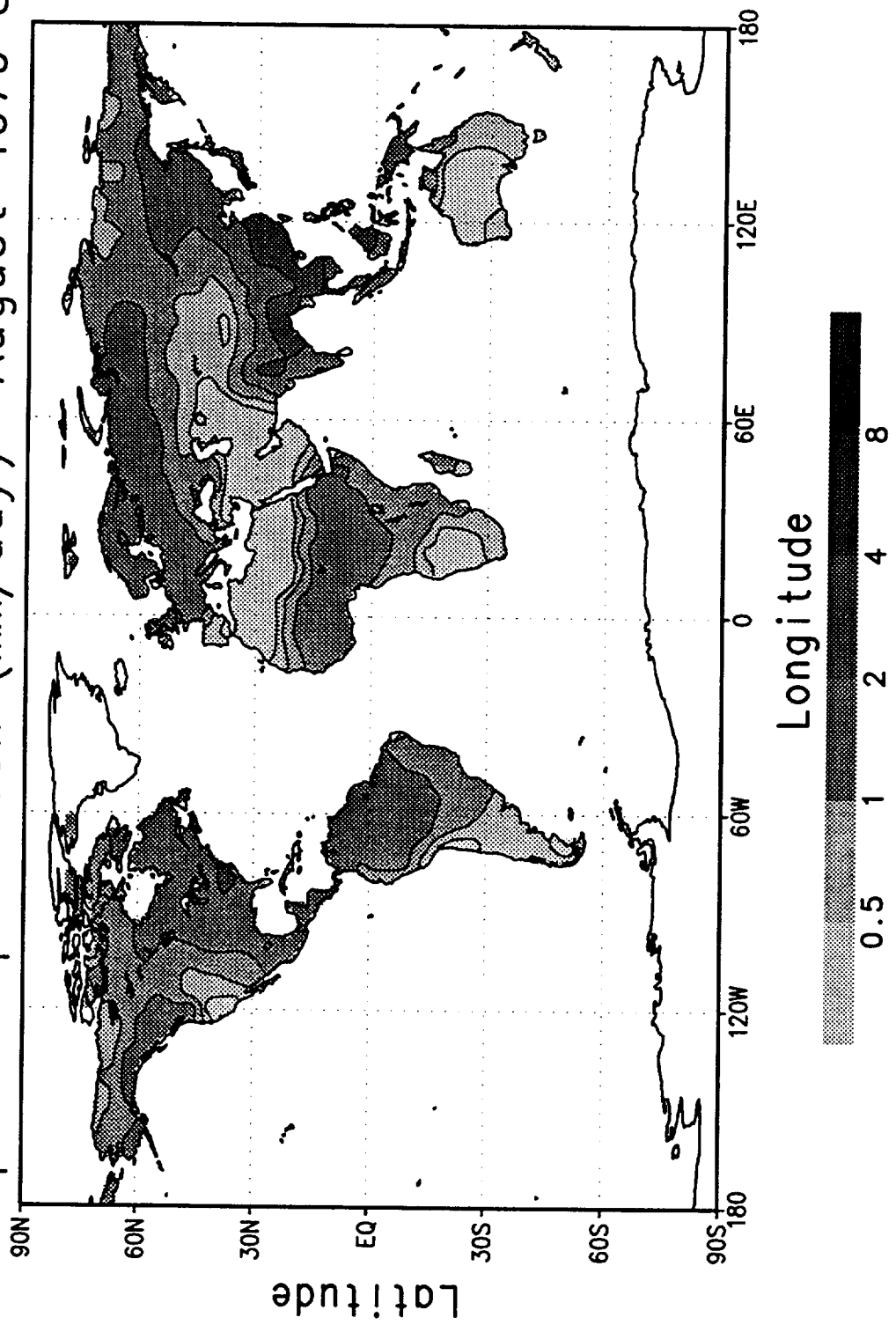
Evapotranspiration (mm/day) July 1979-88



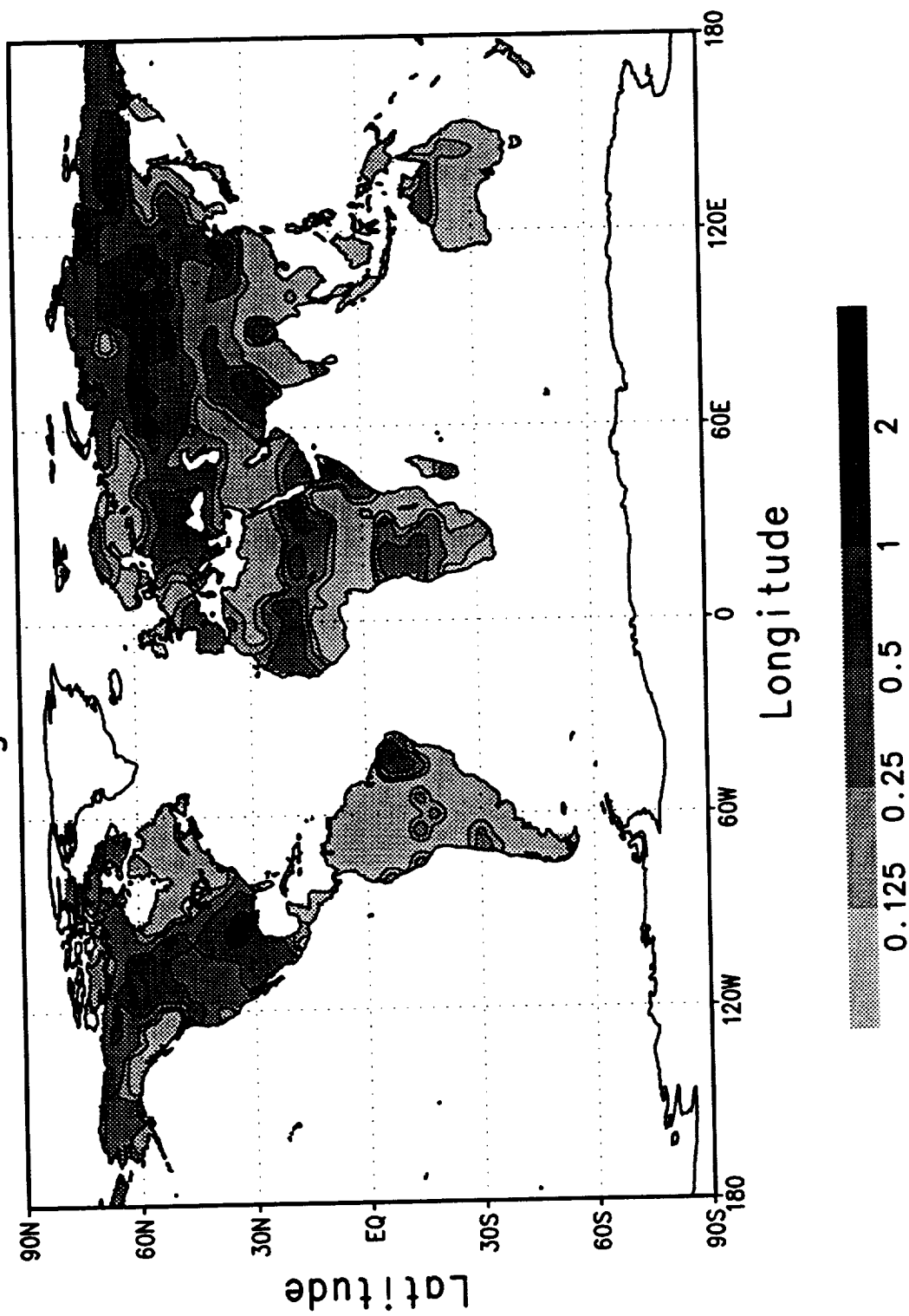
Evapotranspiration Standard Deviation (mm/day)
July 1979-88



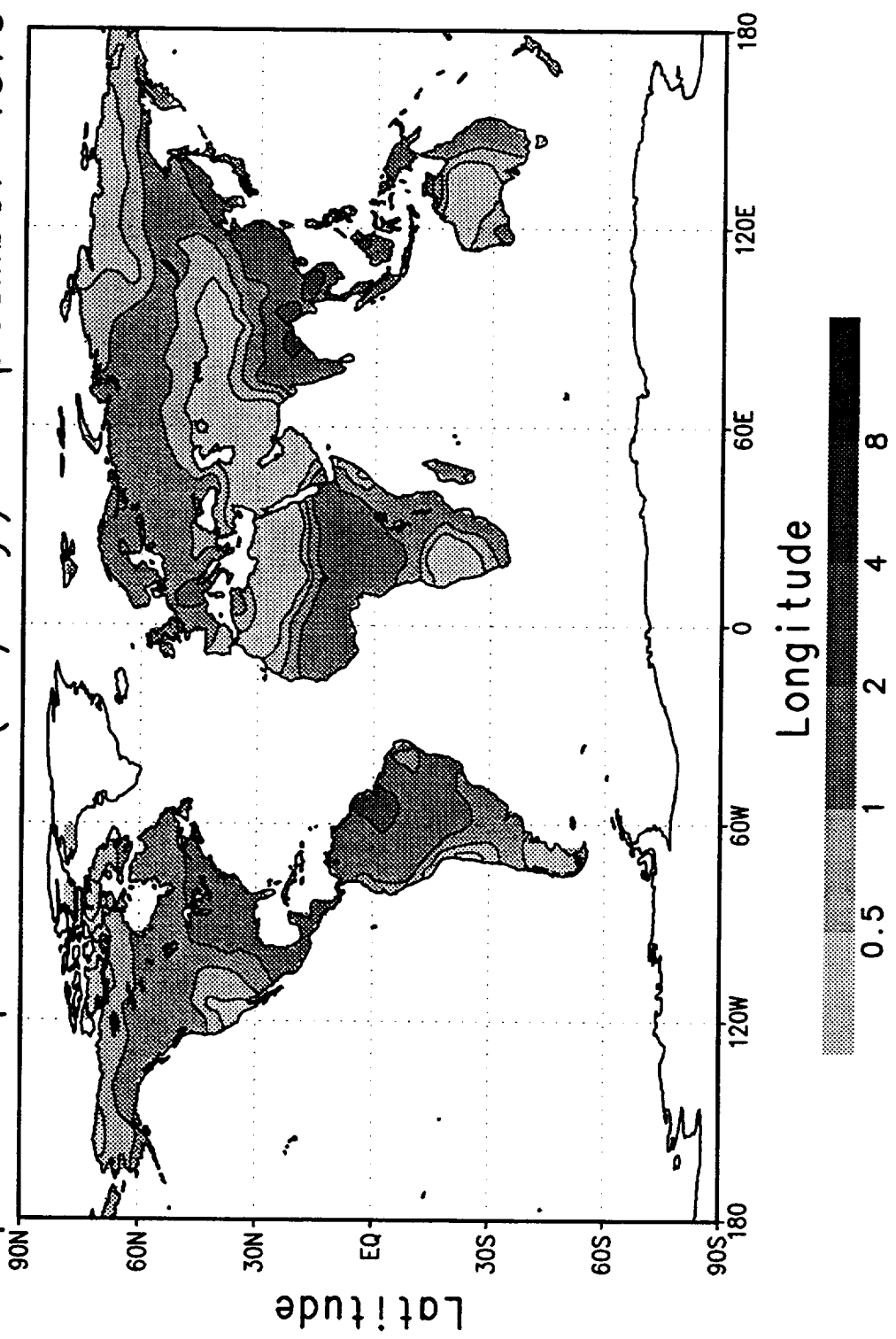
Evapotranspiration (mm/day) August 1979-88



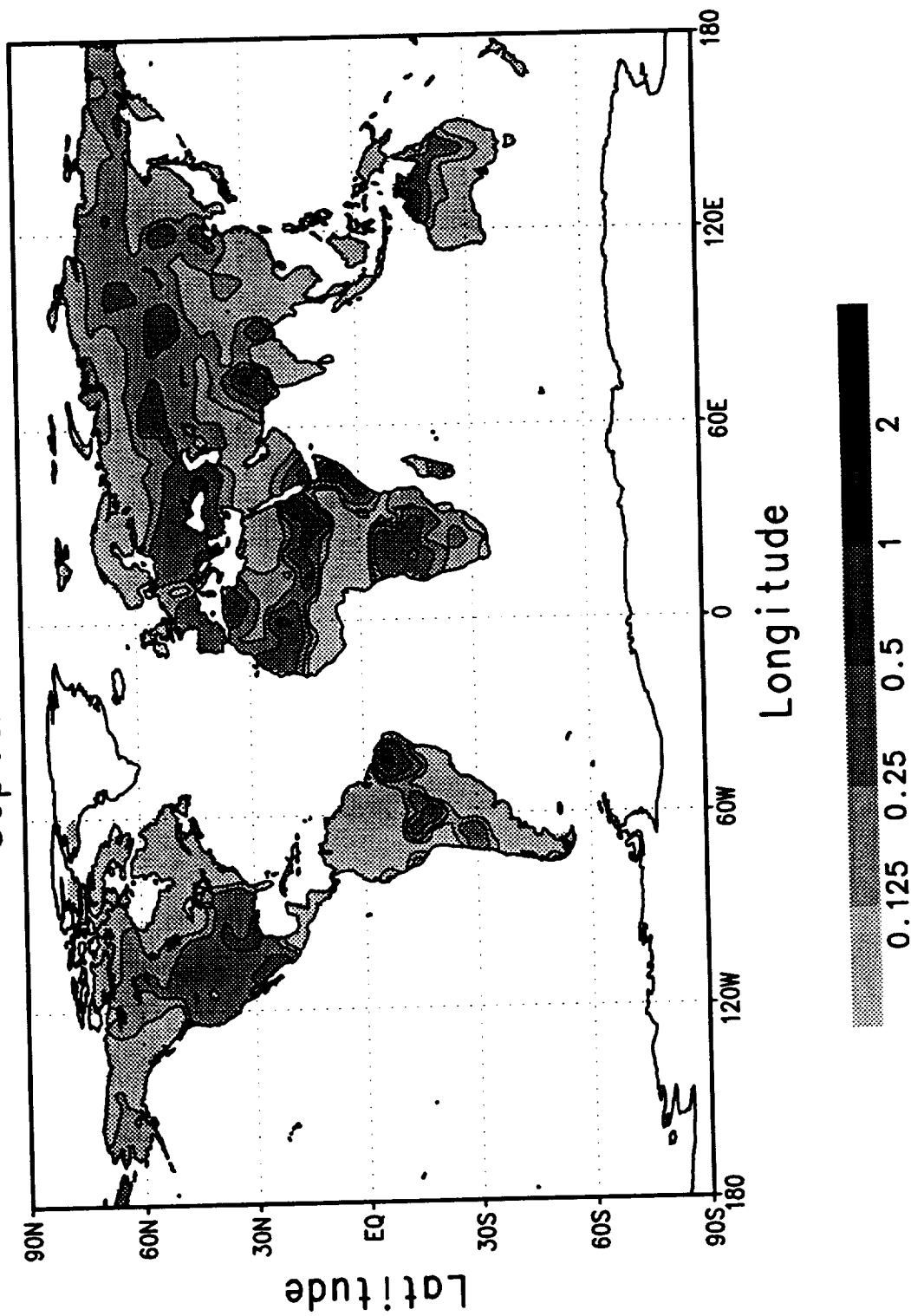
Evapotranspiration Standard Deviation (mm/day)
August 1979-88



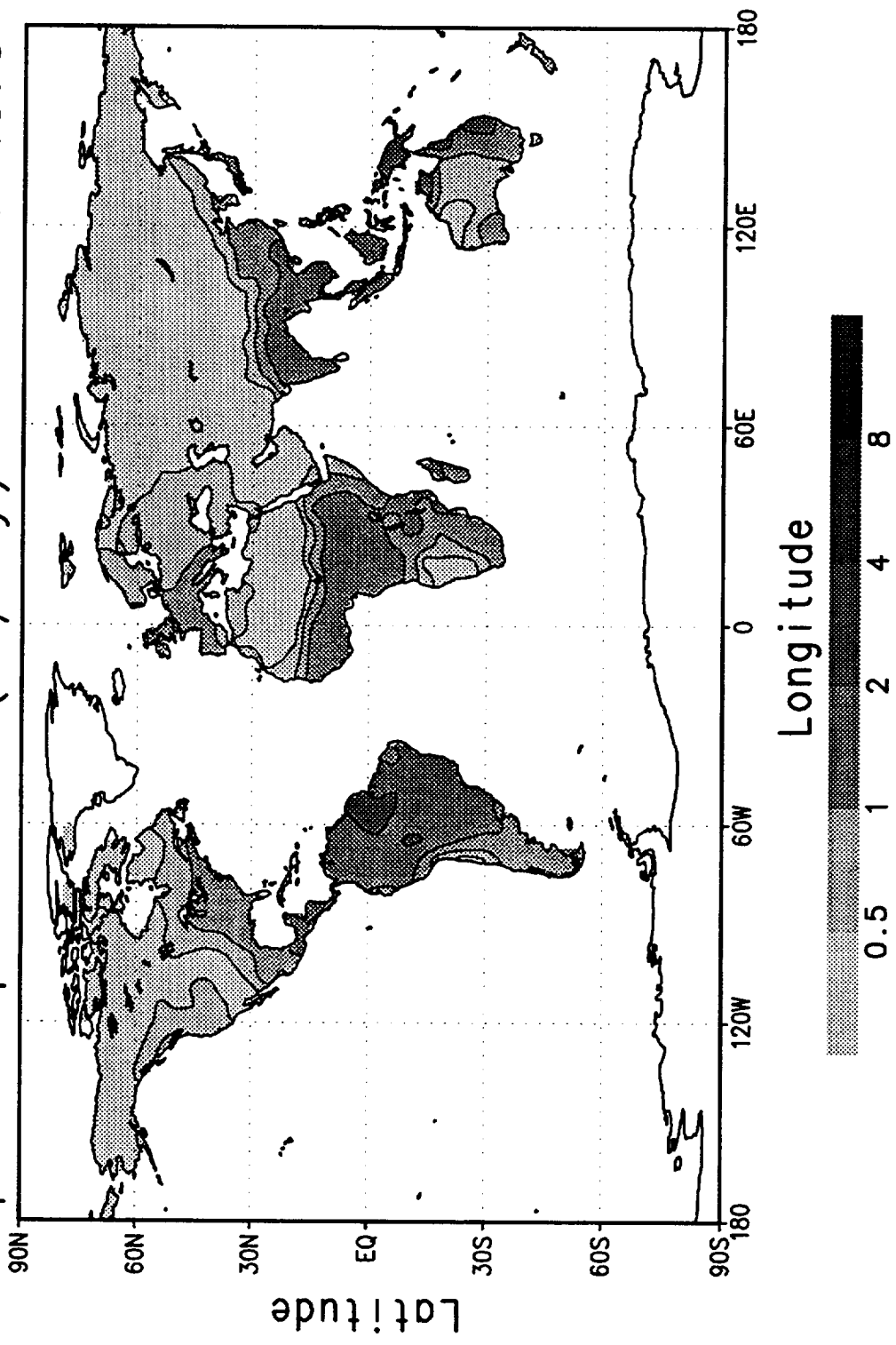
Evapotranspiration (mm/day) September 1979–88



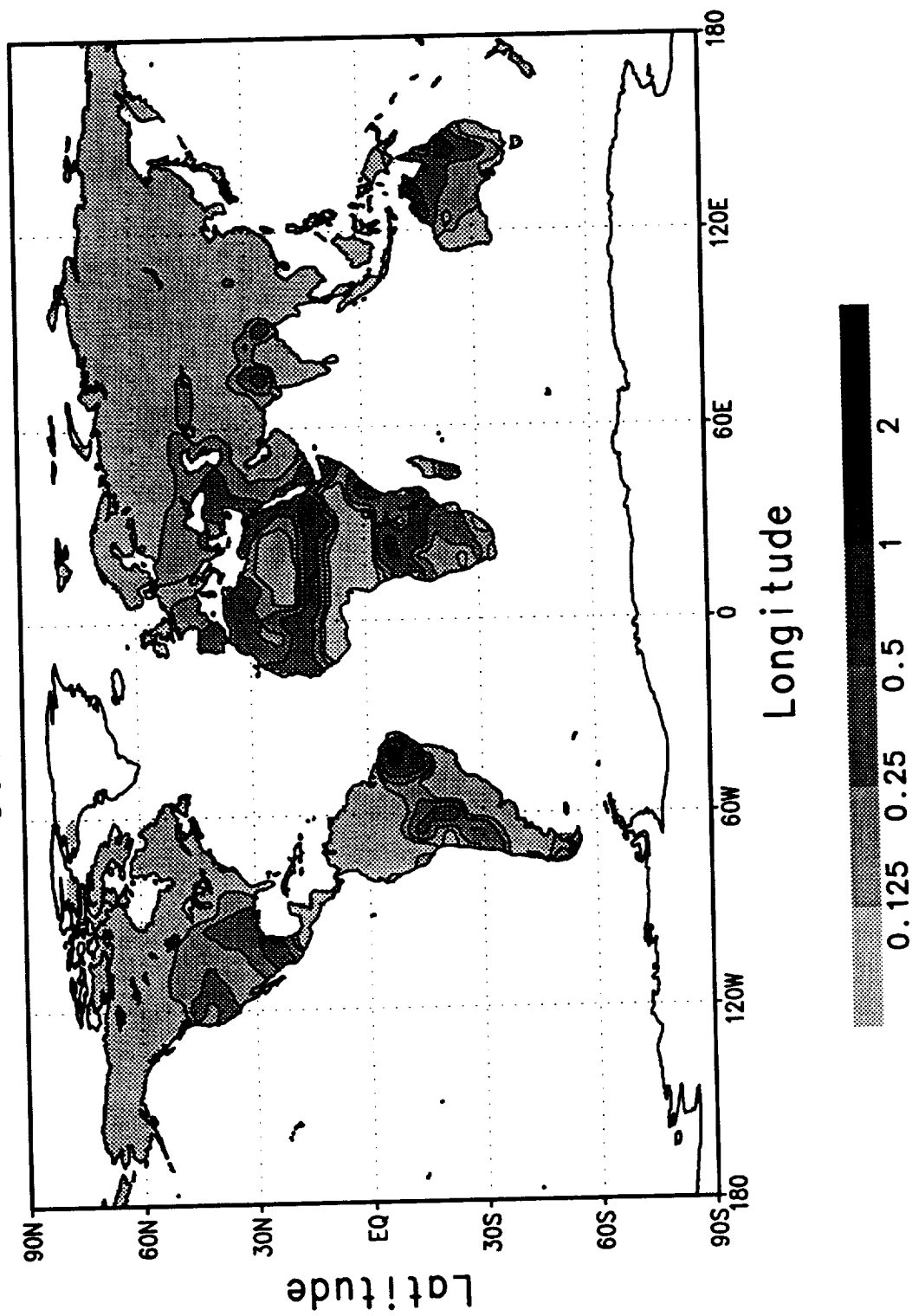
Evapotranspiration Standard Deviation (mm/day)
September 1979-88



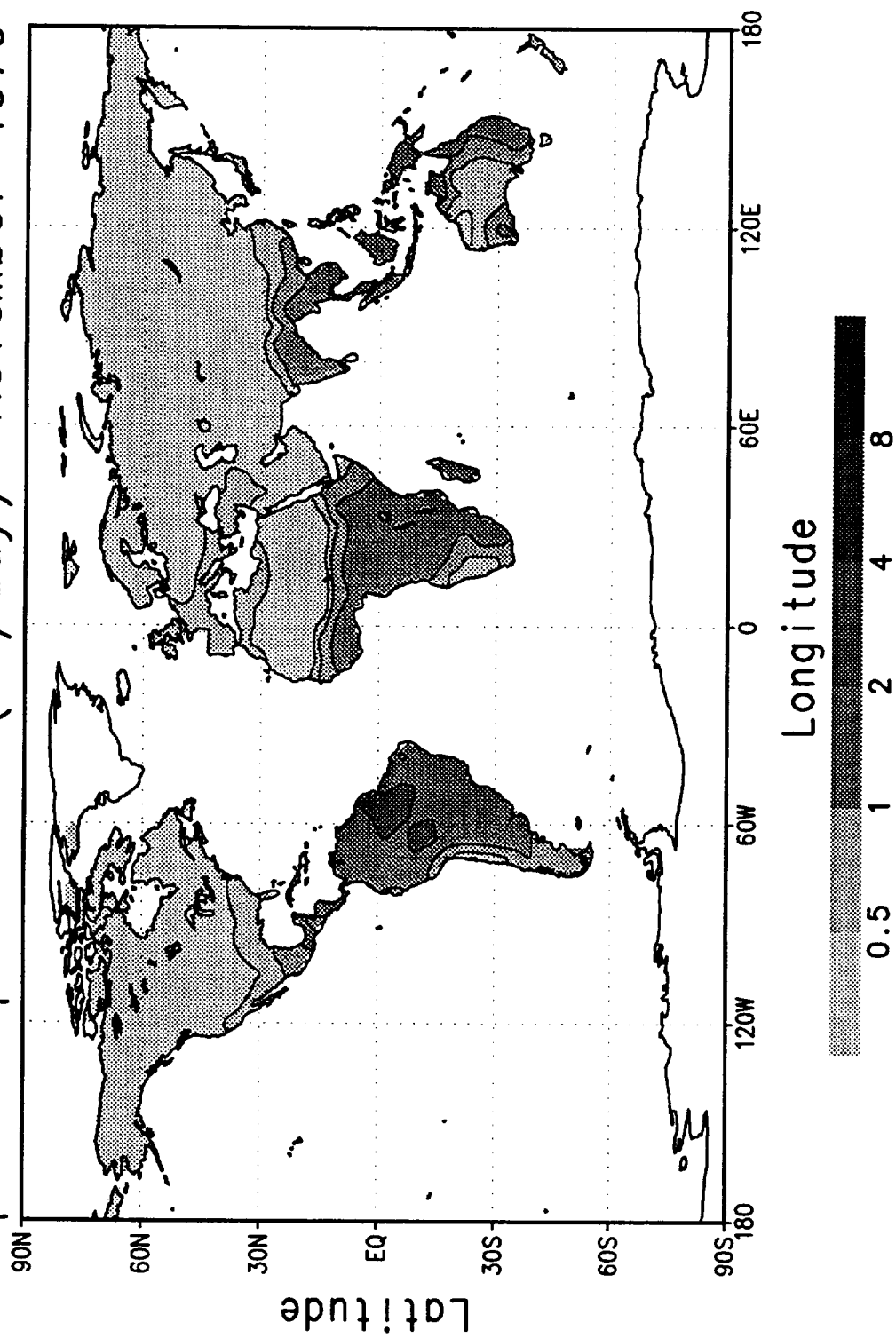
Evapotranspiration (mm/day) October 1979–88



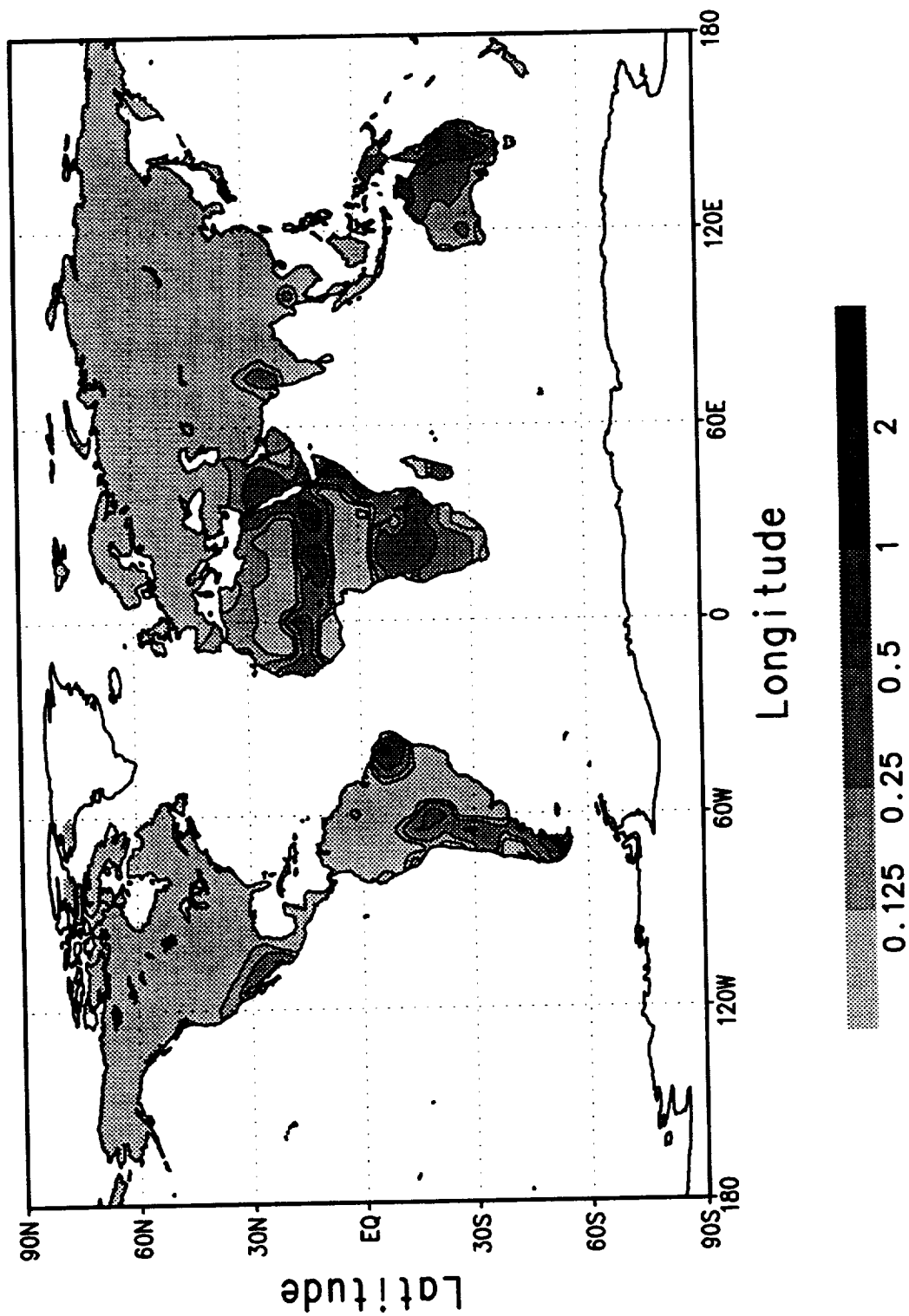
Evapotranspiration Standard Deviation (mm/day)
October 1979-88



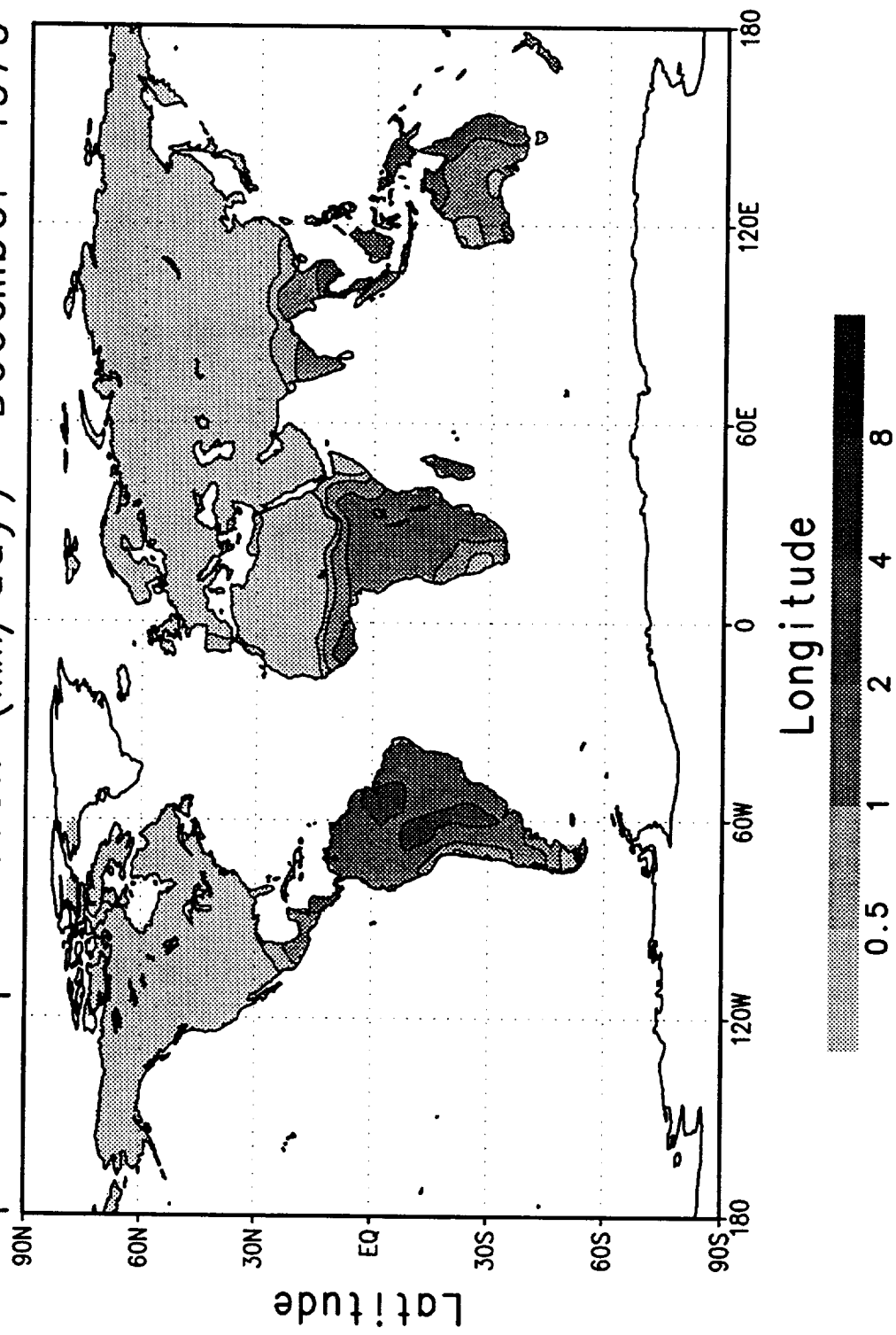
Evapotranspiration (mm/day) November 1979–88



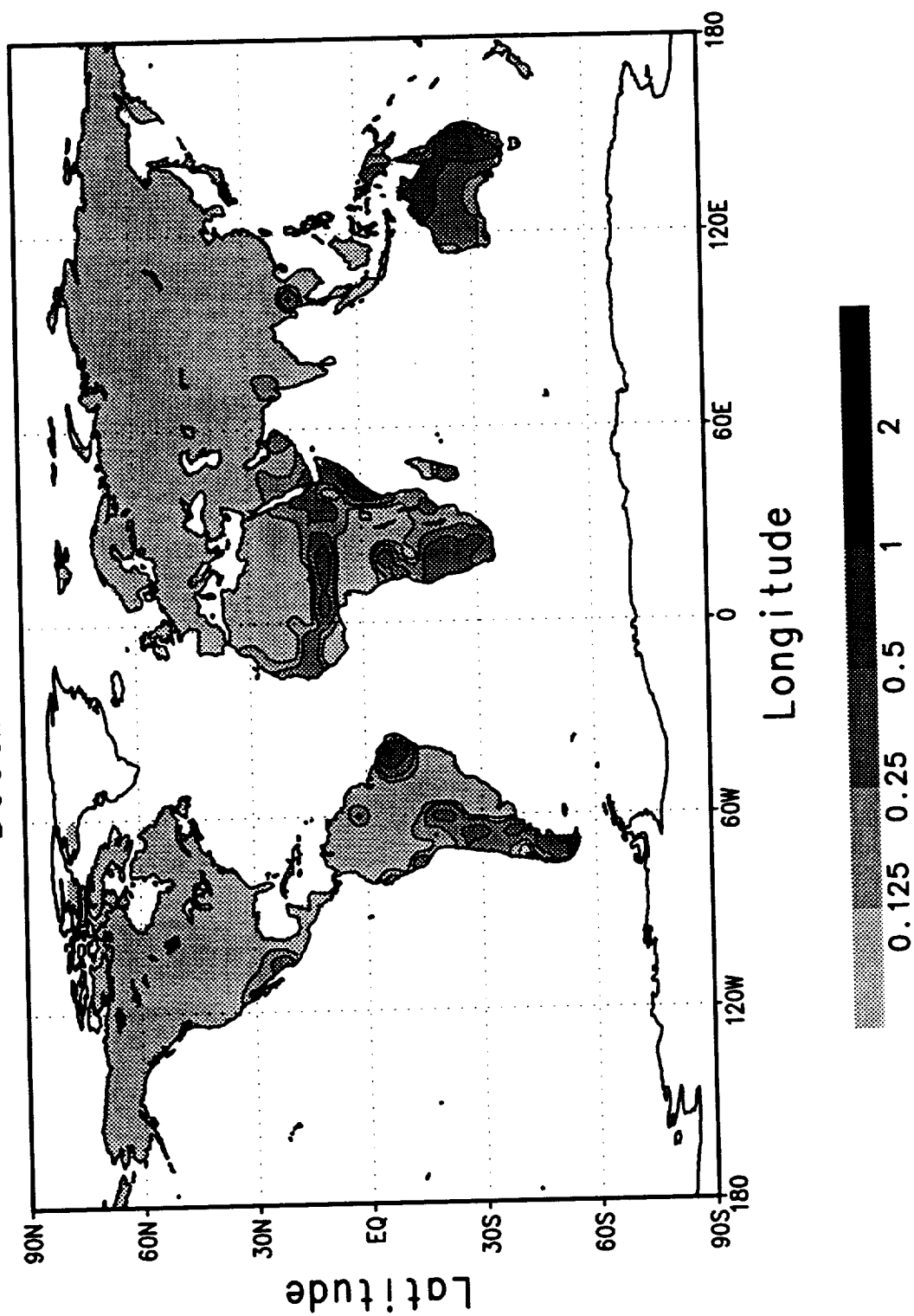
Evapotranspiration Standard Deviation (mm/day)
November 1979-88



Evapotranspiration (mm/day) December 1979–88



Evapotranspiration Standard Deviation (mm/day)
December 1979-88

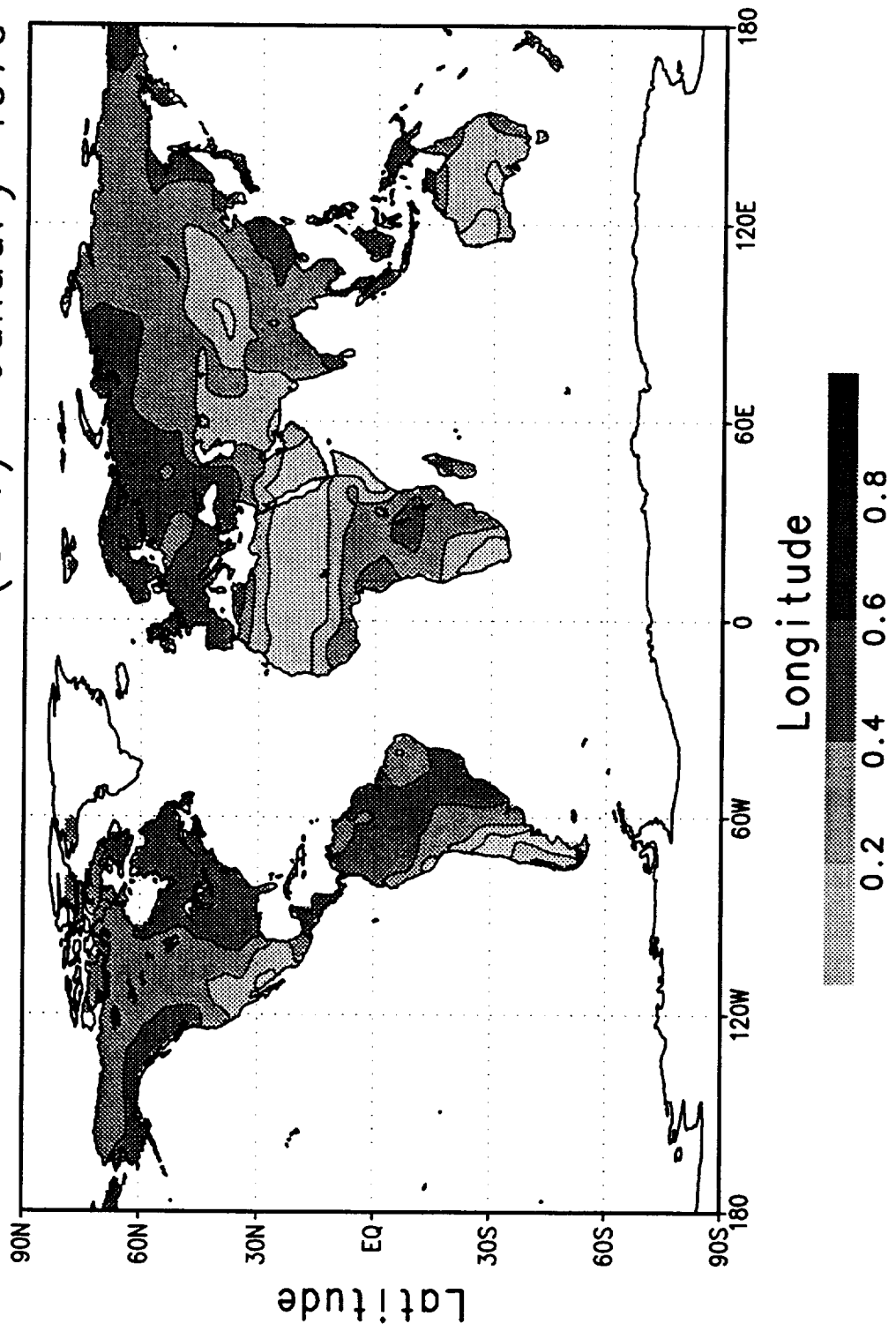


ROOT ZONE SOIL WETNESS

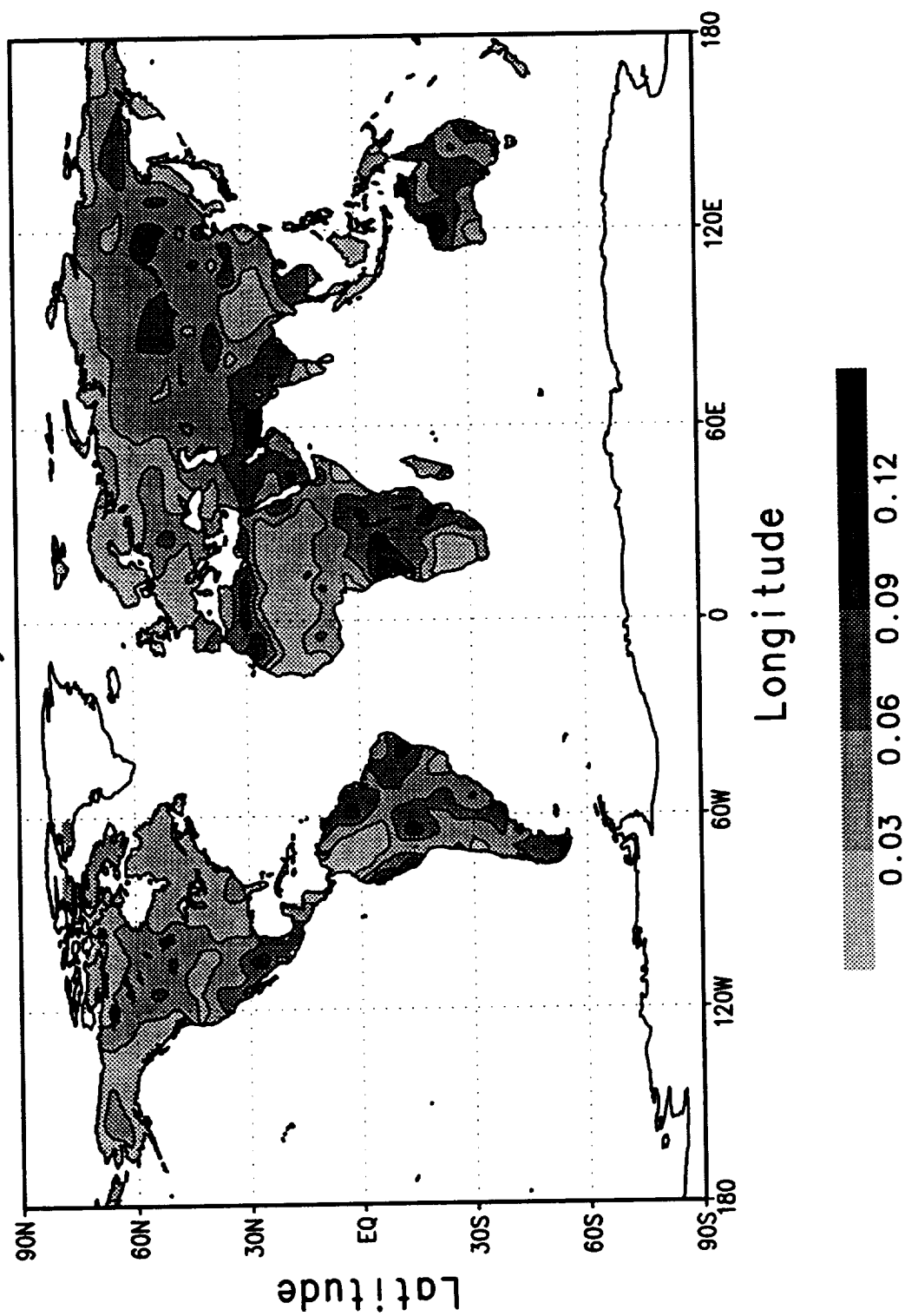
(January - December)

Ten-year average (1979 - 1988) of the monthly mean root zone soil wetness (0 - 1), computed from soil moisture initialization scheme. Also plotted are the standard deviations of the monthly mean fields as determined from the 10-year data set.

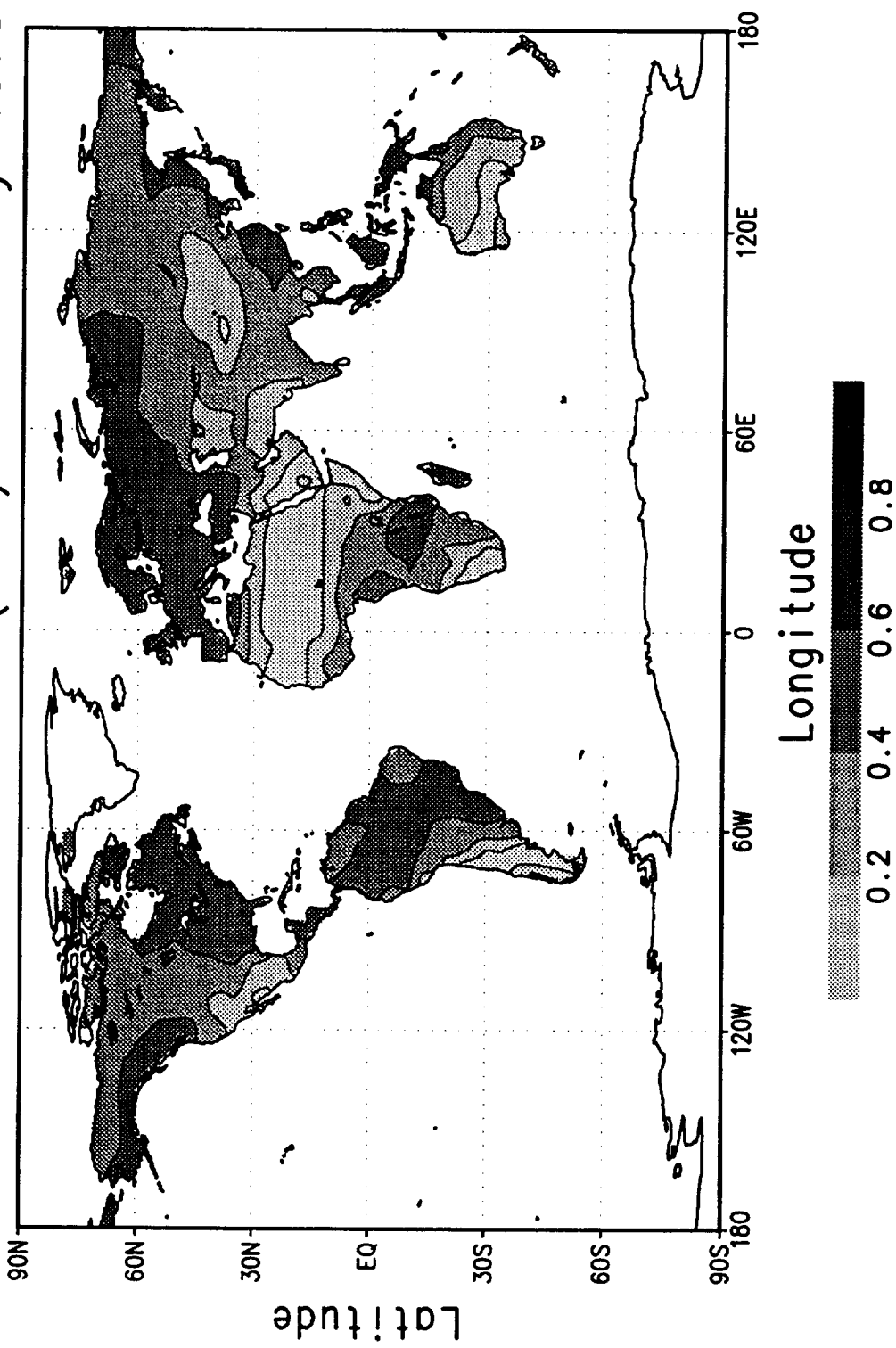
Root Zone Soil Wetness (0-1) January 1979-88



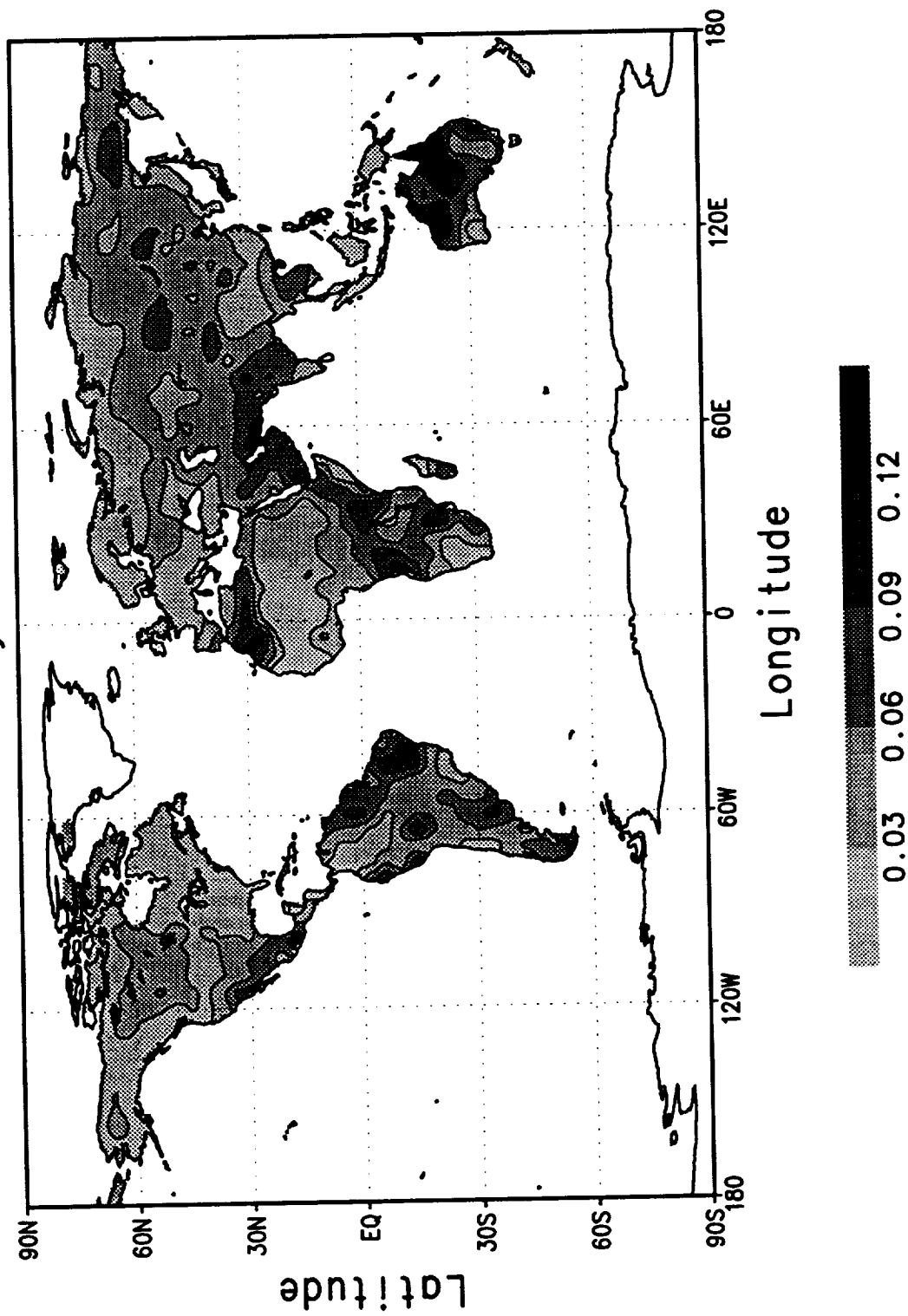
Soil Moisture Standard Deviation (0-1) January 1979-88



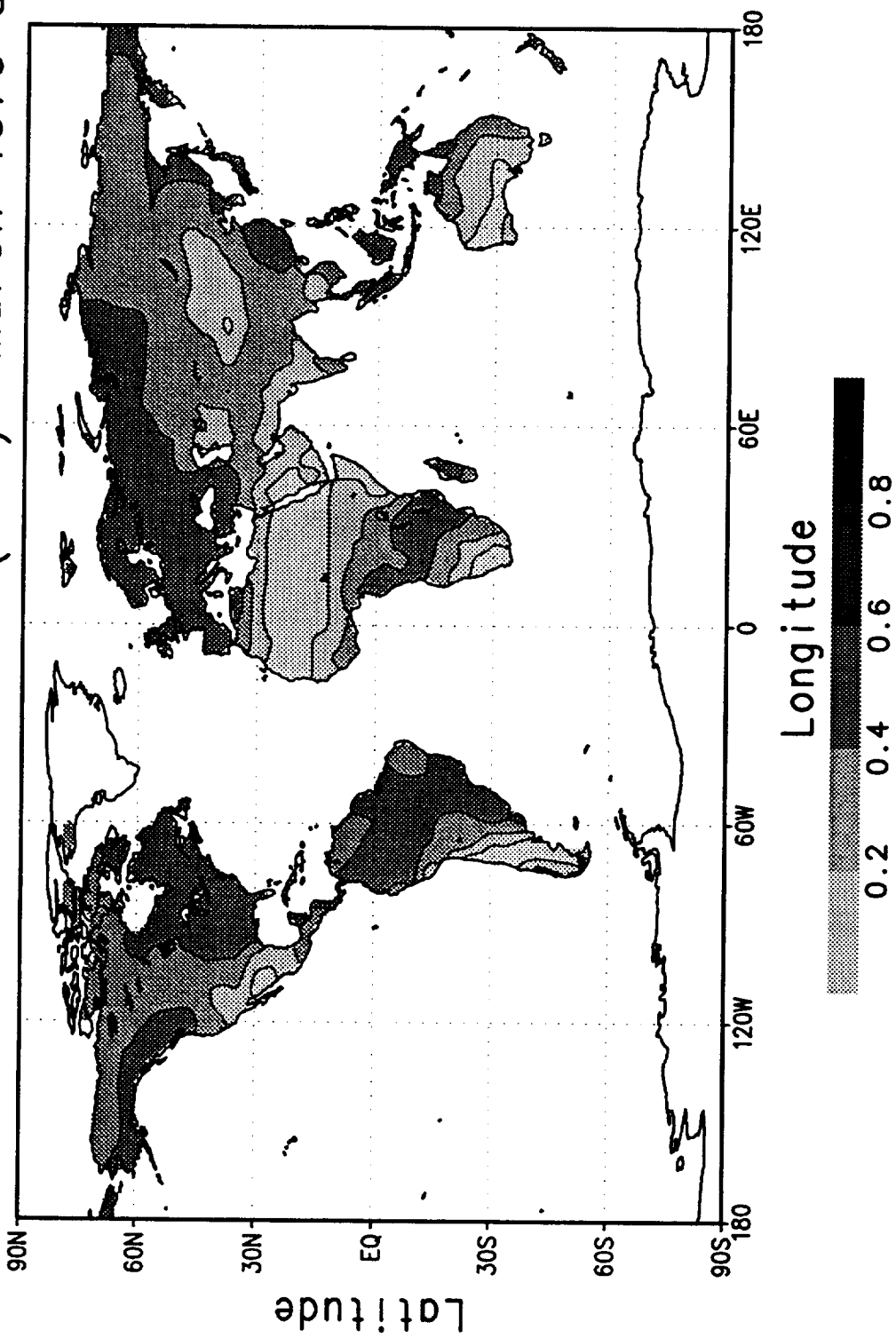
Root Zone Soil Wetness (0-1) February 1979-88



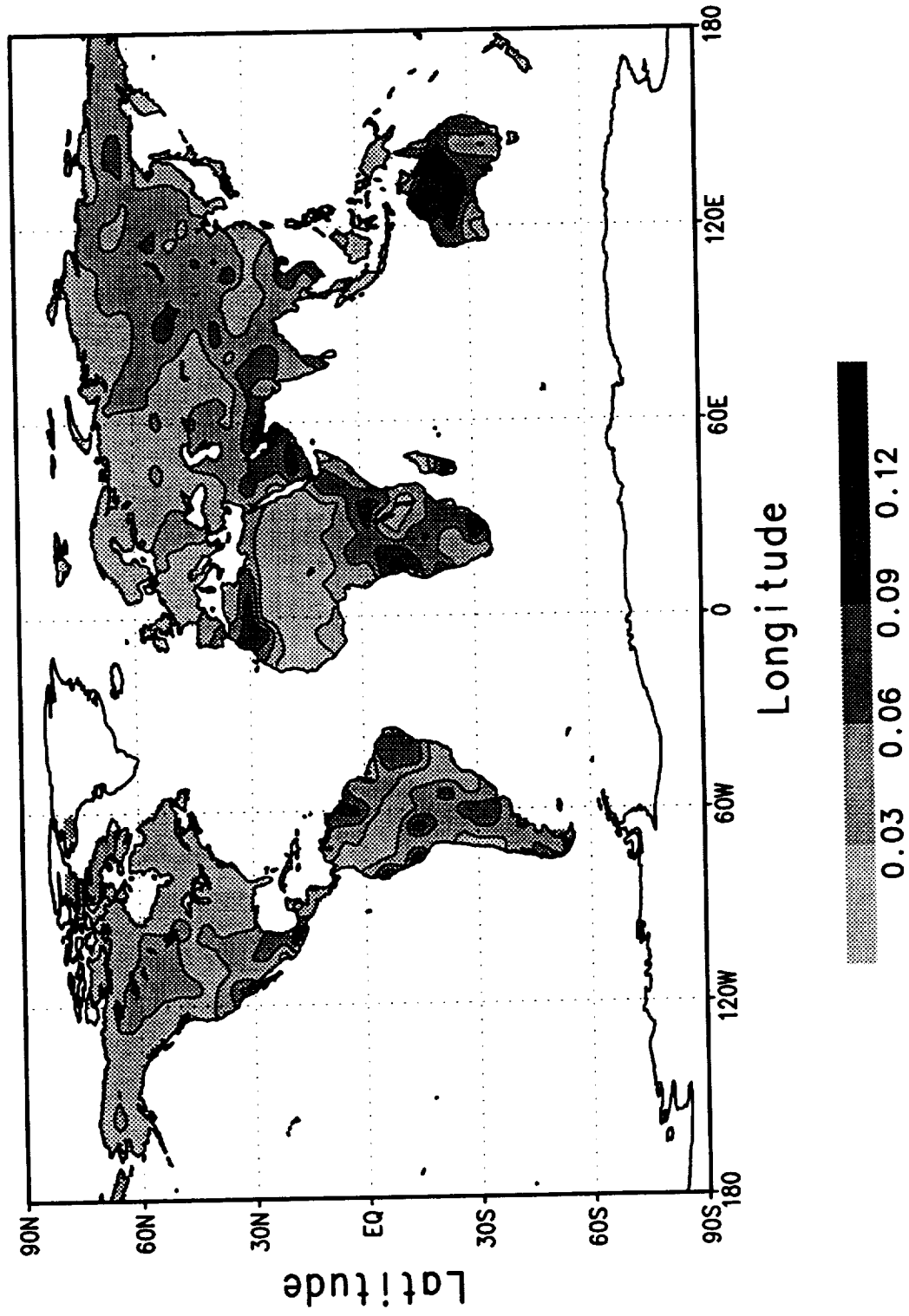
Soil Moisture Standard Deviation (0-1)
February 1979-88



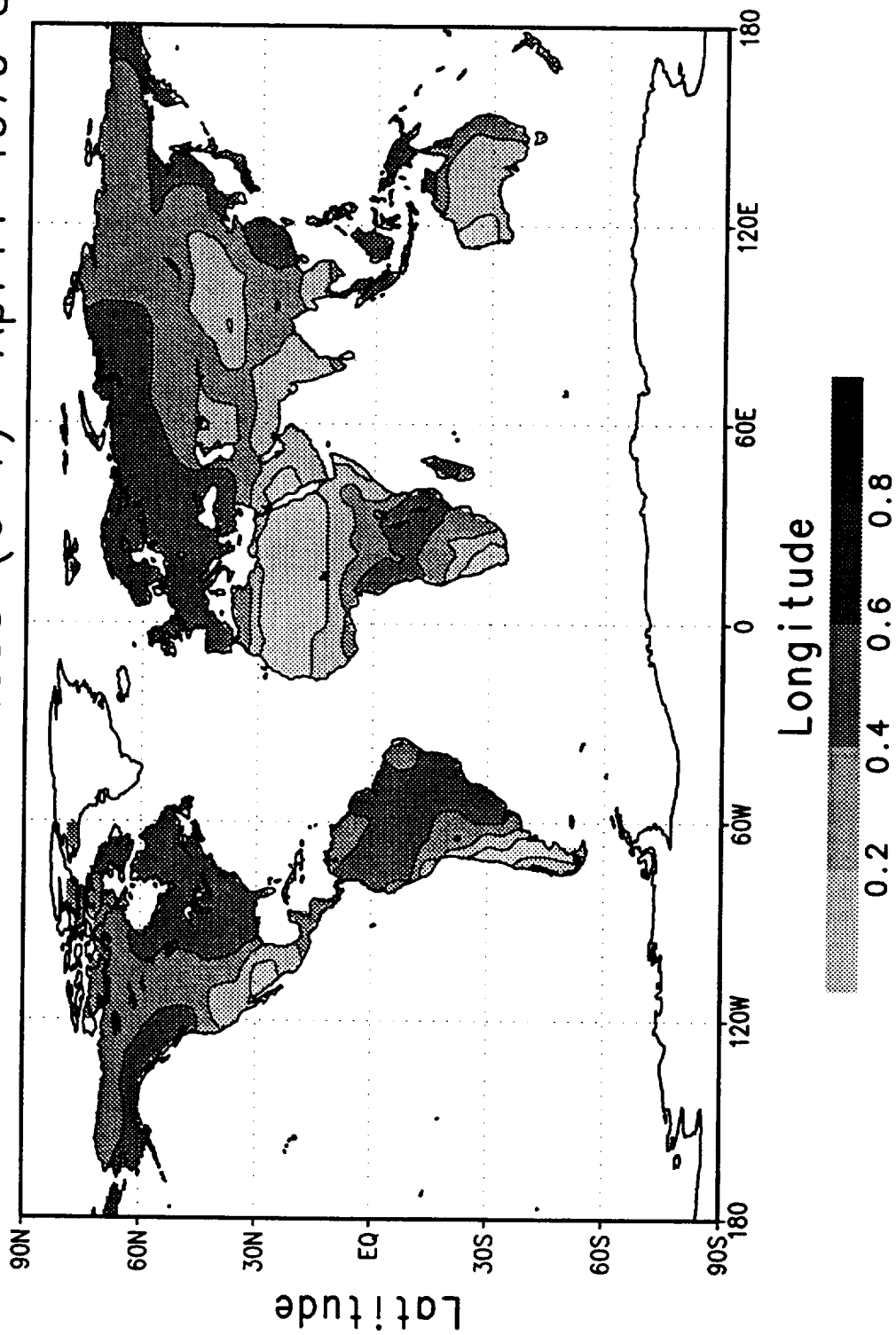
Root Zone Soil Wetness (0-1) March 1979-88



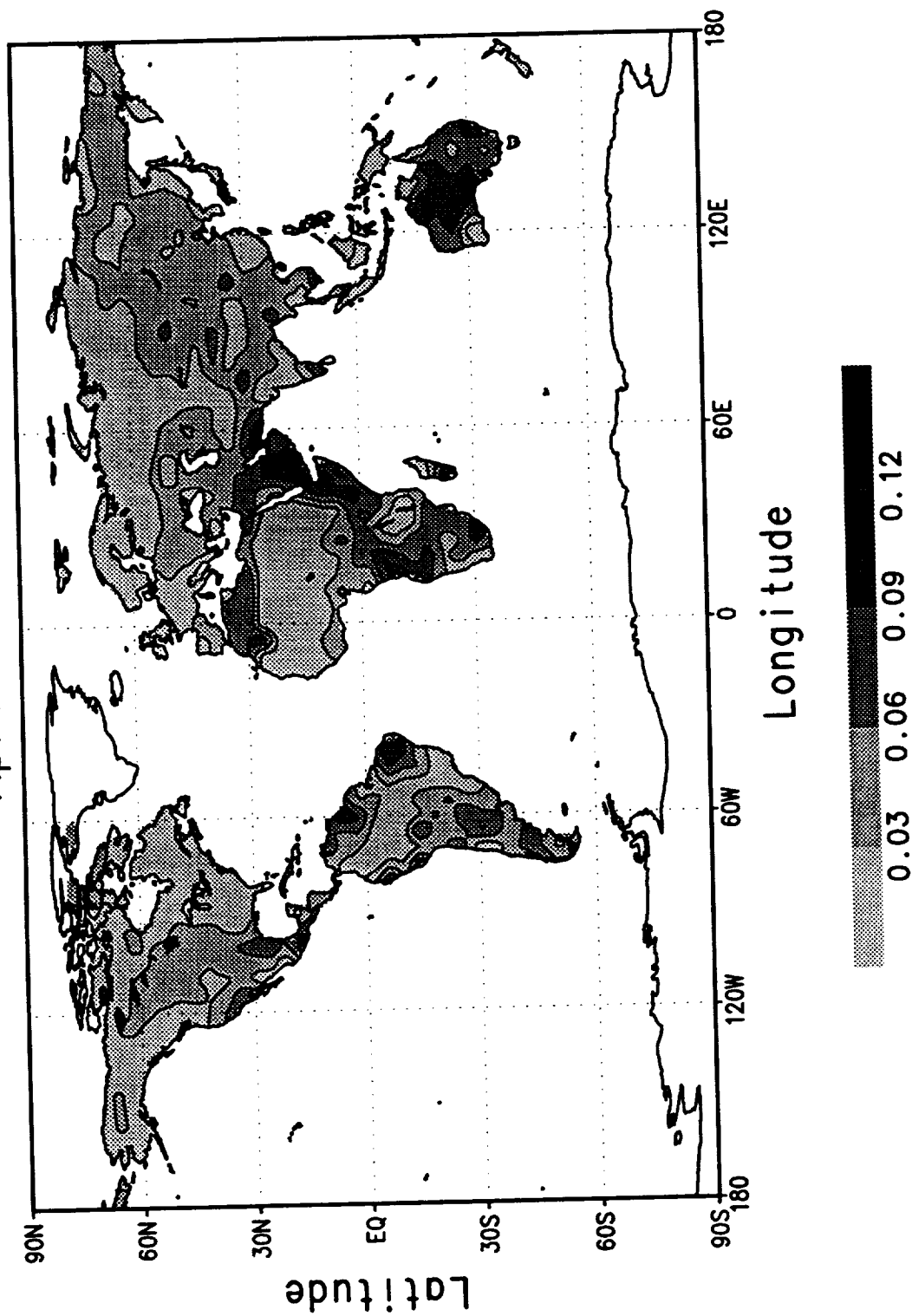
Soil Moisture Standard Deviation (0-1) March 1979-88



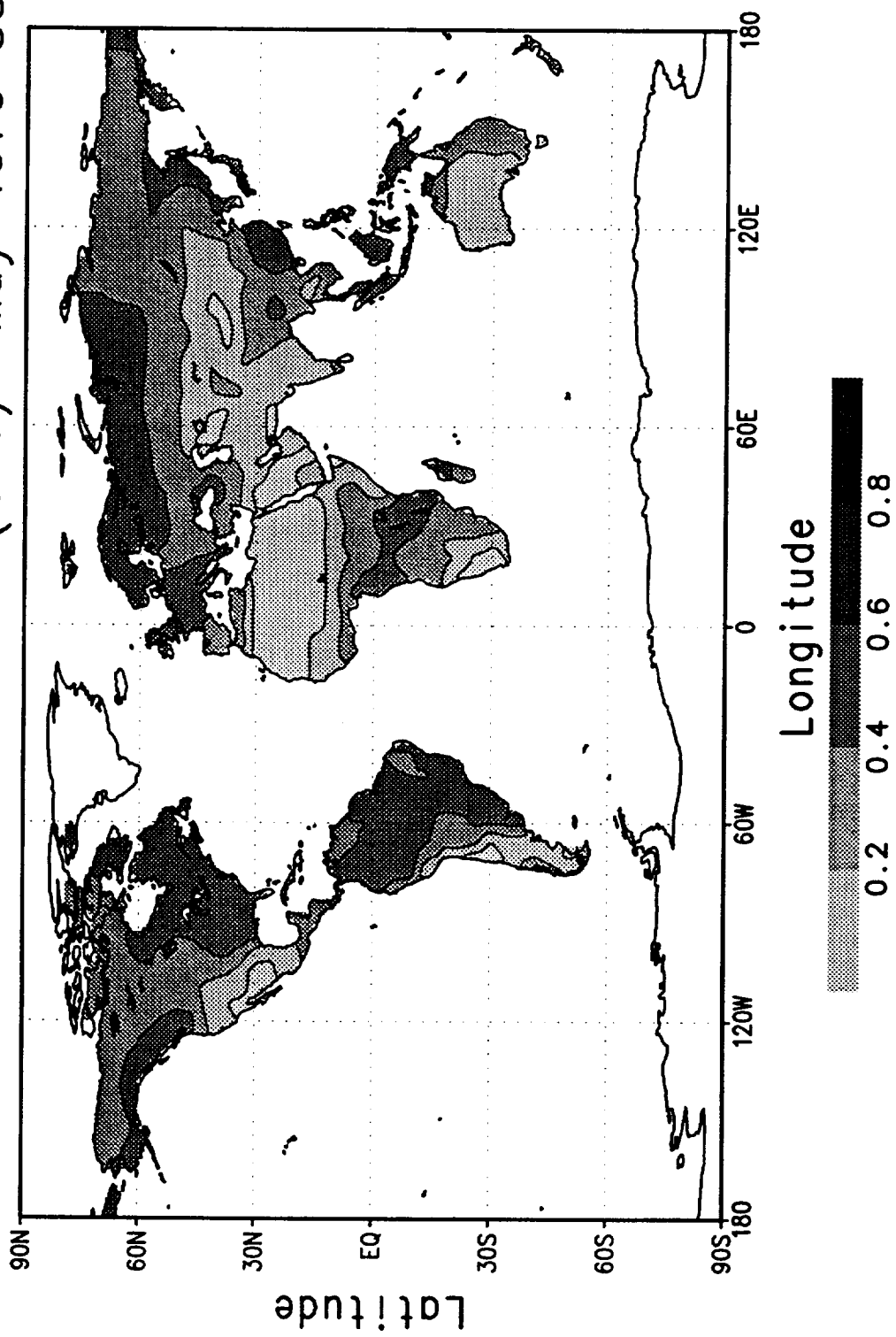
Root Zone Soil Wetness (0-1) April 1979-88



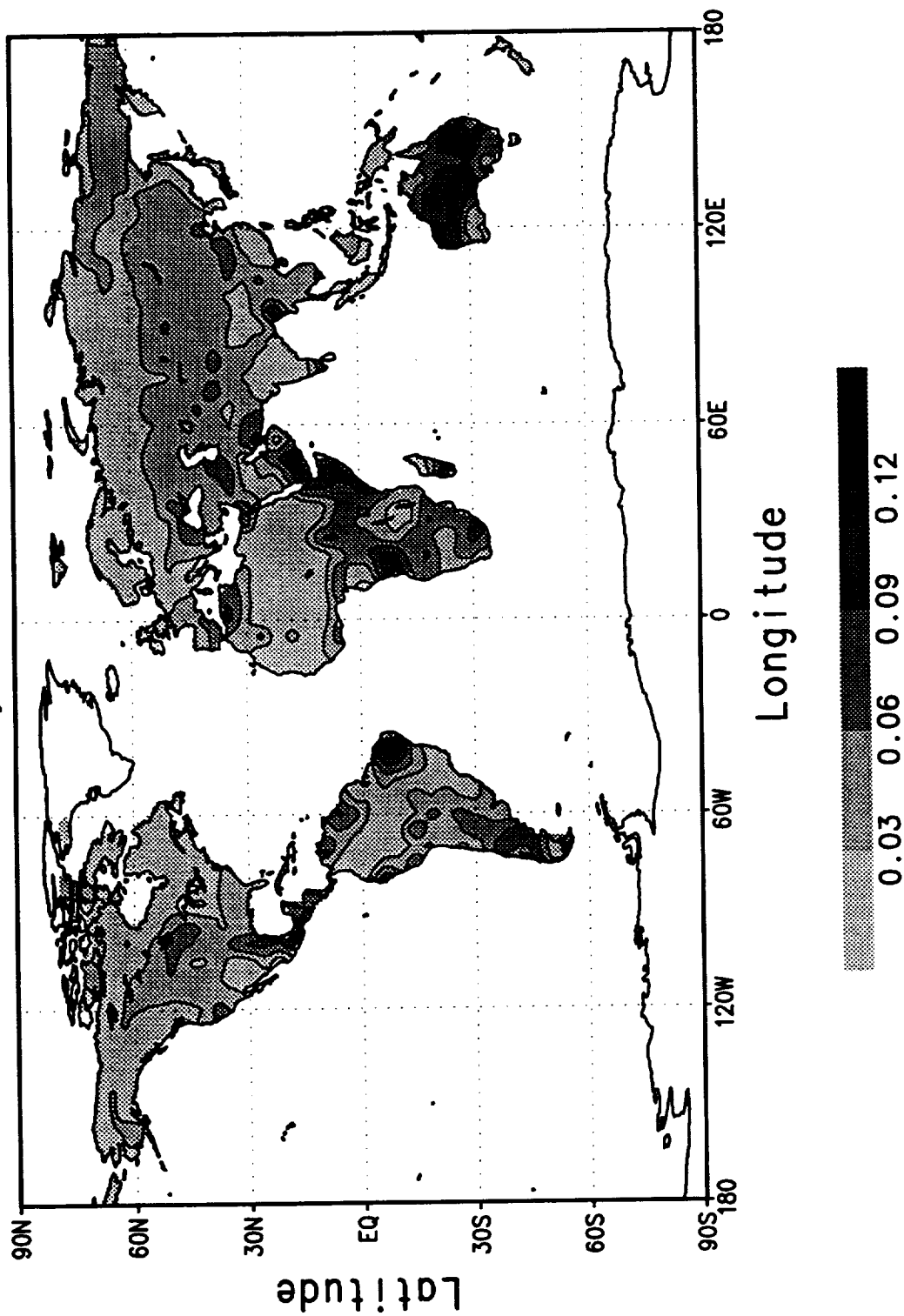
Soil Moisture Standard Deviation (0-1)
April 1979-88



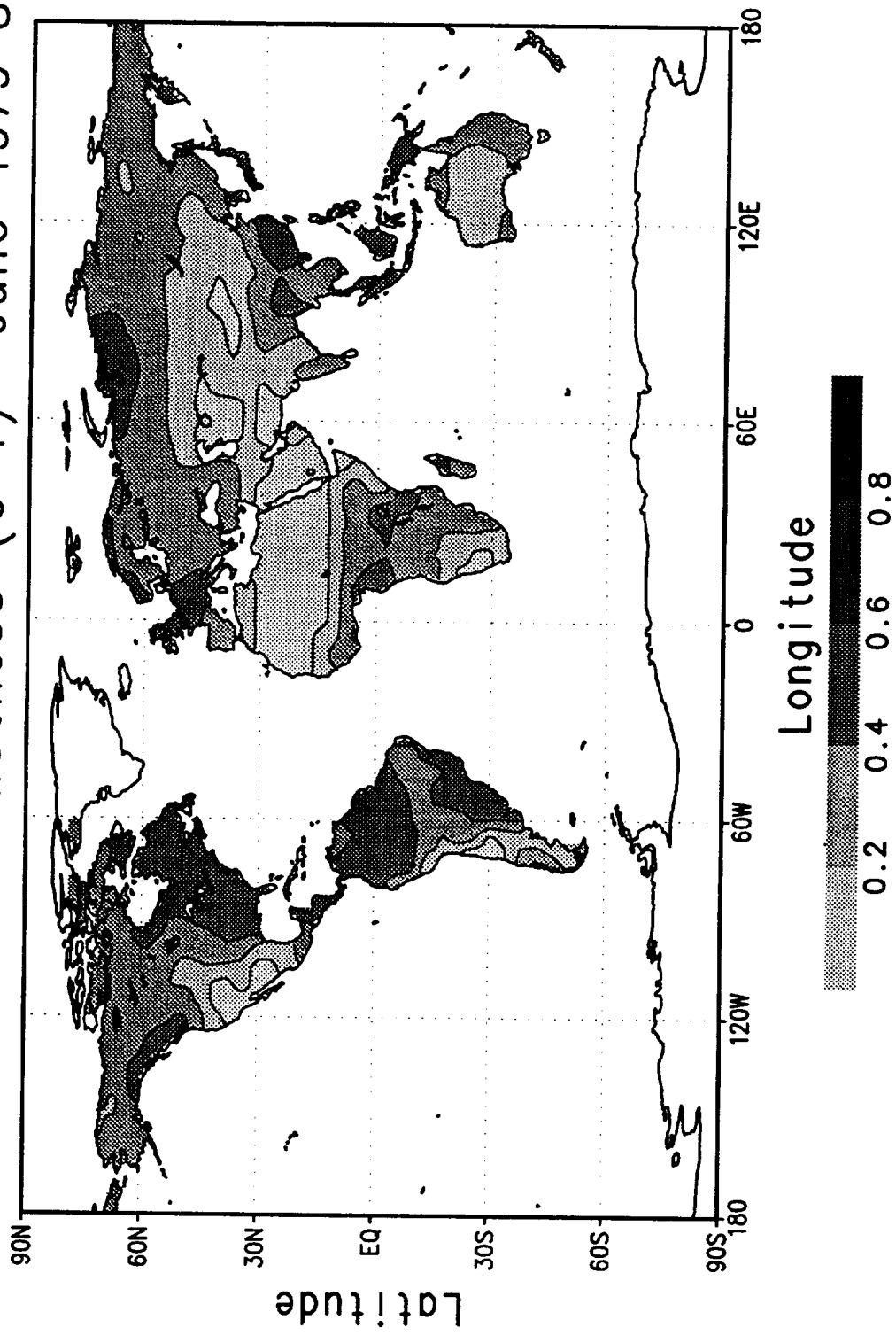
Root Zone Soil Wetness (0-1) May 1979-88



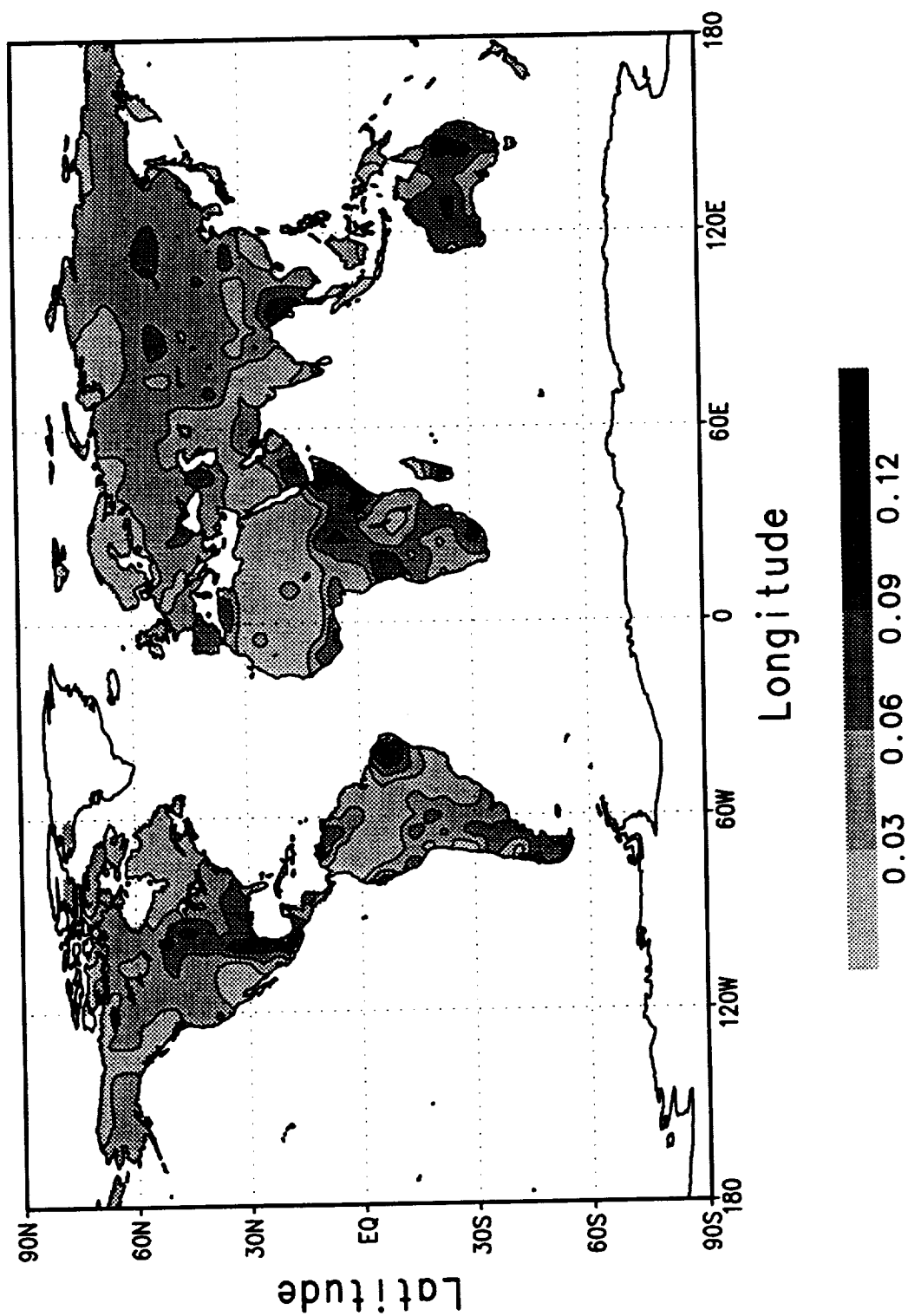
Soil Moisture Standard Deviation (0-1) May 1979-88



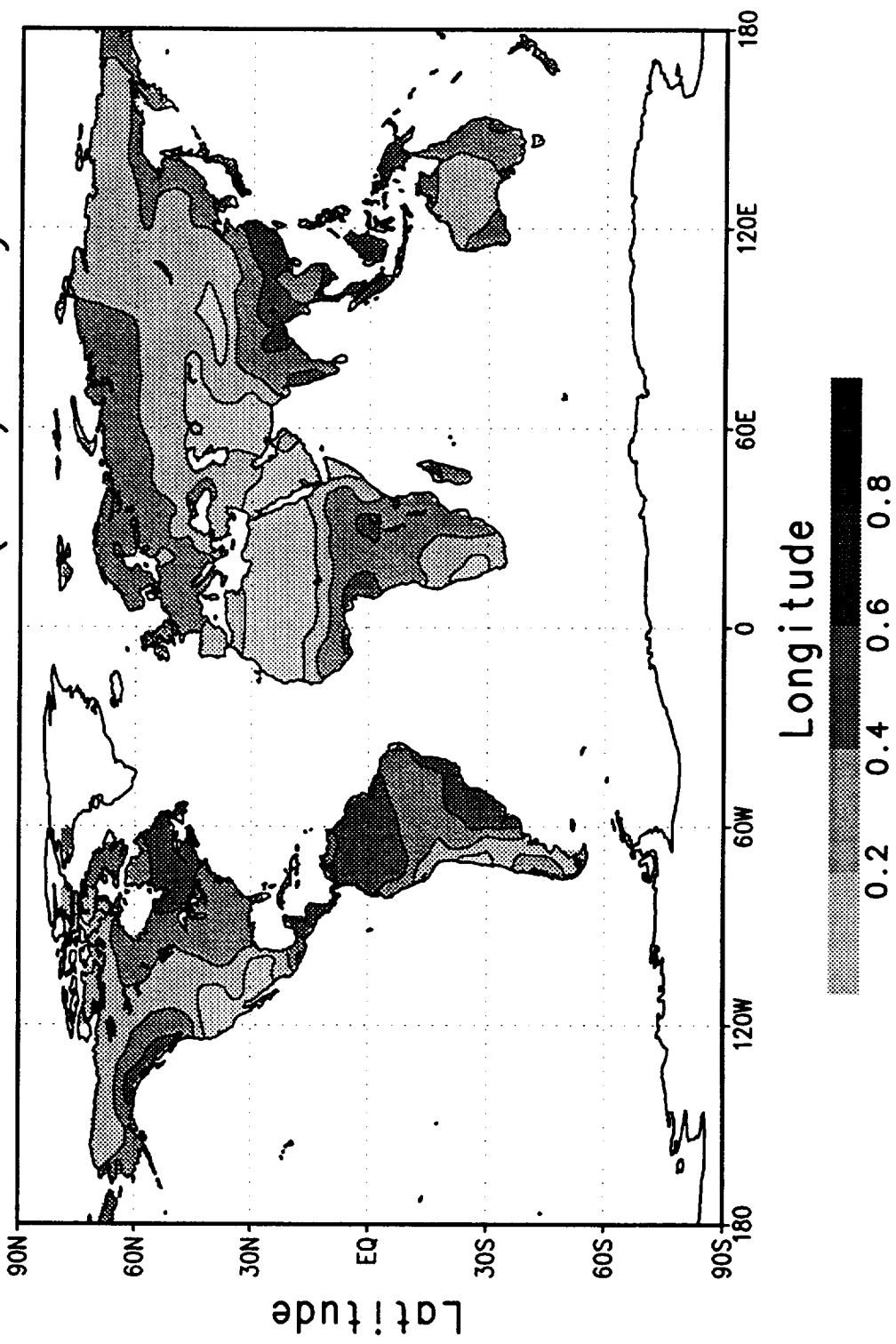
Root Zone Soil Wetness (0-1) June 1979-88



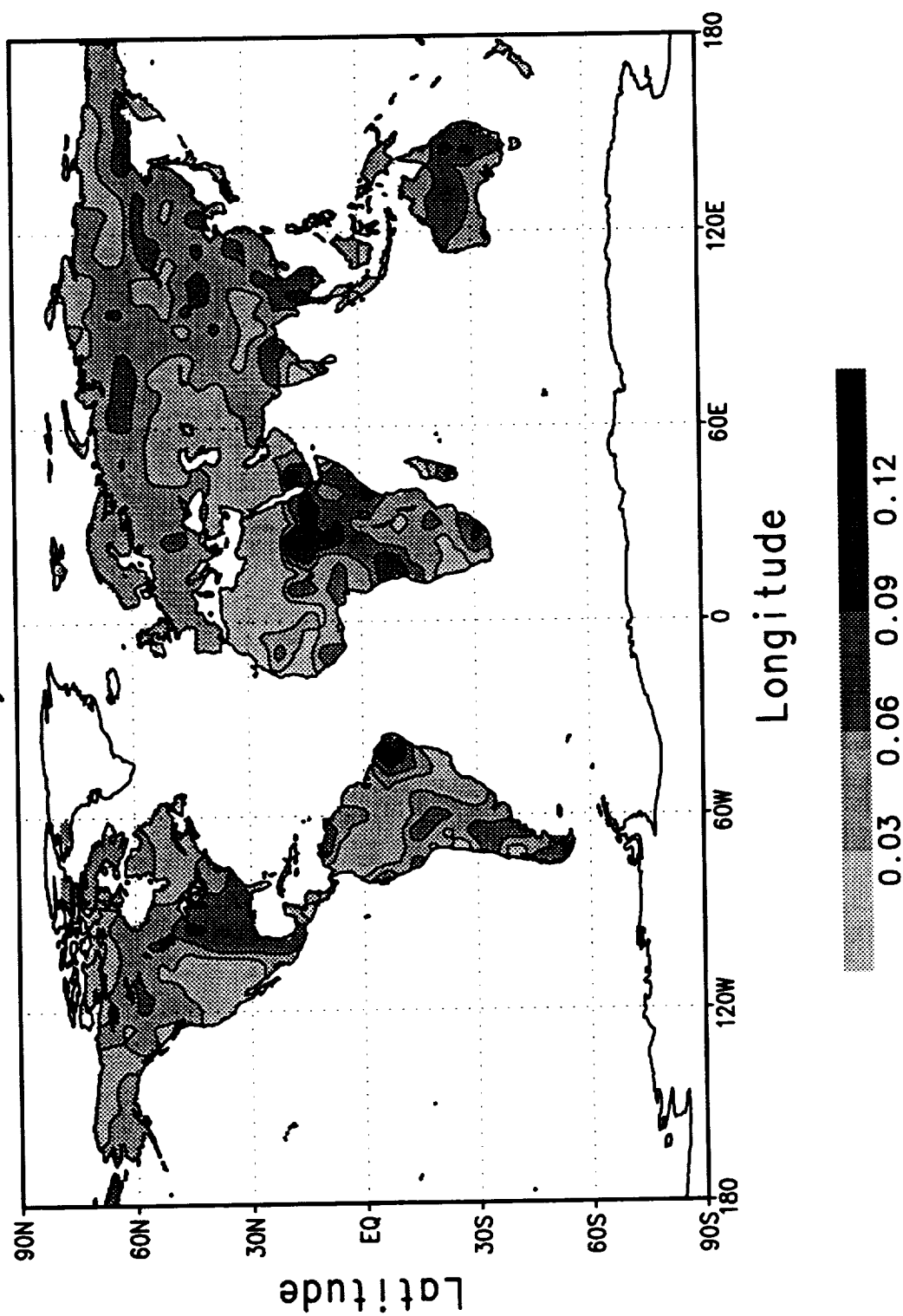
Soil Moisture Standard Deviation (0-1) June 1979-88



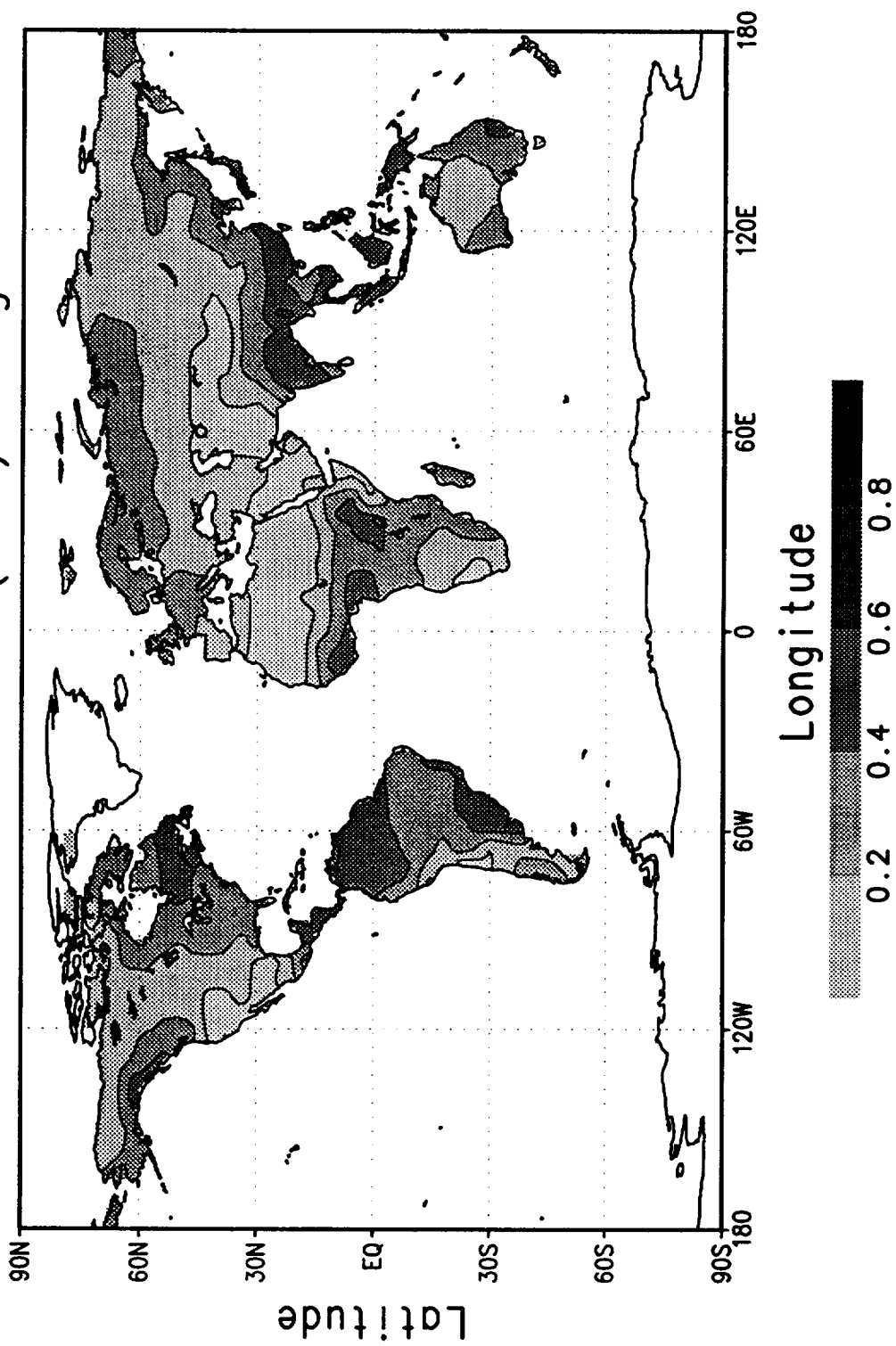
Root Zone Soil Wetness (0-1) July 1979-88



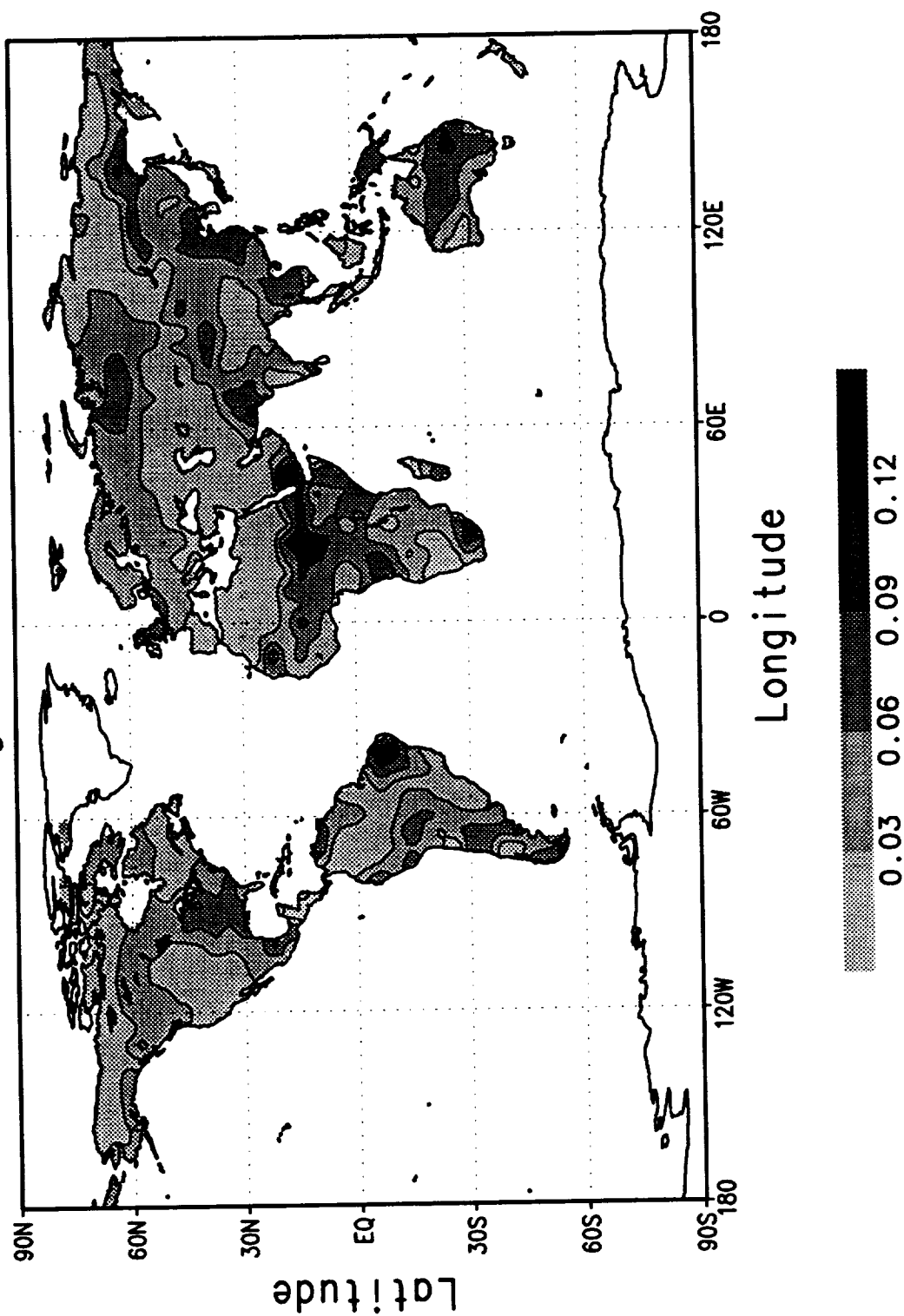
Soil Moisture Standard Deviation (0-1) July 1979-88



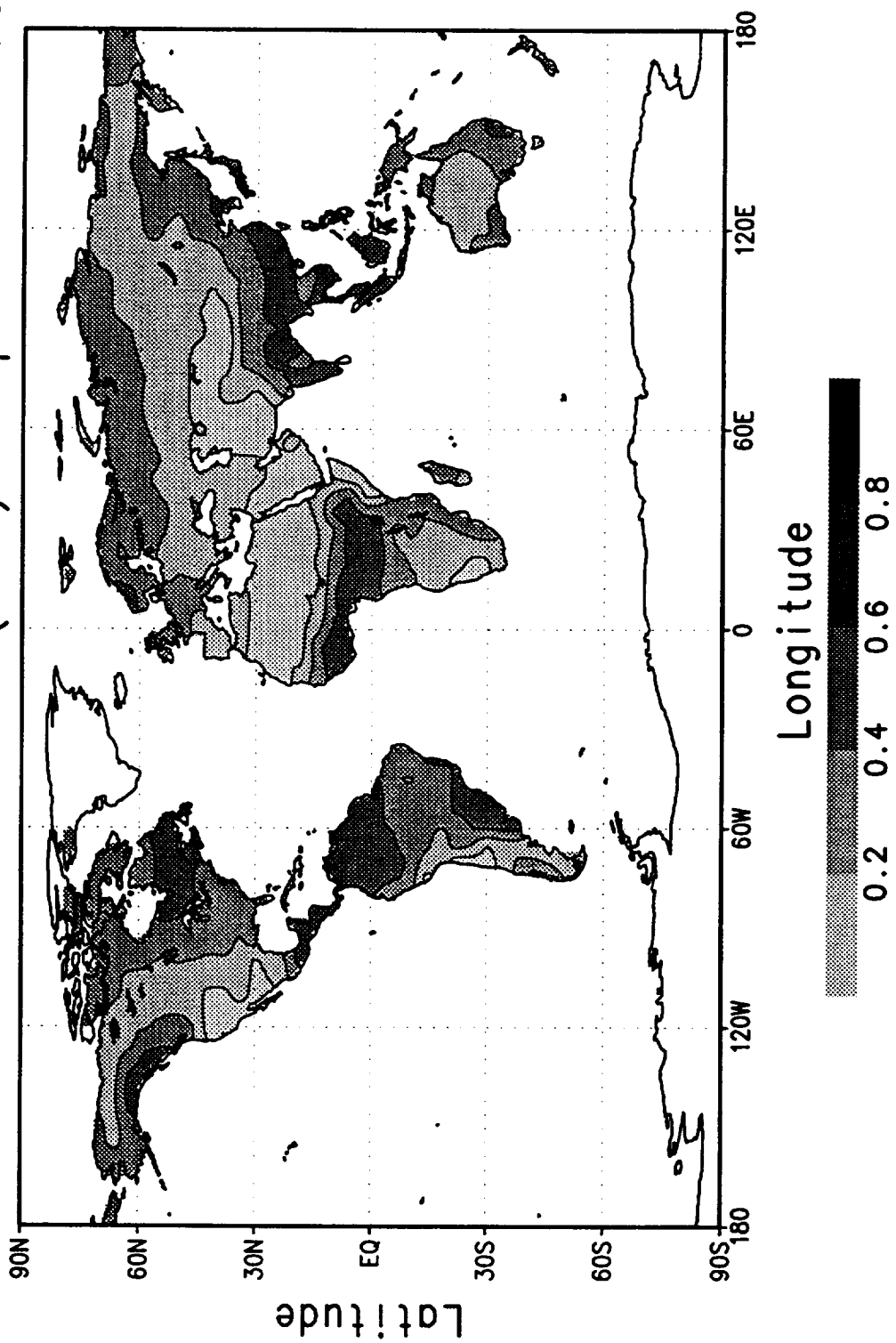
Root Zone Soil Wetness (0-1) August 1979-88



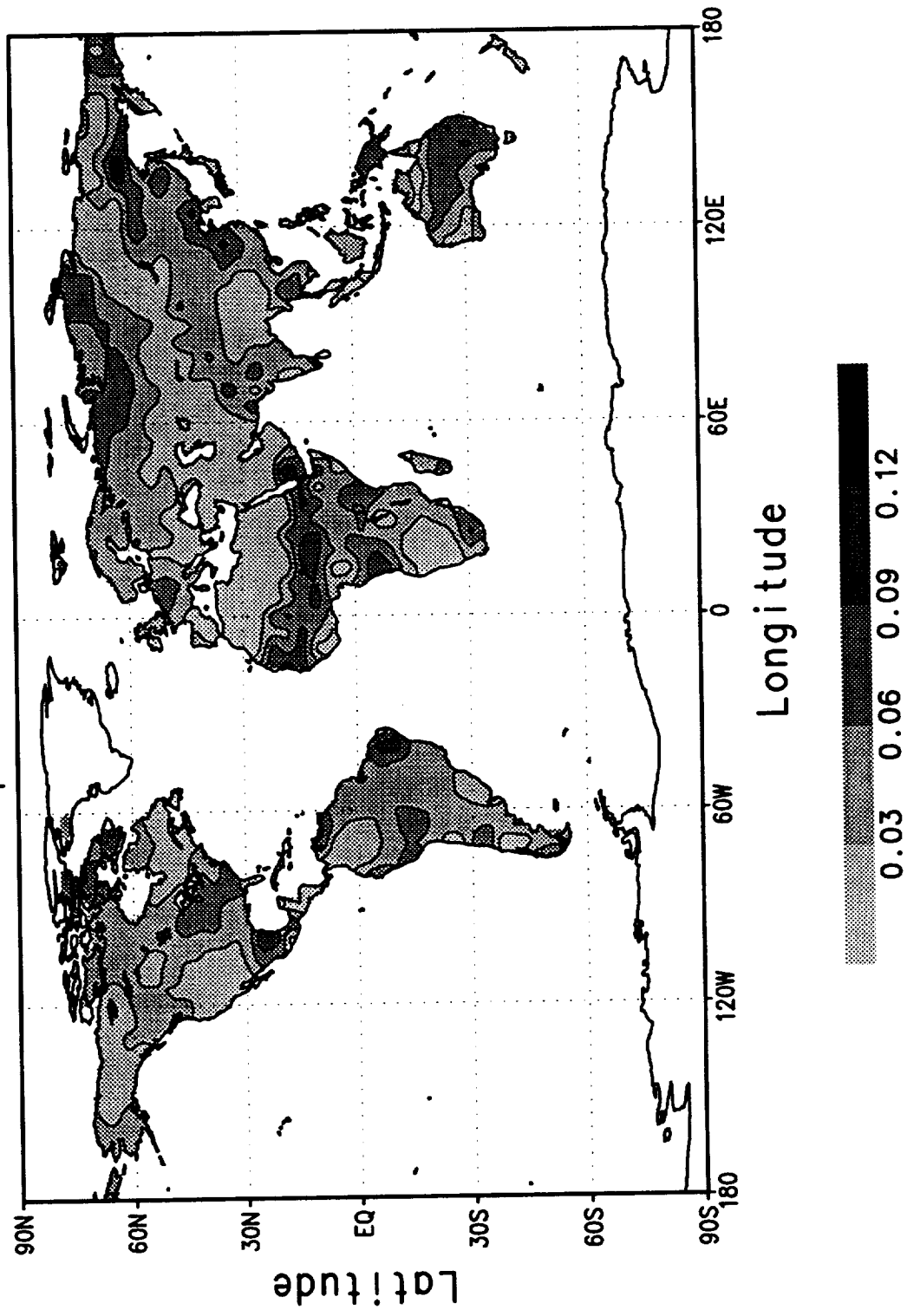
Soil Moisture Standard Deviation (0-1)
August 1979-88



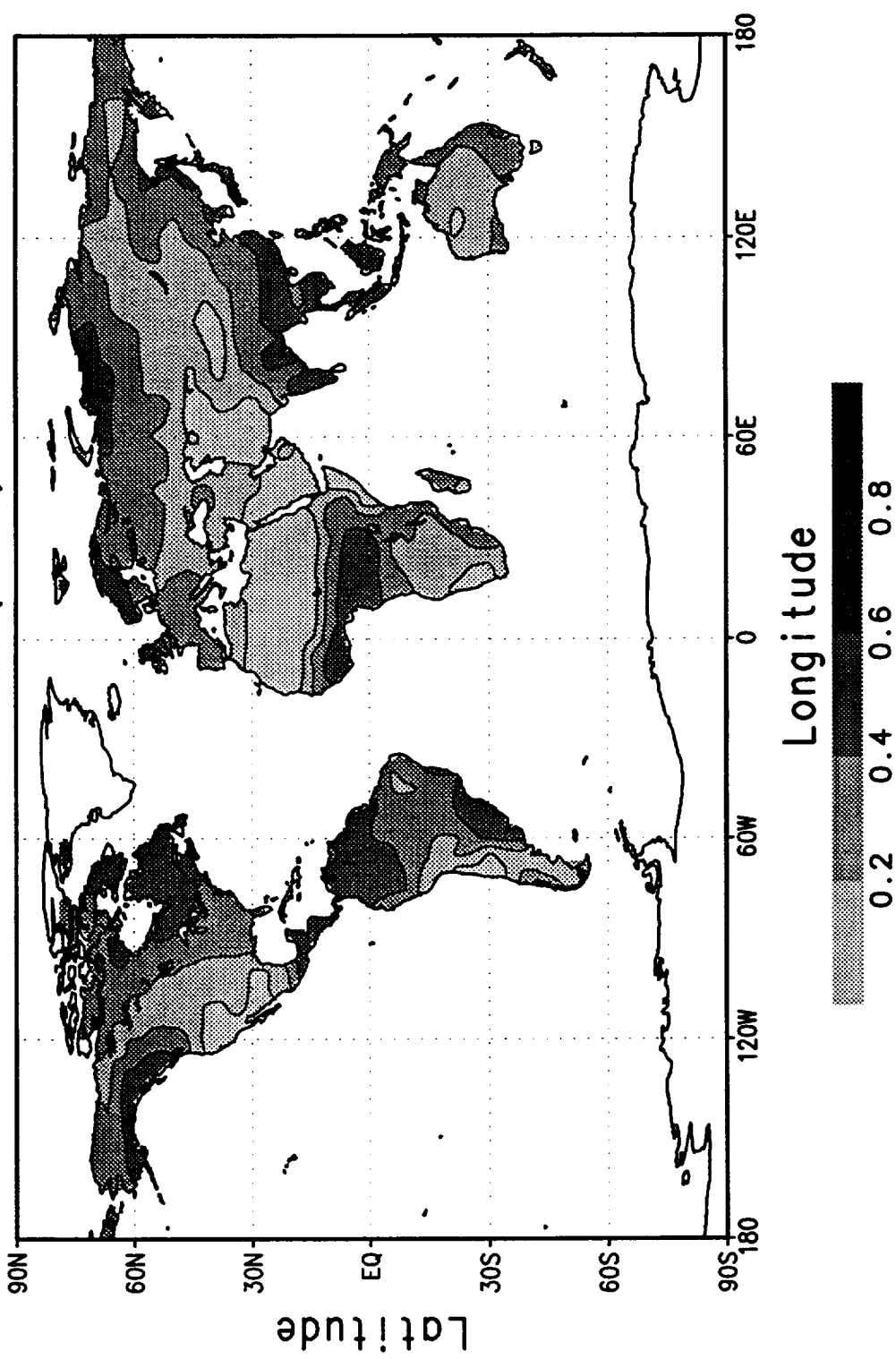
Root Zone Soil Wetness (0-1) September 1979-88



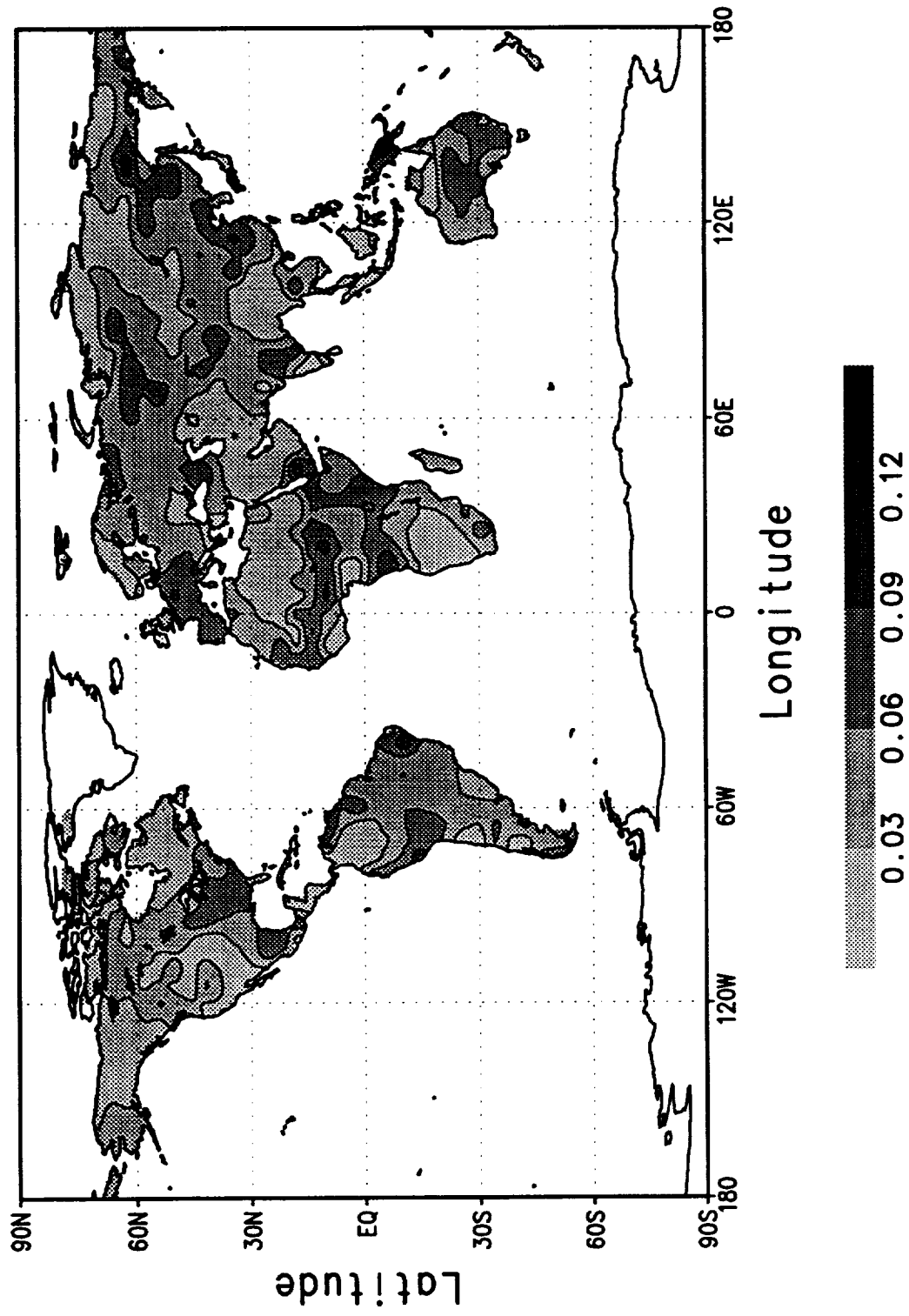
Soil Moisture Standard Deviation (0-1) September 1979-88



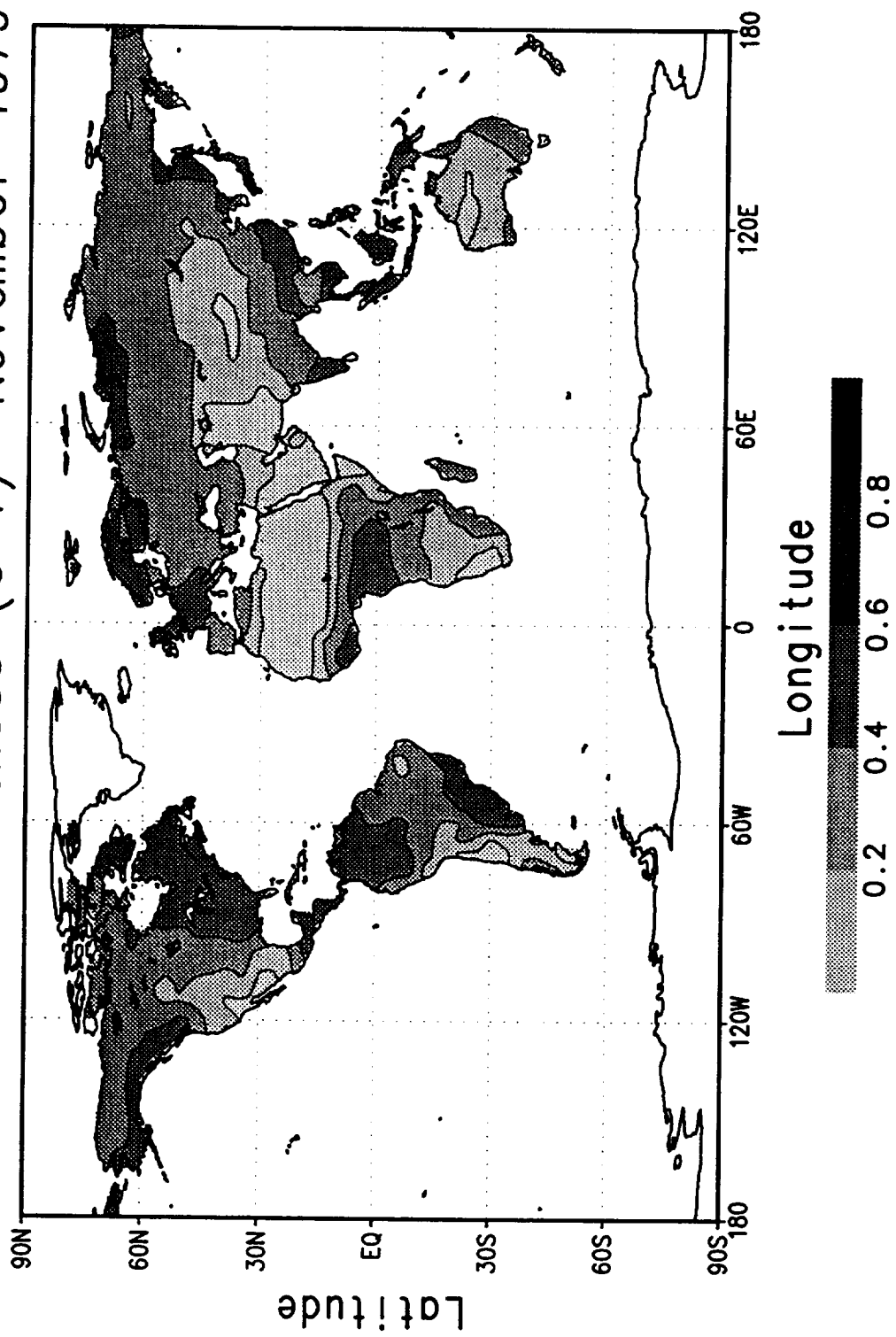
Root Zone Soil Wetness (0-1) October 1979-88



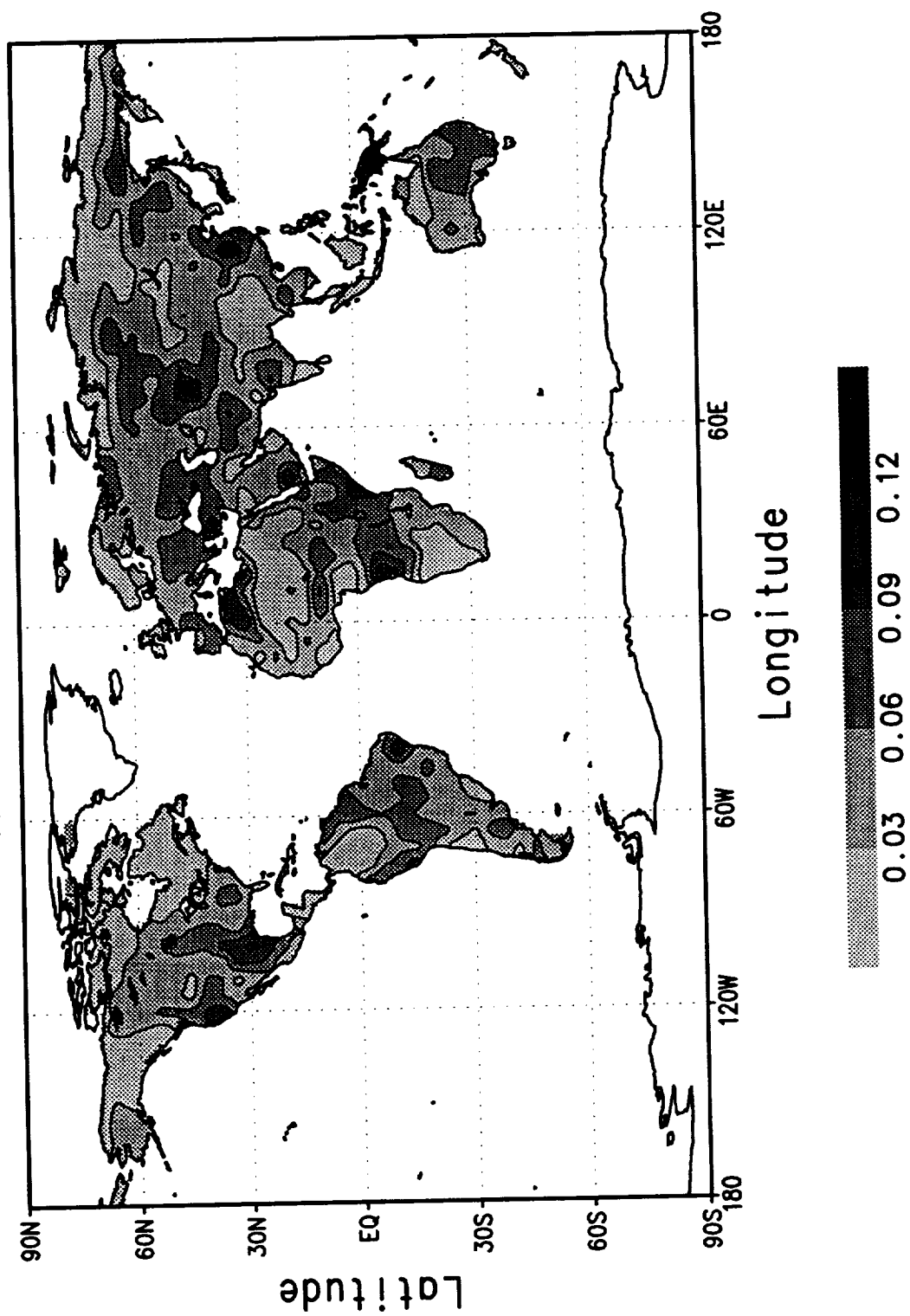
Soil Moisture Standard Deviation (0-1) October 1979-88



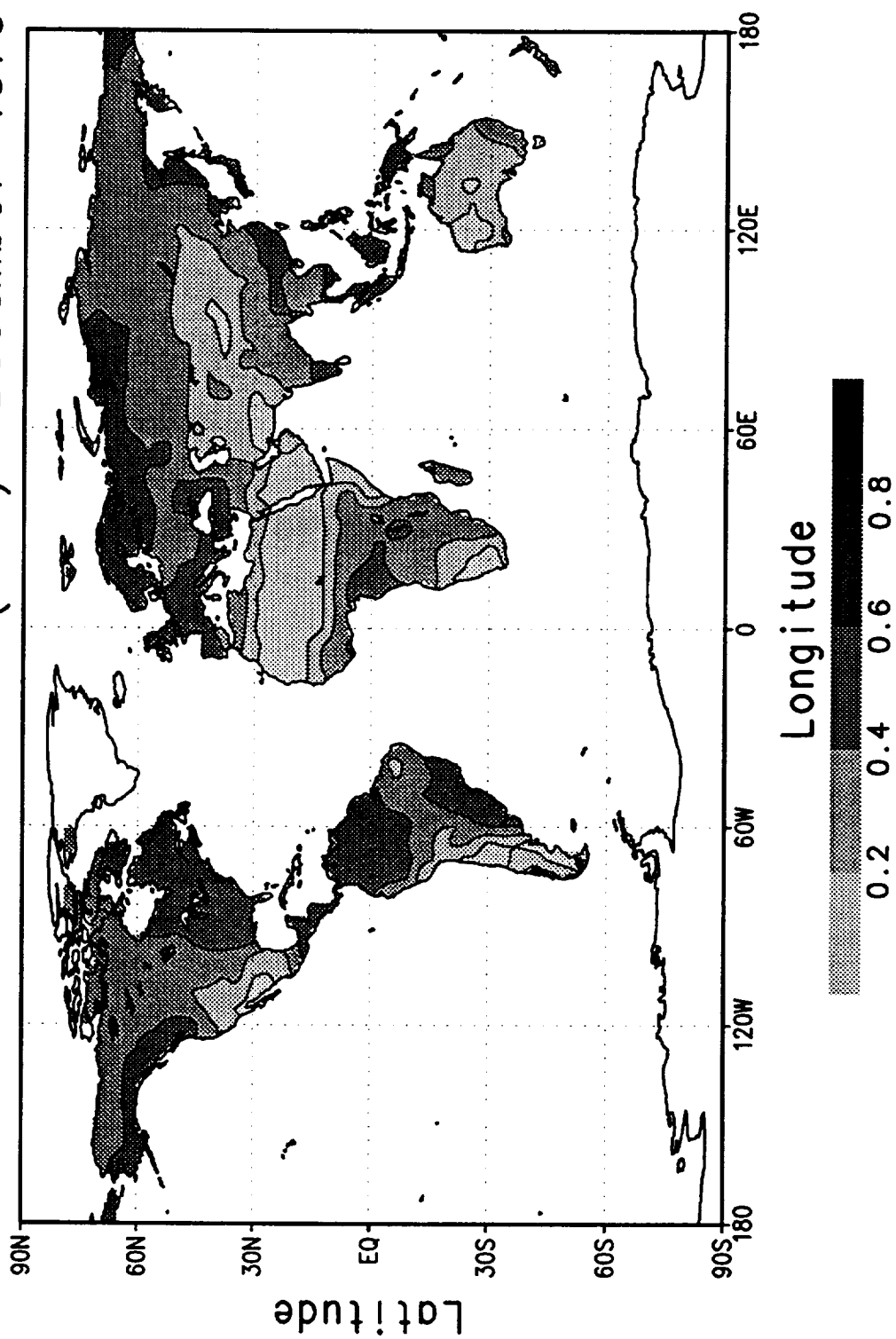
Root Zone Soil Wetness (0-1) November 1979-88



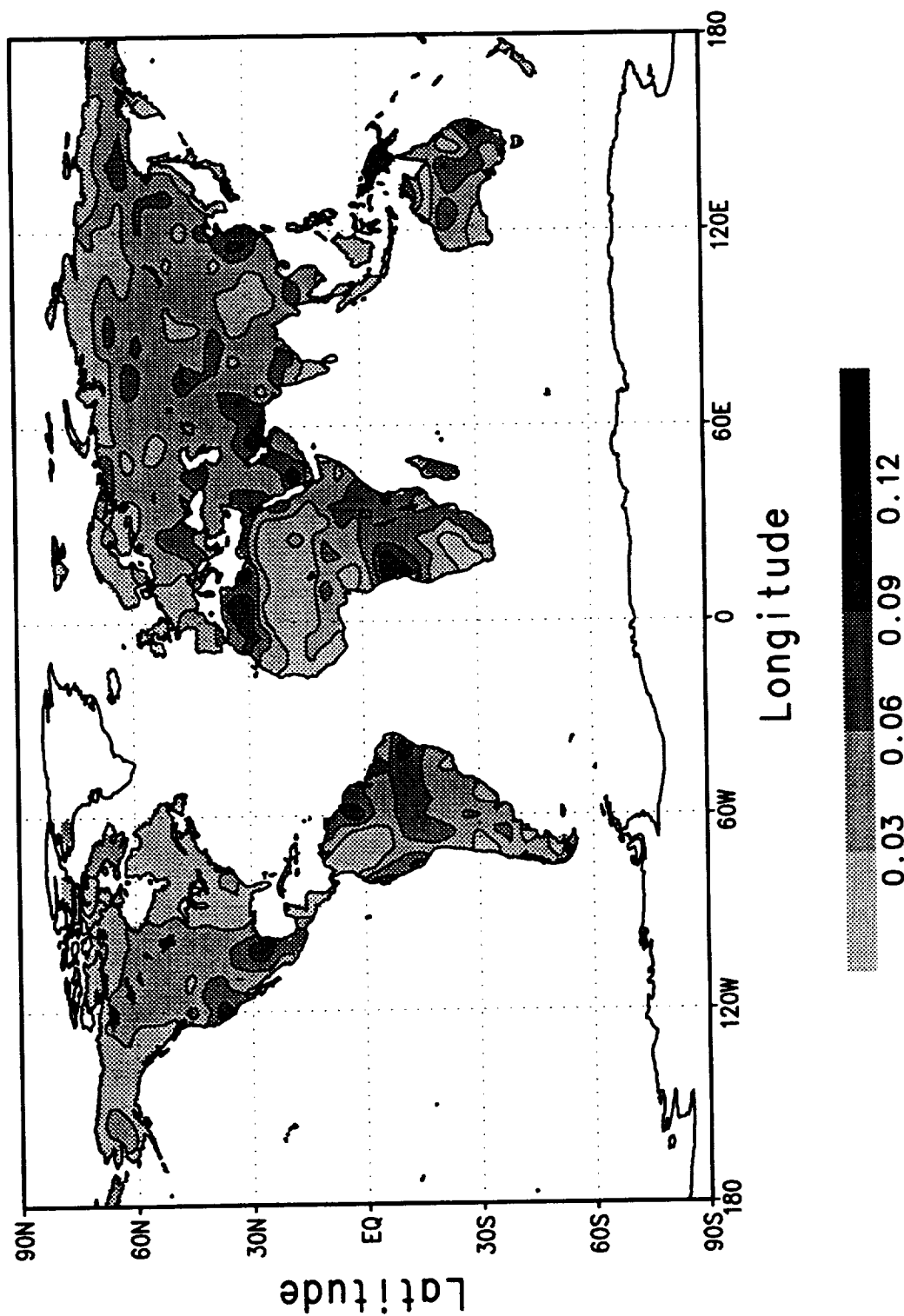
Soil Moisture Standard Deviation (0-1)
November 1979-88



Root Zone Soil Wetness (0-1) December 1979-88



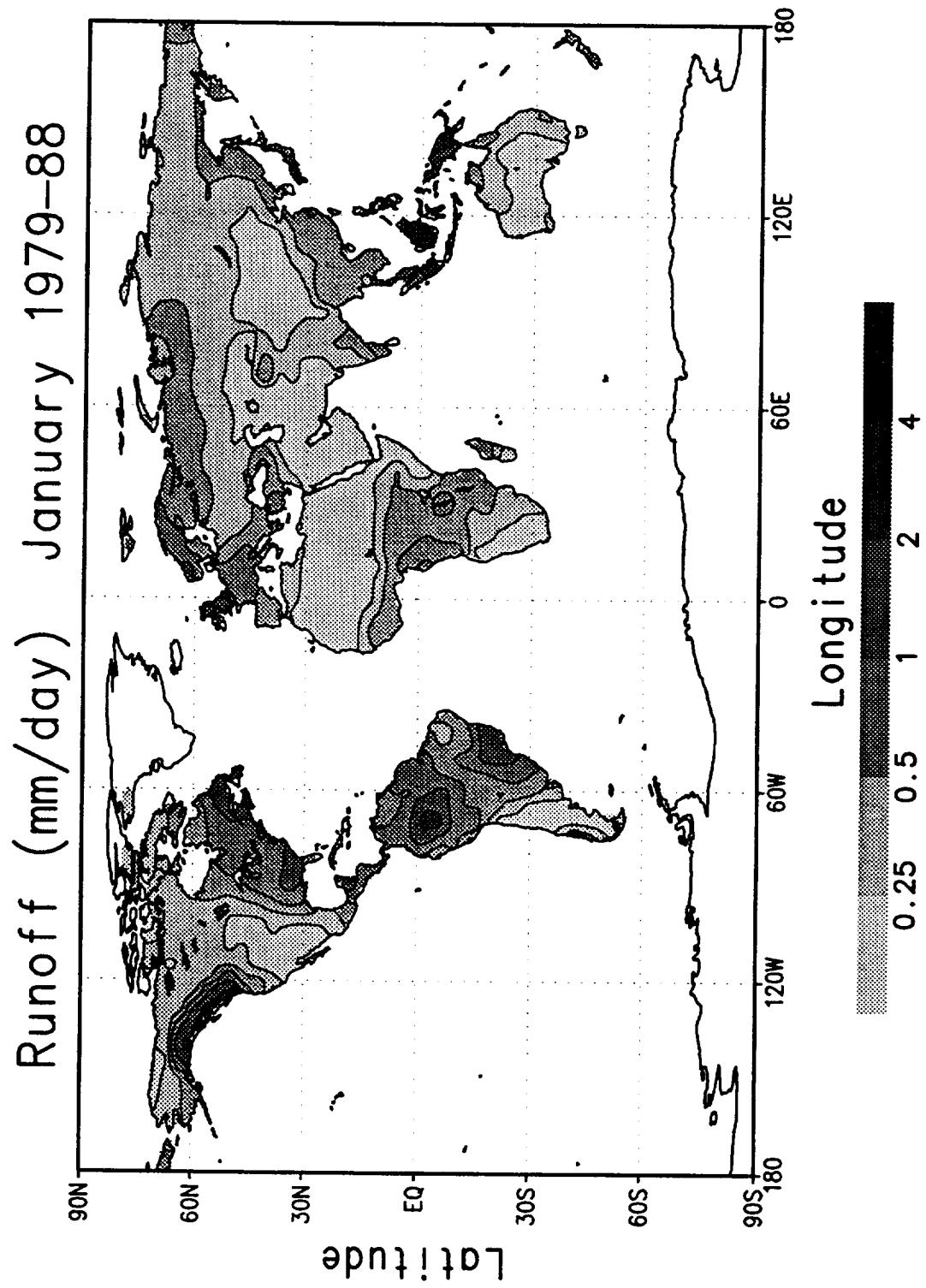
Soil Moisture Standard Deviation (0-1) December 1979-88



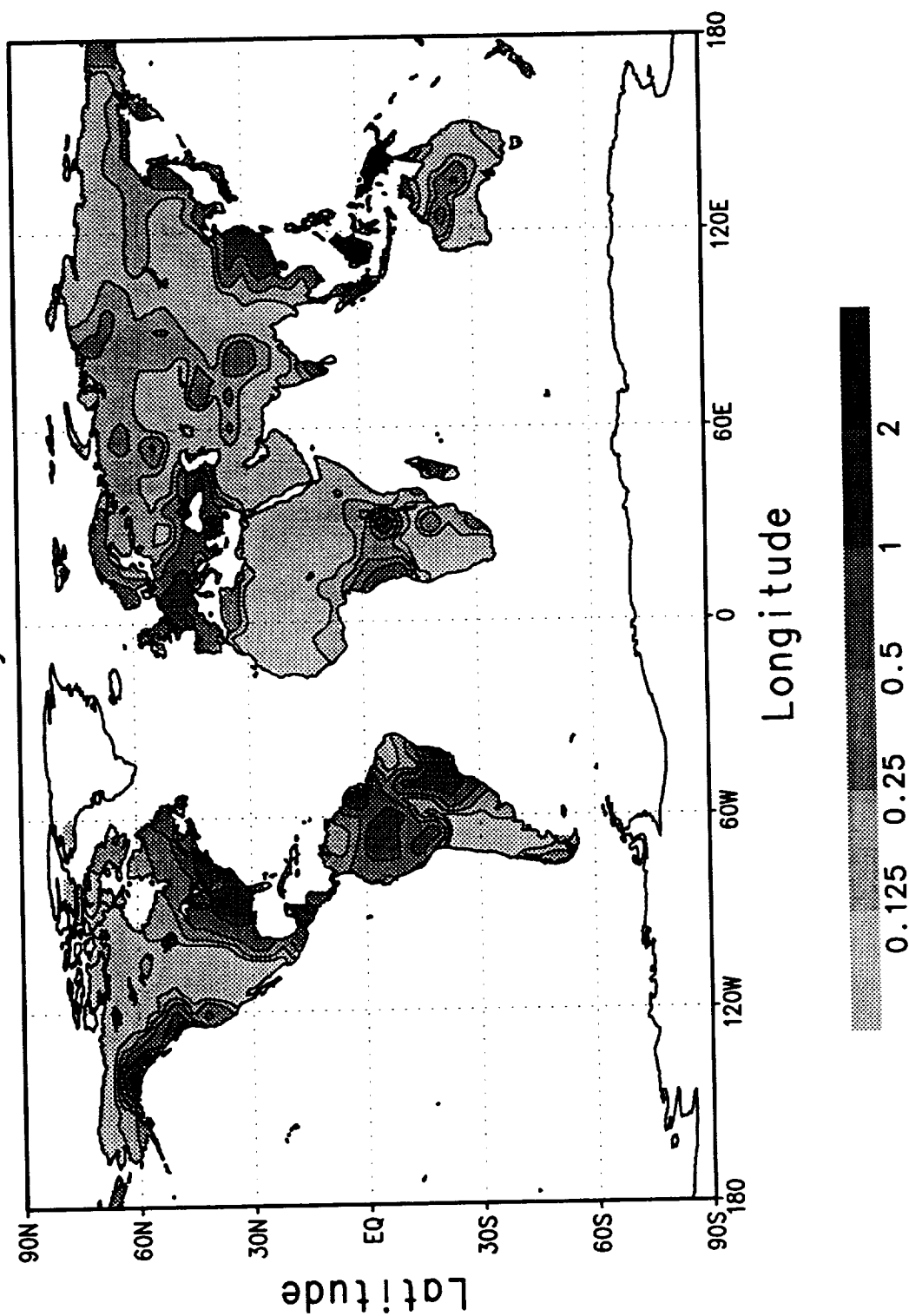
RUNOFF

(January - December)

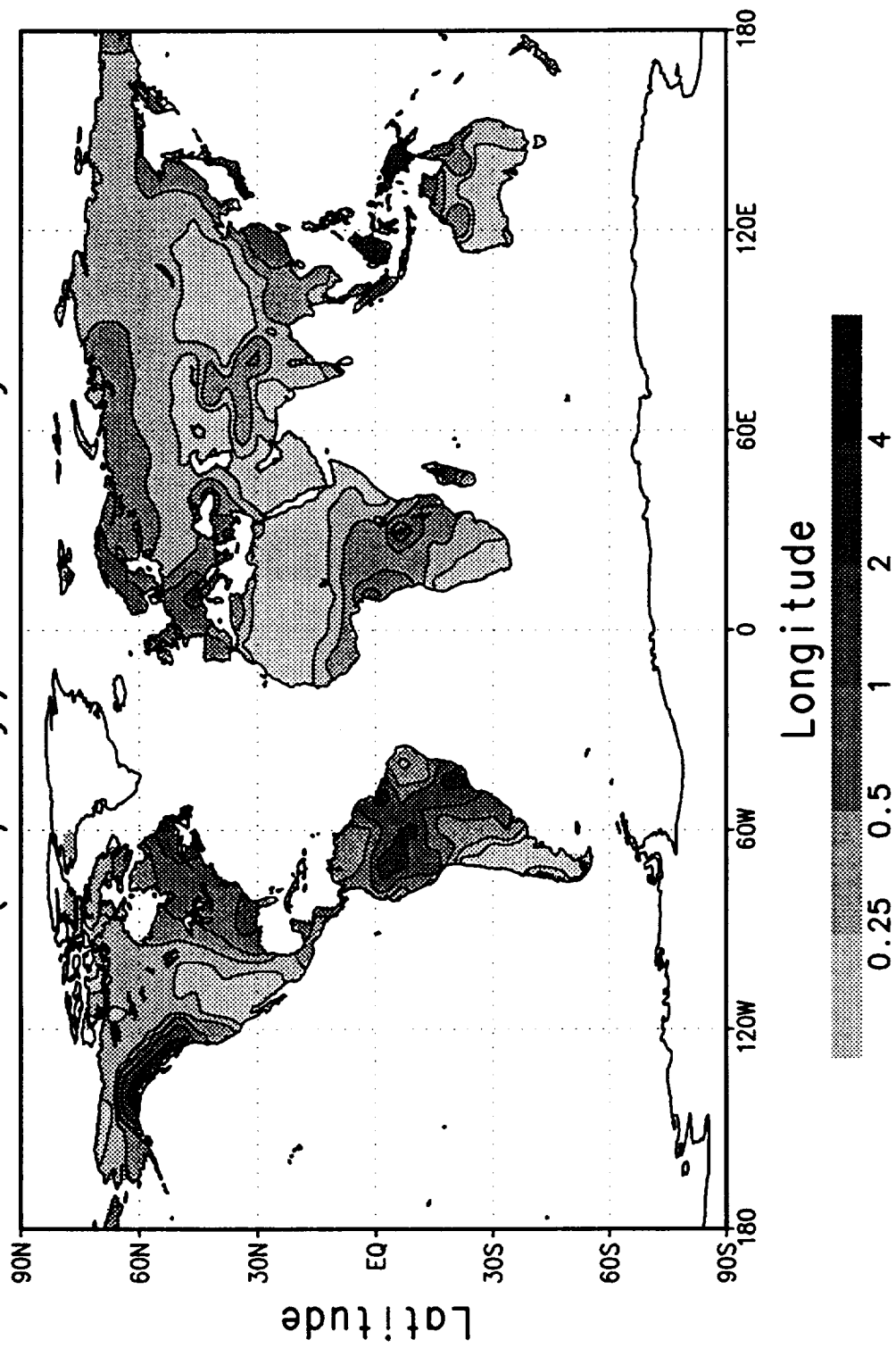
Ten-year average (1979 - 1988) of the monthly mean runoff (mm day^{-1}), computed from soil moisture initialization scheme. Also plotted are the standard deviations of the monthly mean fields as determined from the 10-year data set.



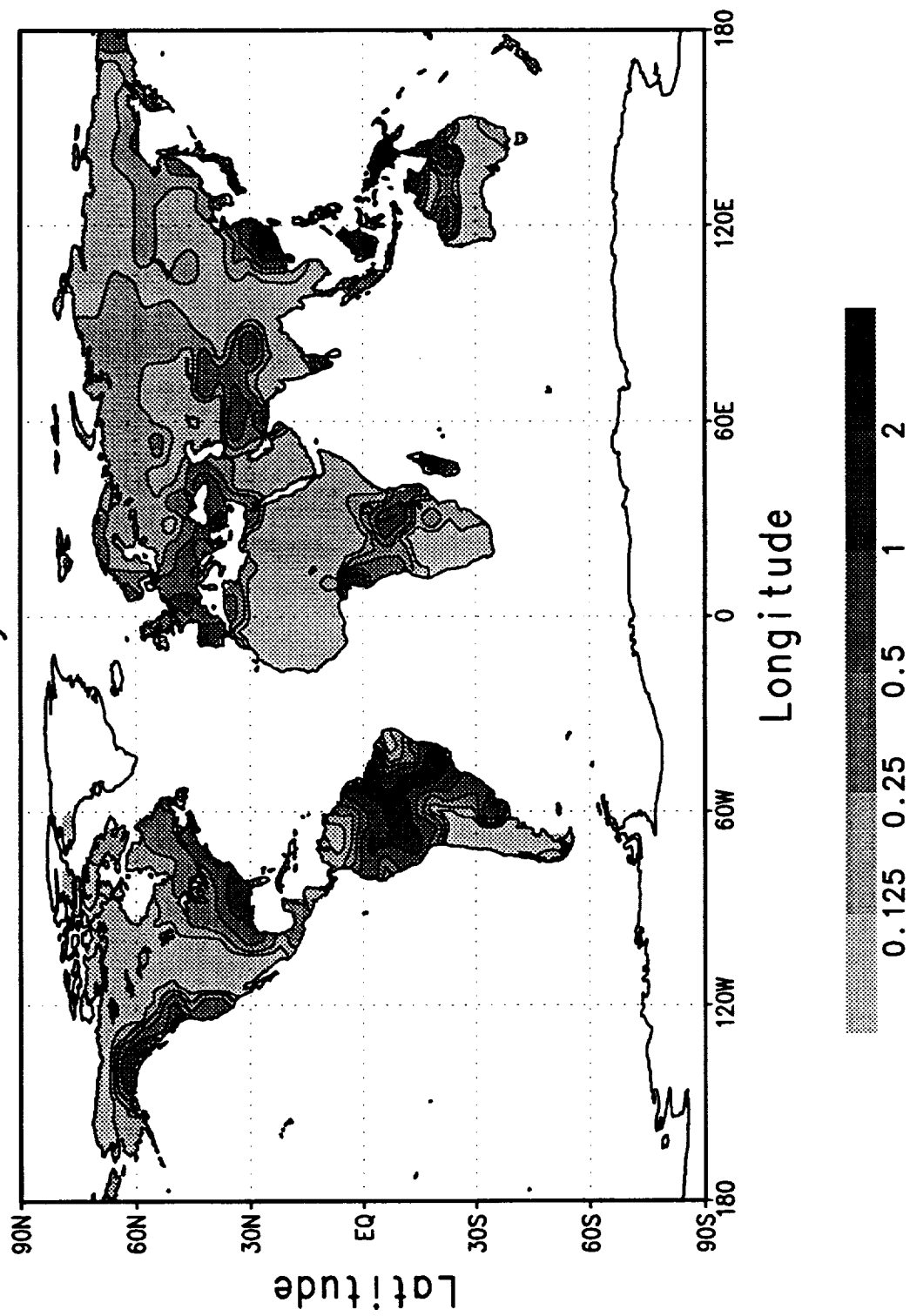
Runoff Standard Deviation (mm/day)
January 1979-88

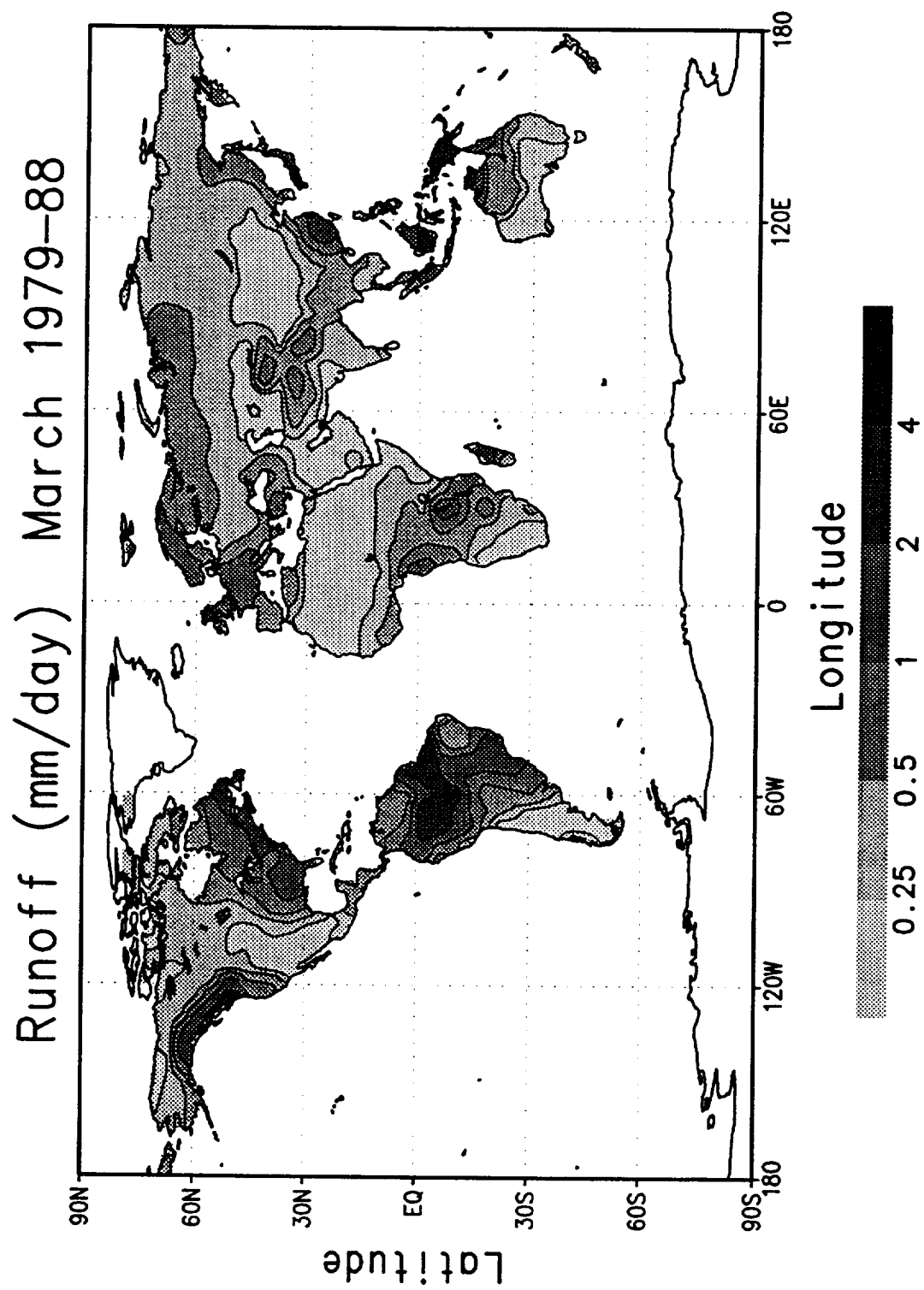


Runoff (mm/day) February 1979-88

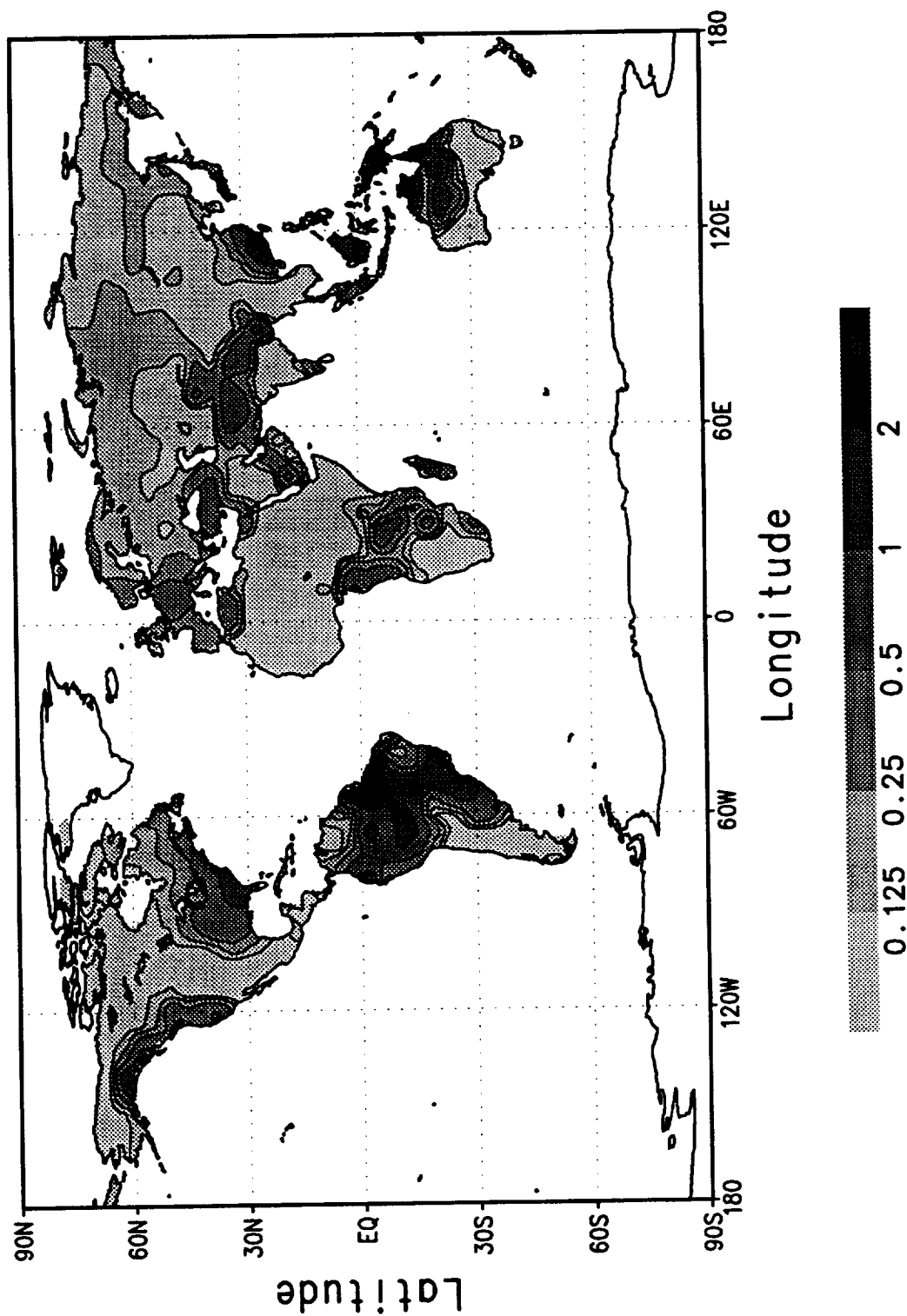


Runoff Standard Deviation (mm/day)
February 1979-88

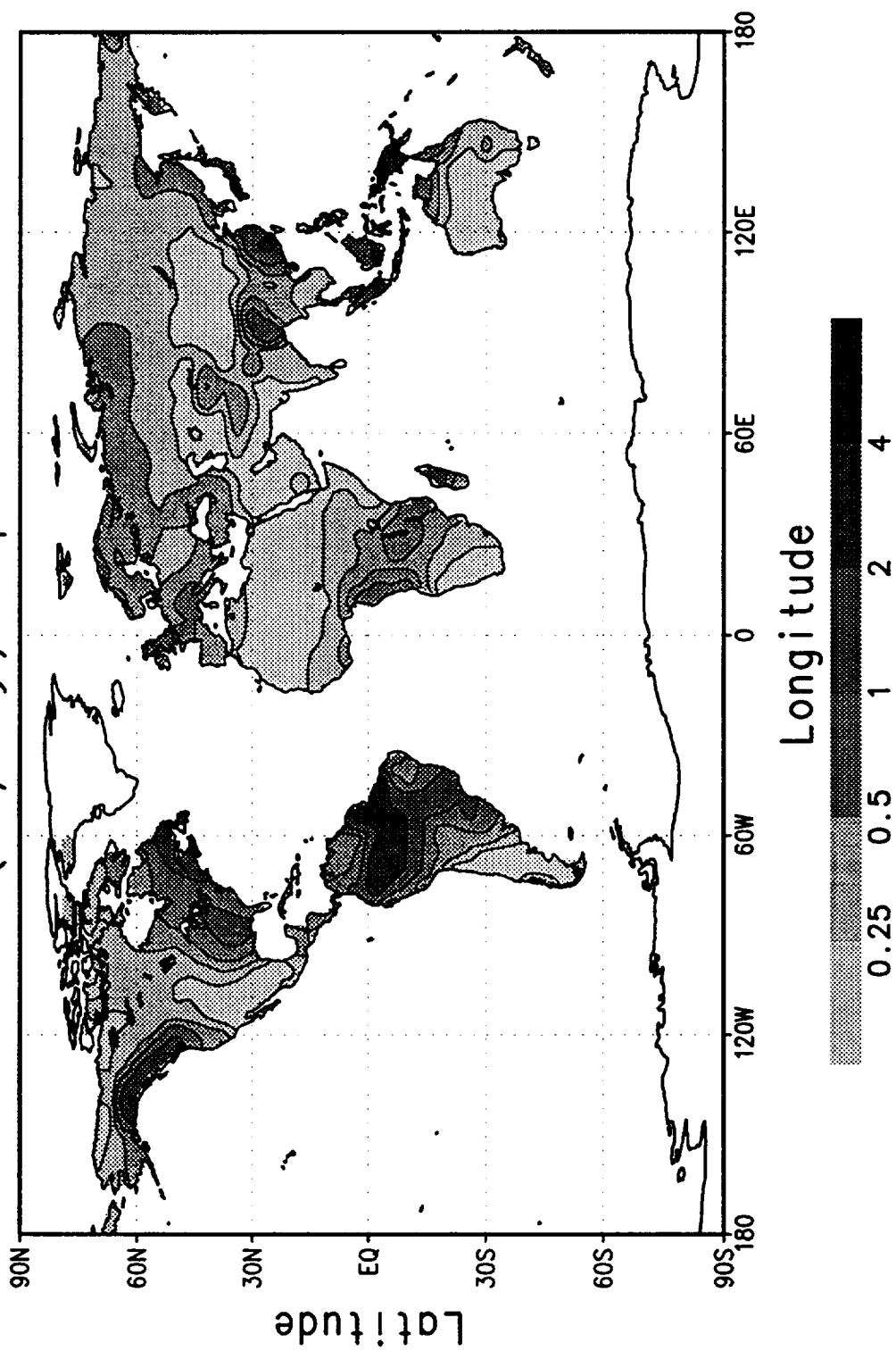




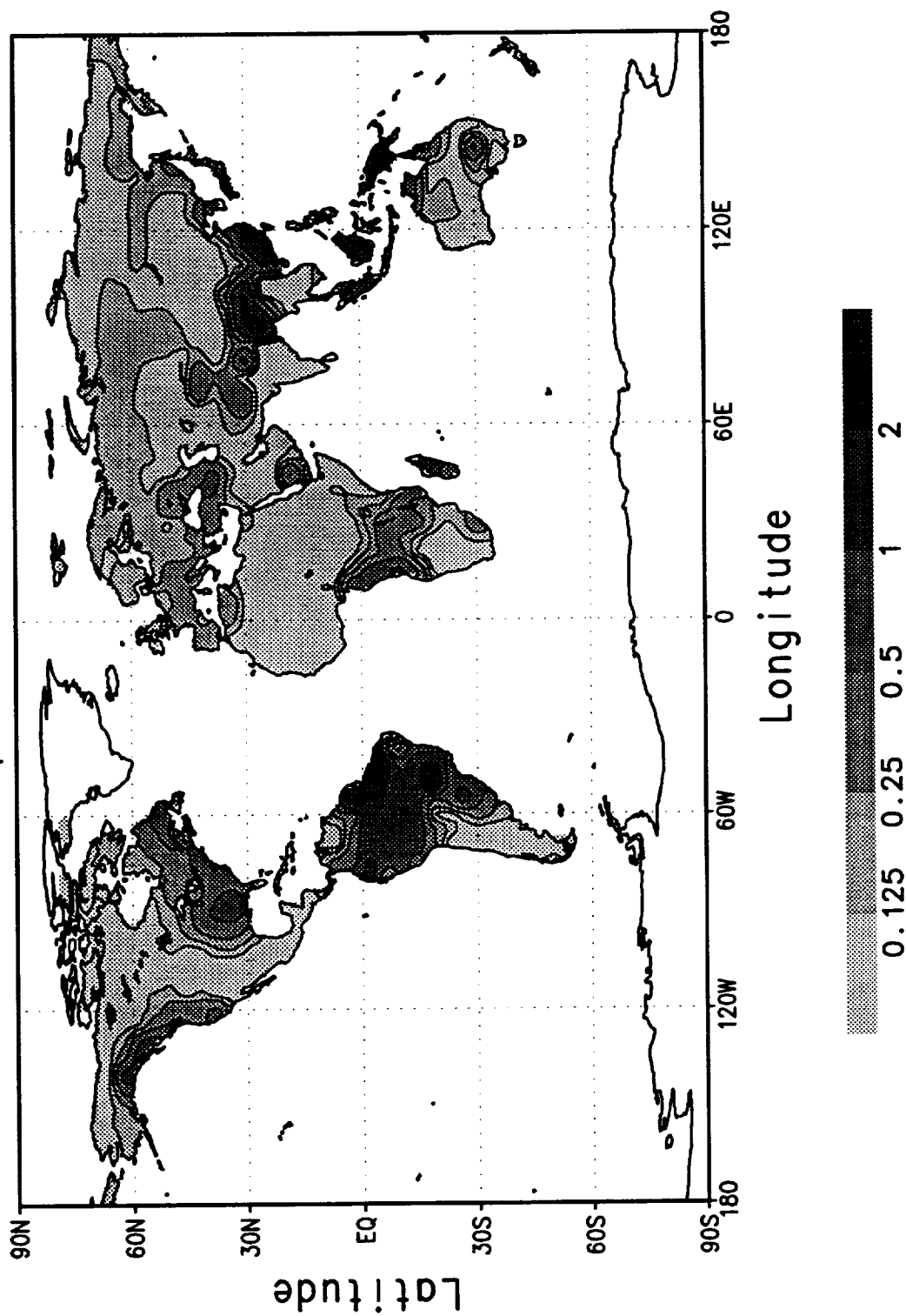
Runoff Standard Deviation (mm/day)
March 1979-88



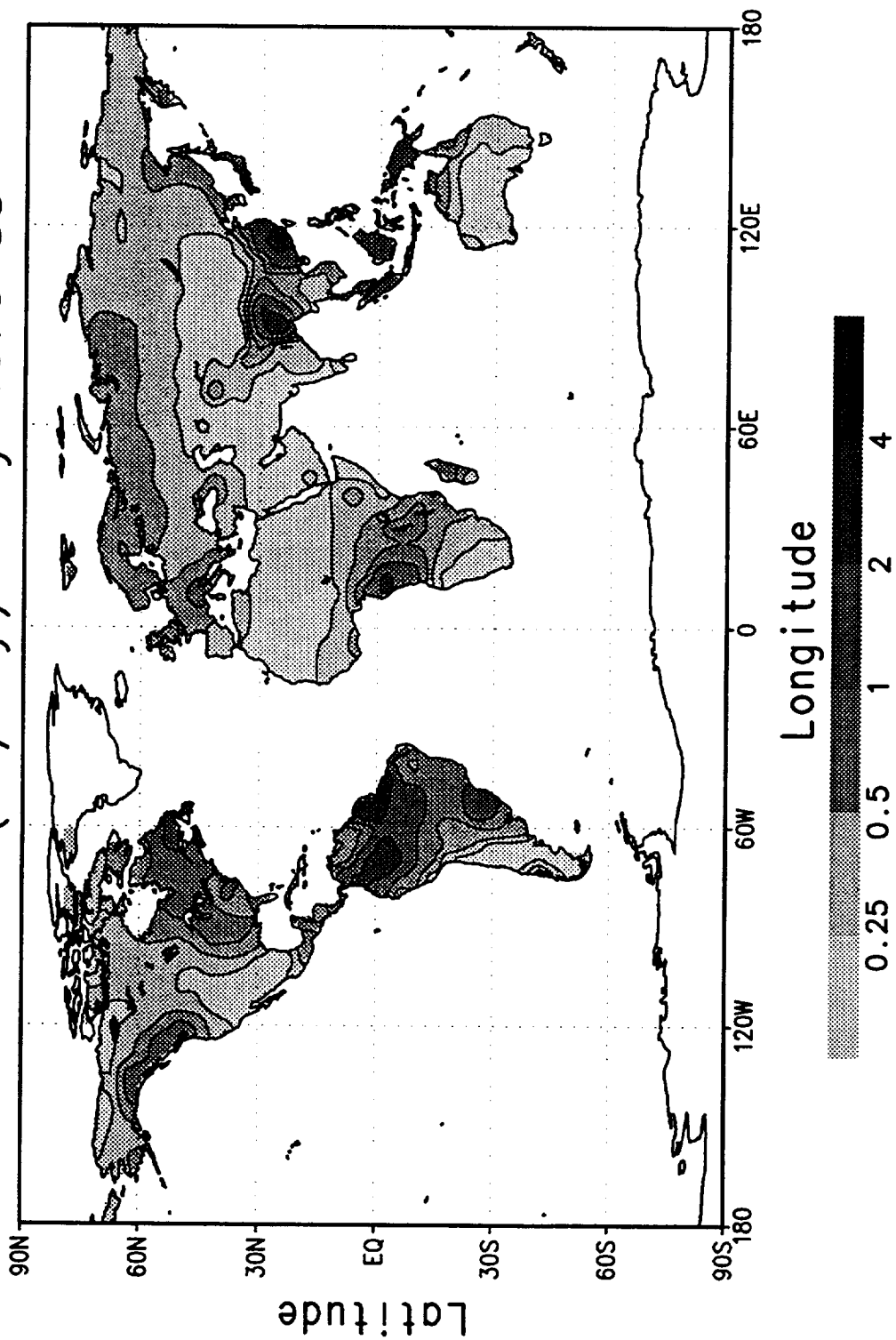
Runoff (mm/day) April 1979-88



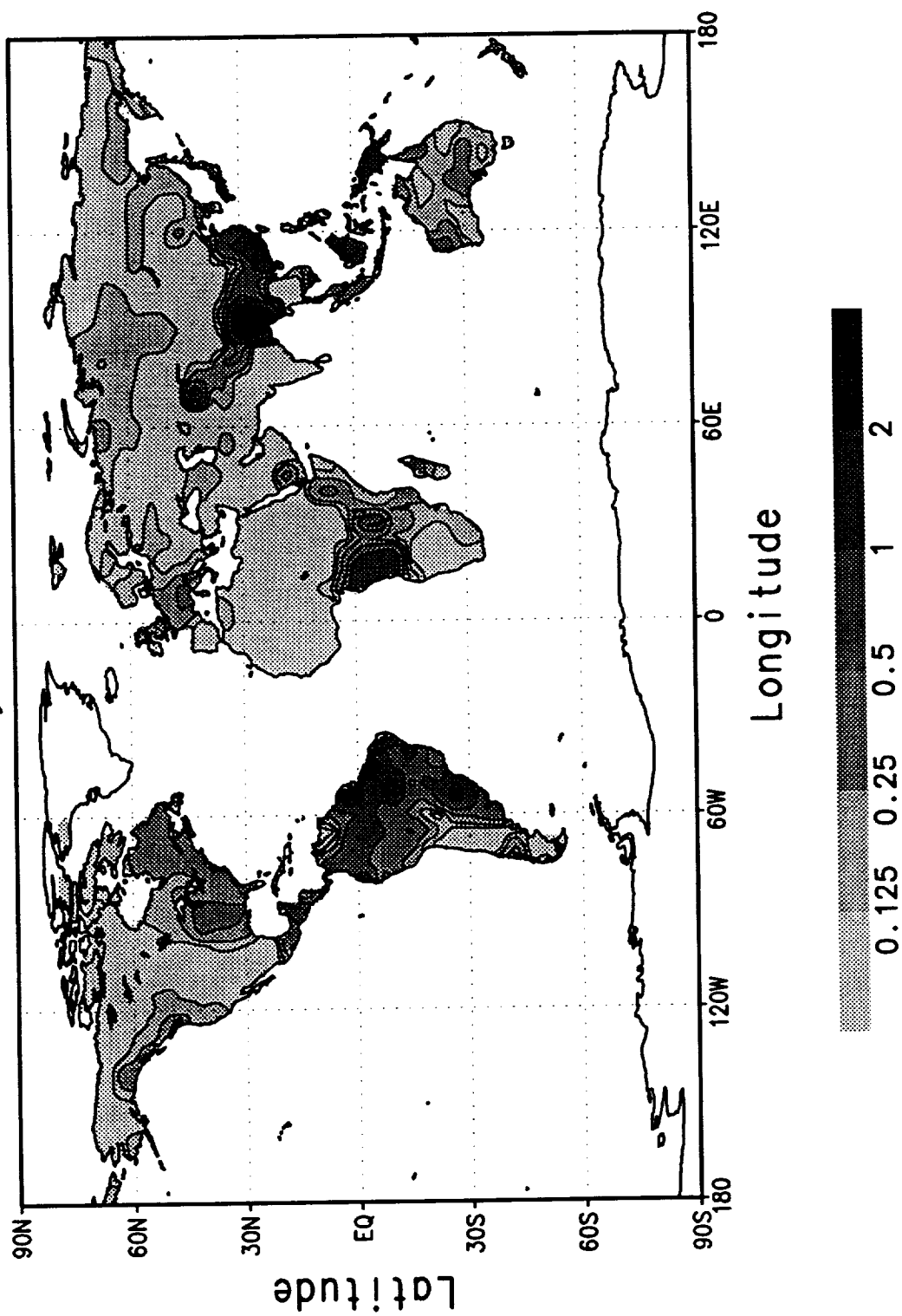
Runoff Standard Deviation (mm/day)
April 1979-88

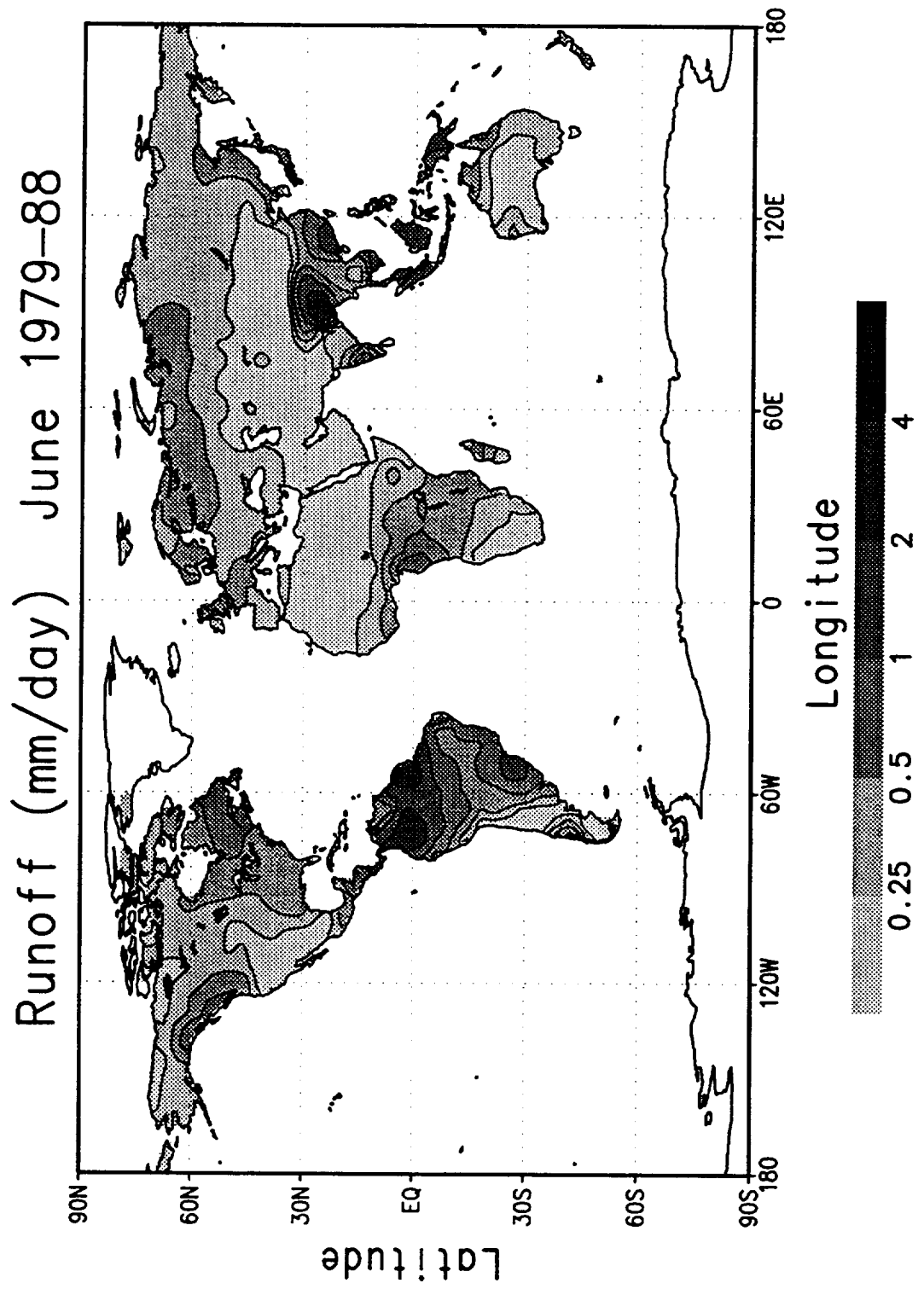


Runoff (mm/day) May 1979-88

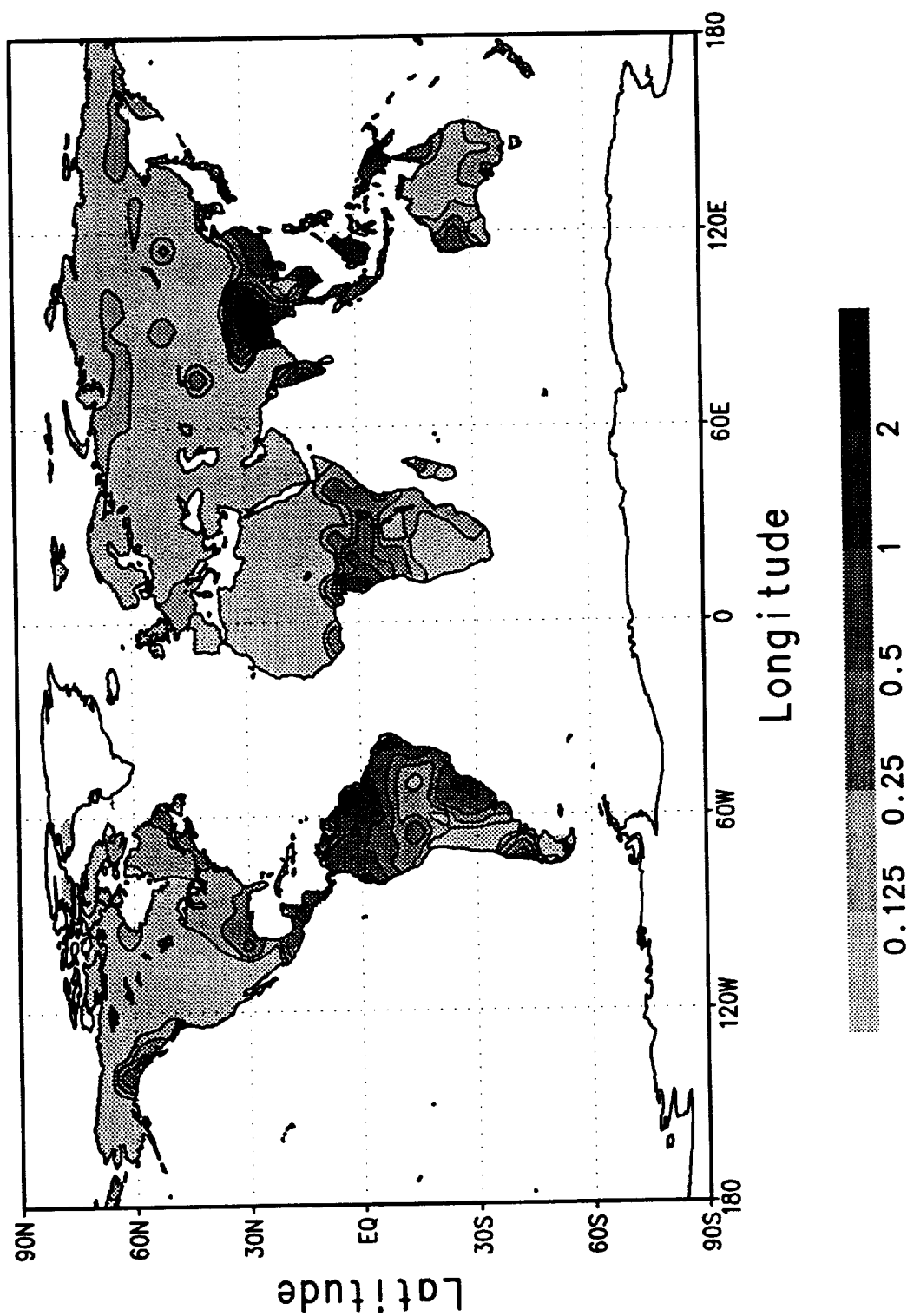


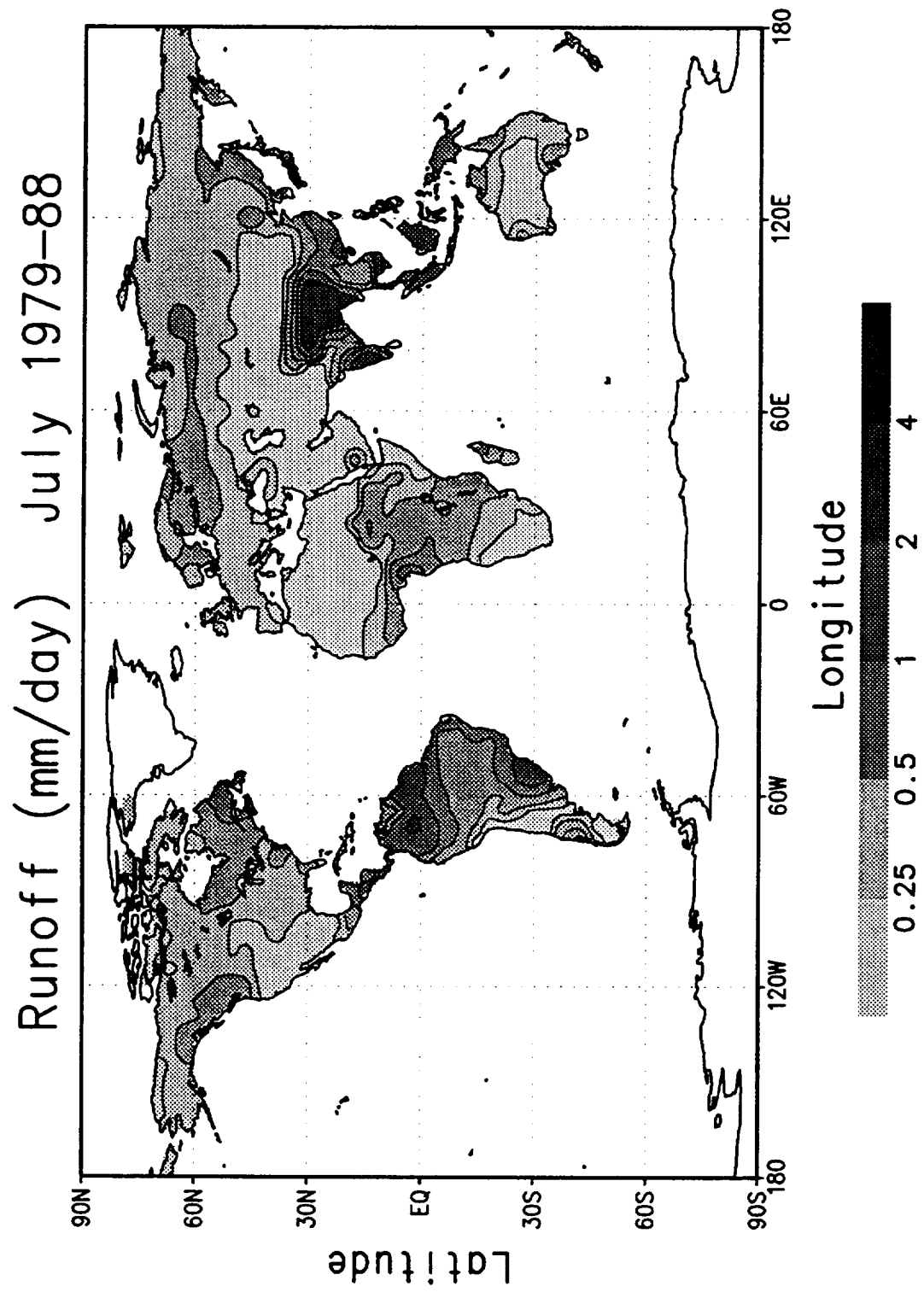
Runoff Standard Deviation (mm/day)
May 1979-88



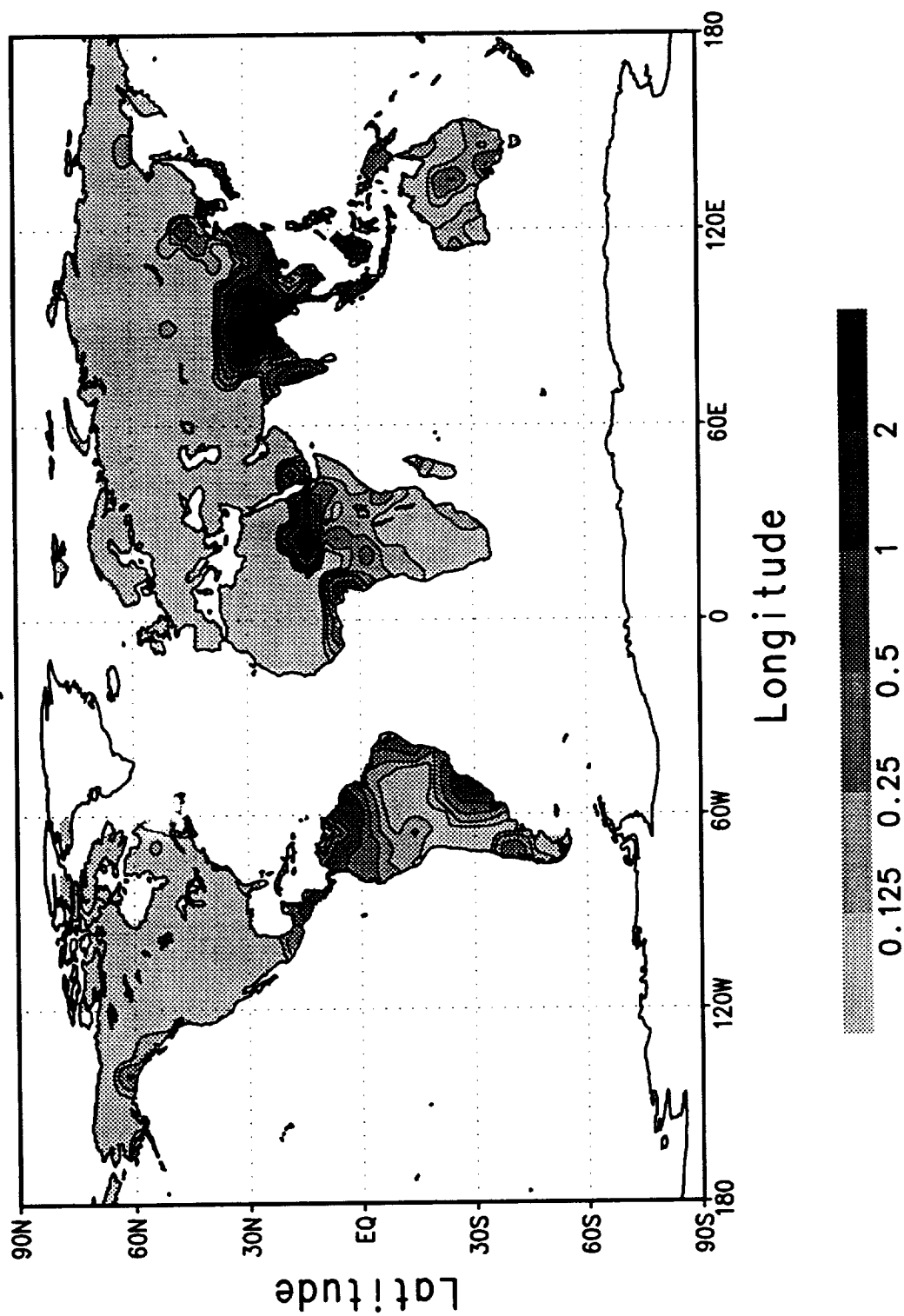


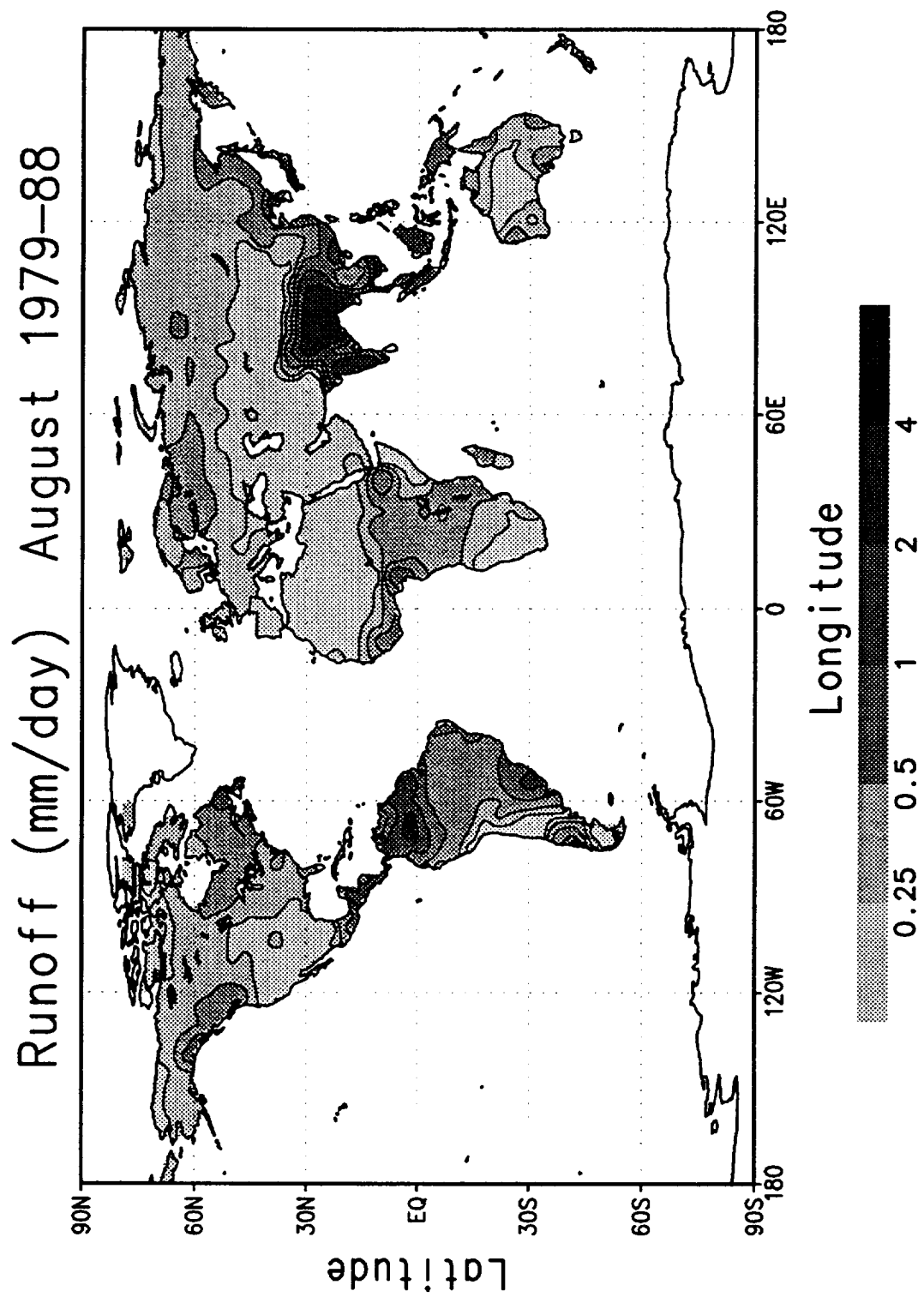
Runoff Standard Deviation (mm/day)
June 1979-88



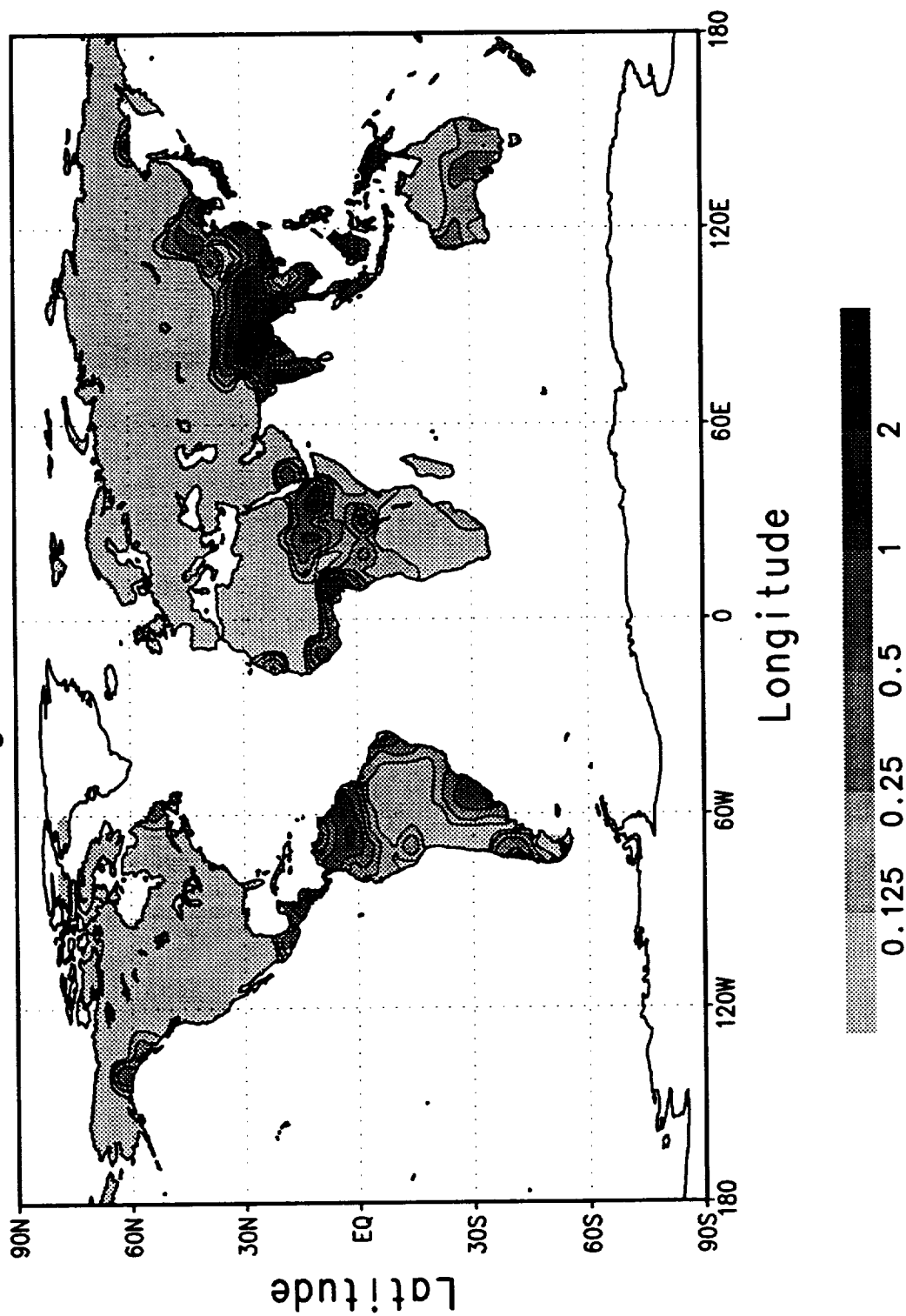


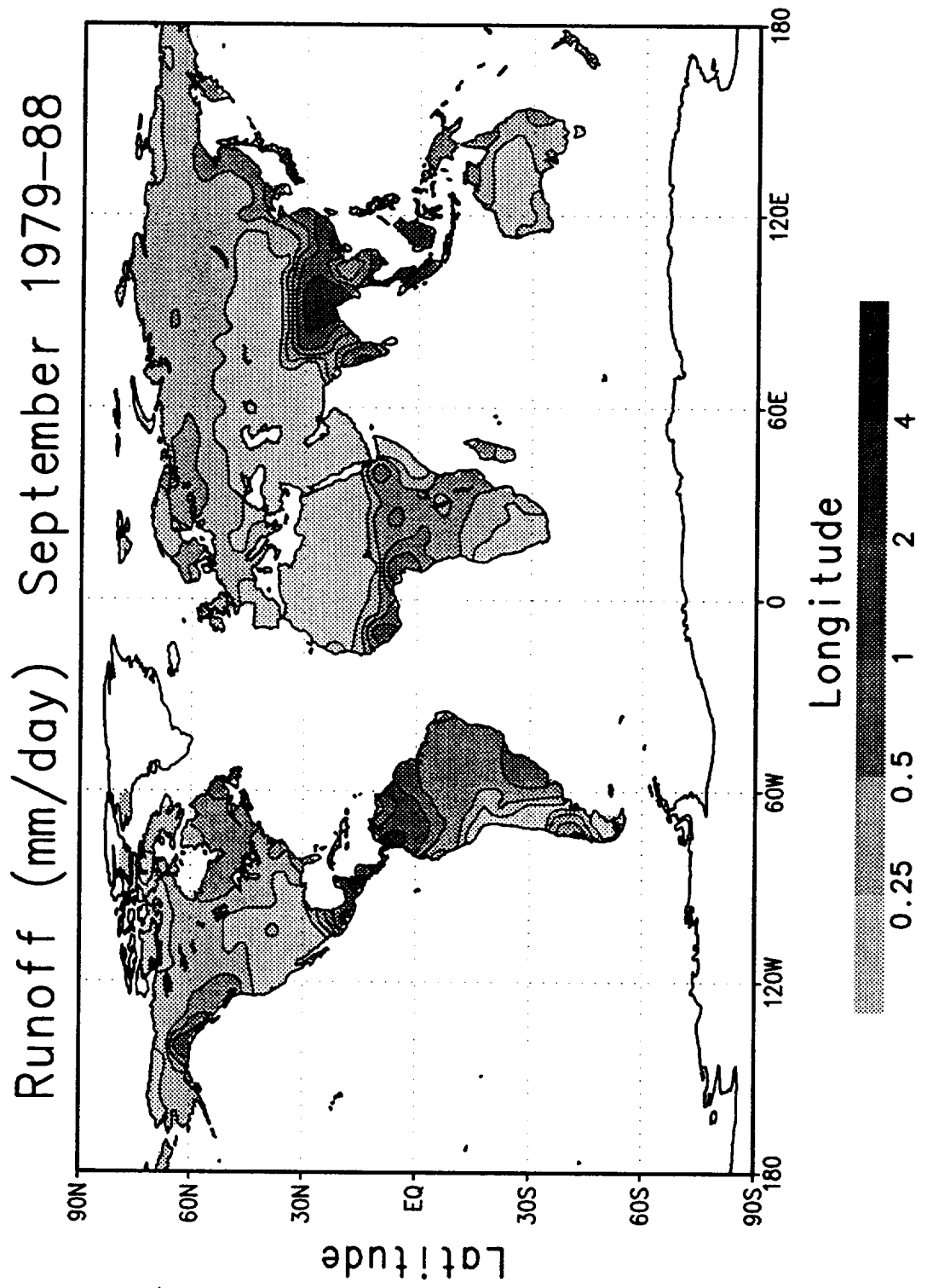
Runoff Standard Deviation (mm/day)
July 1979-88



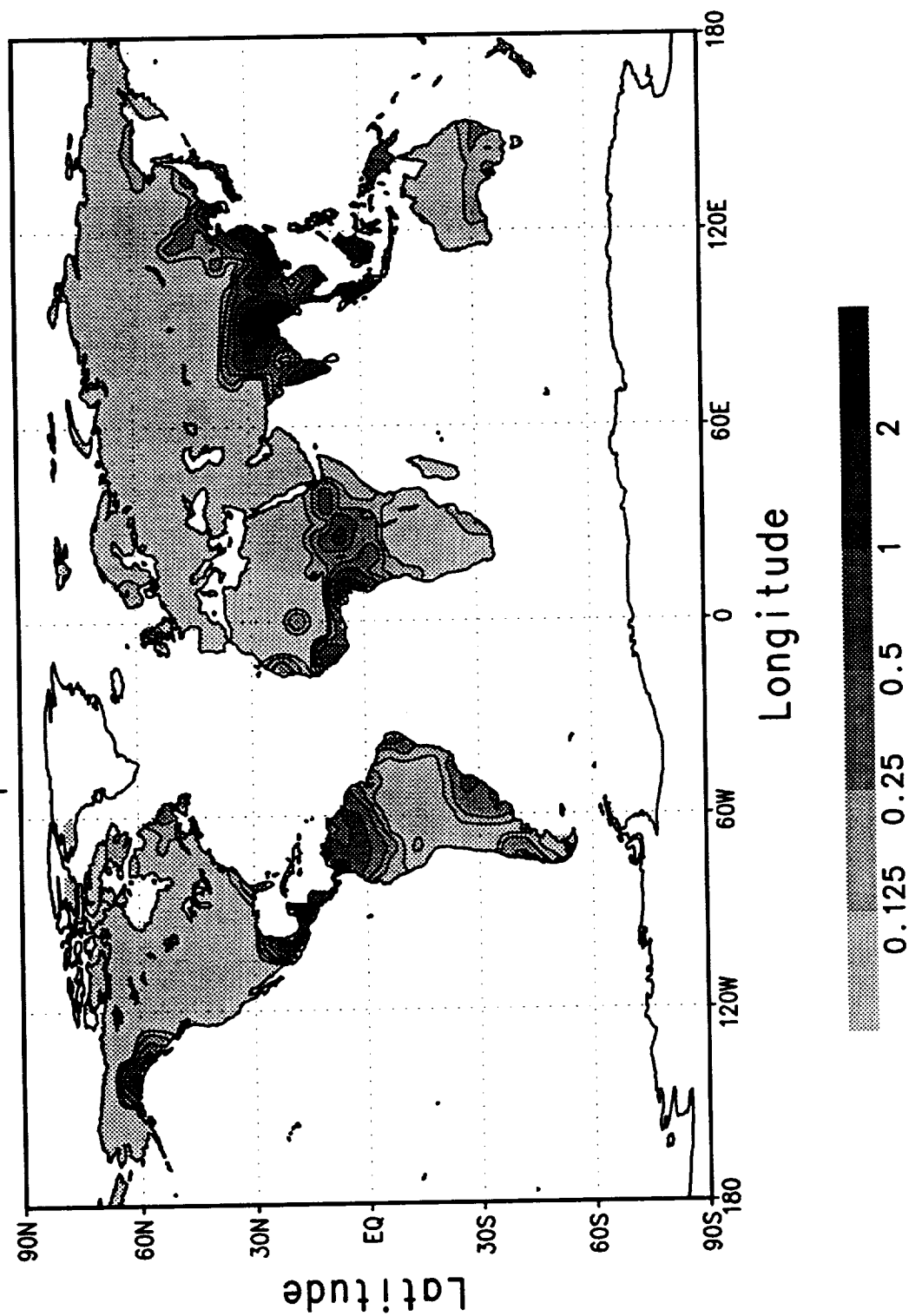


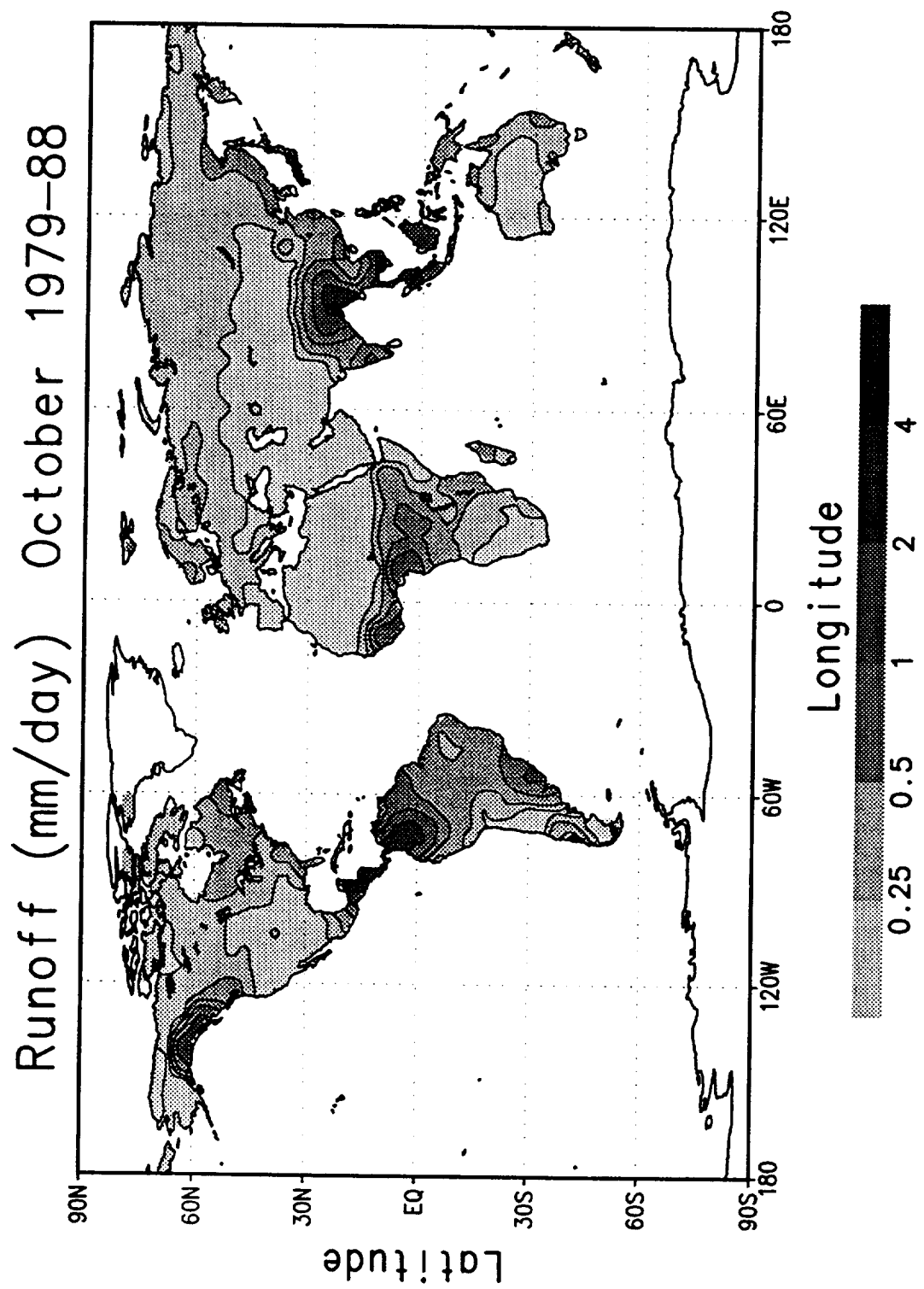
Runoff Standard Deviation (mm/day)
August 1979-88



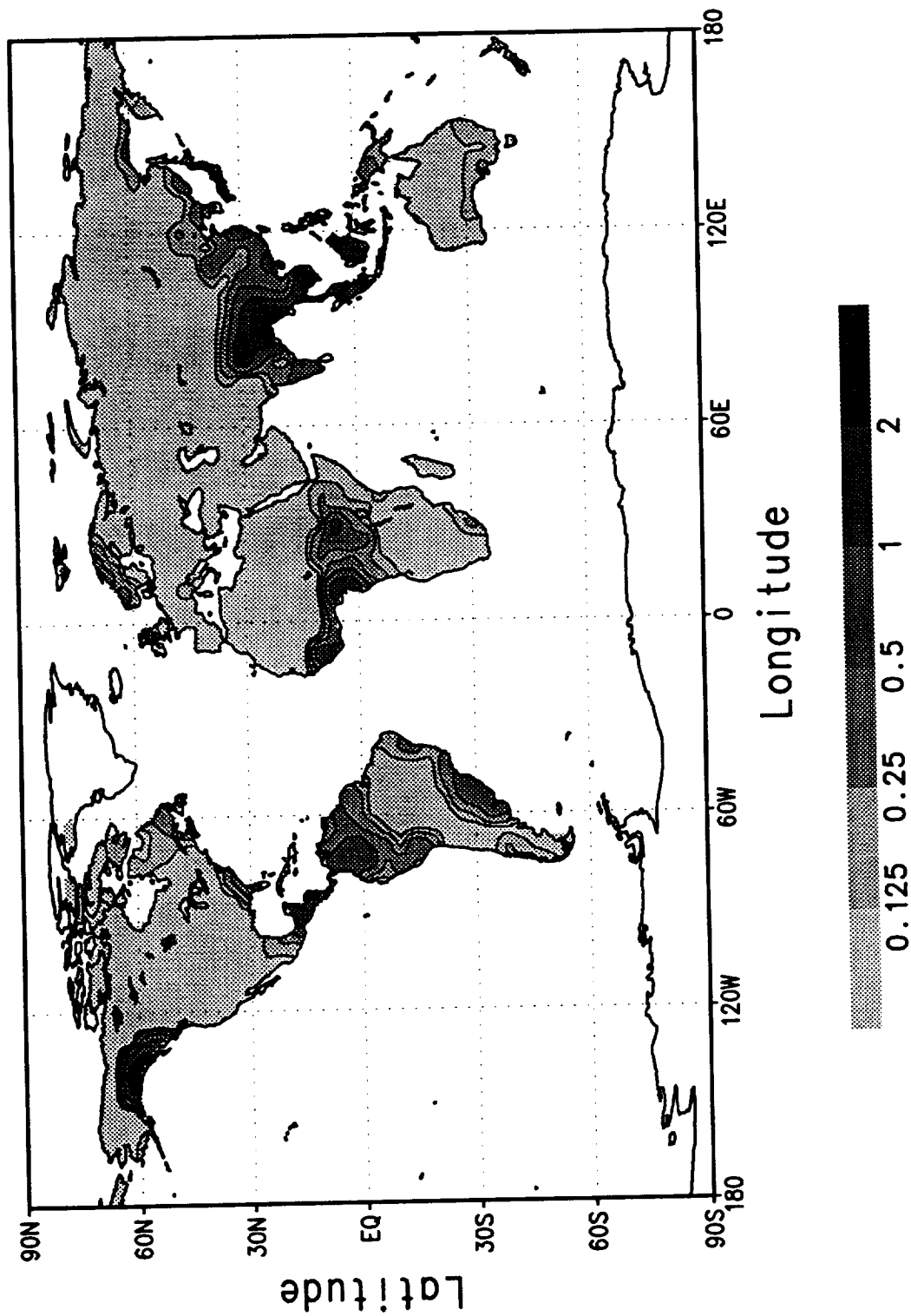


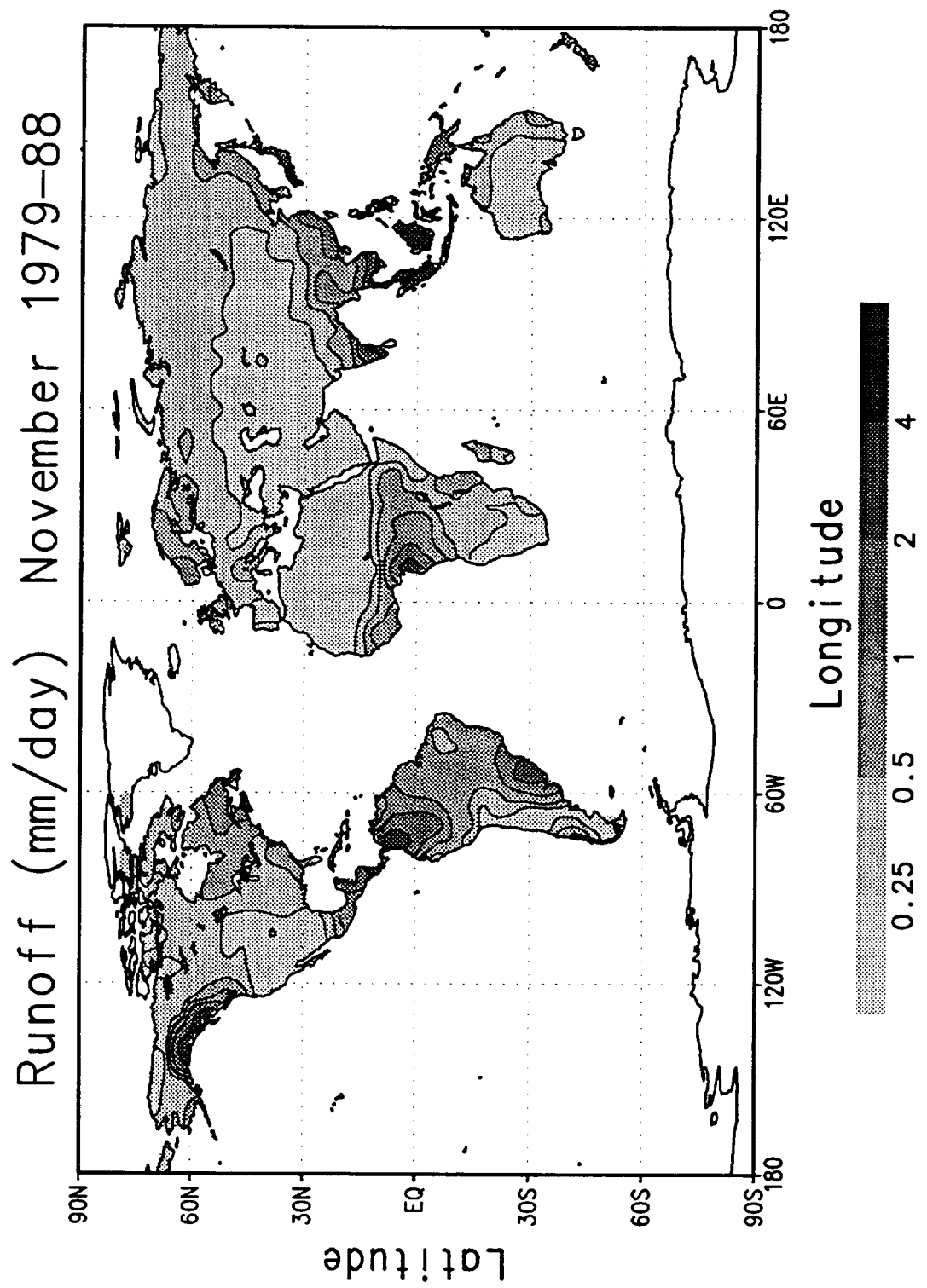
Runoff Standard Deviation (mm/day)
September 1979-88



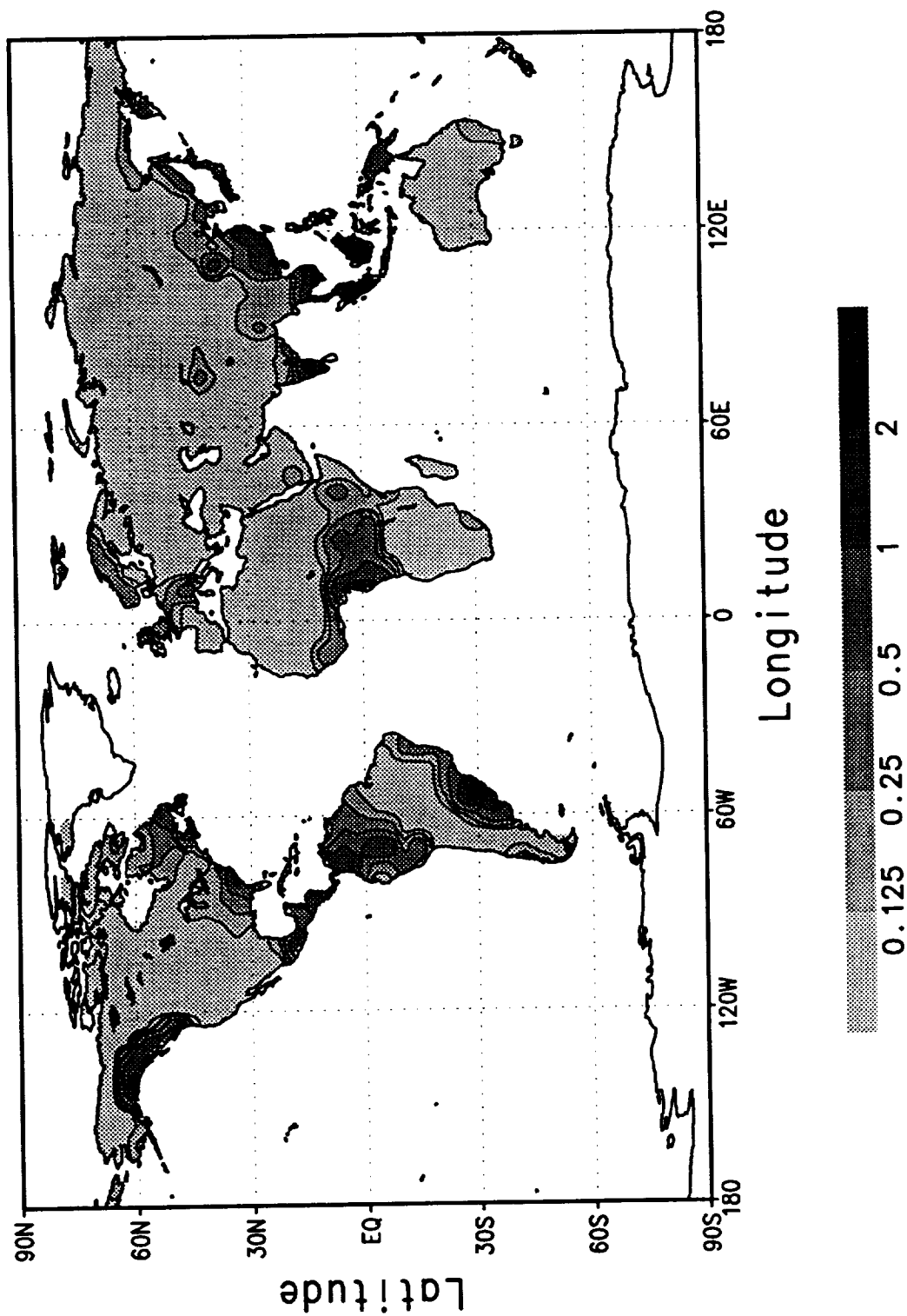


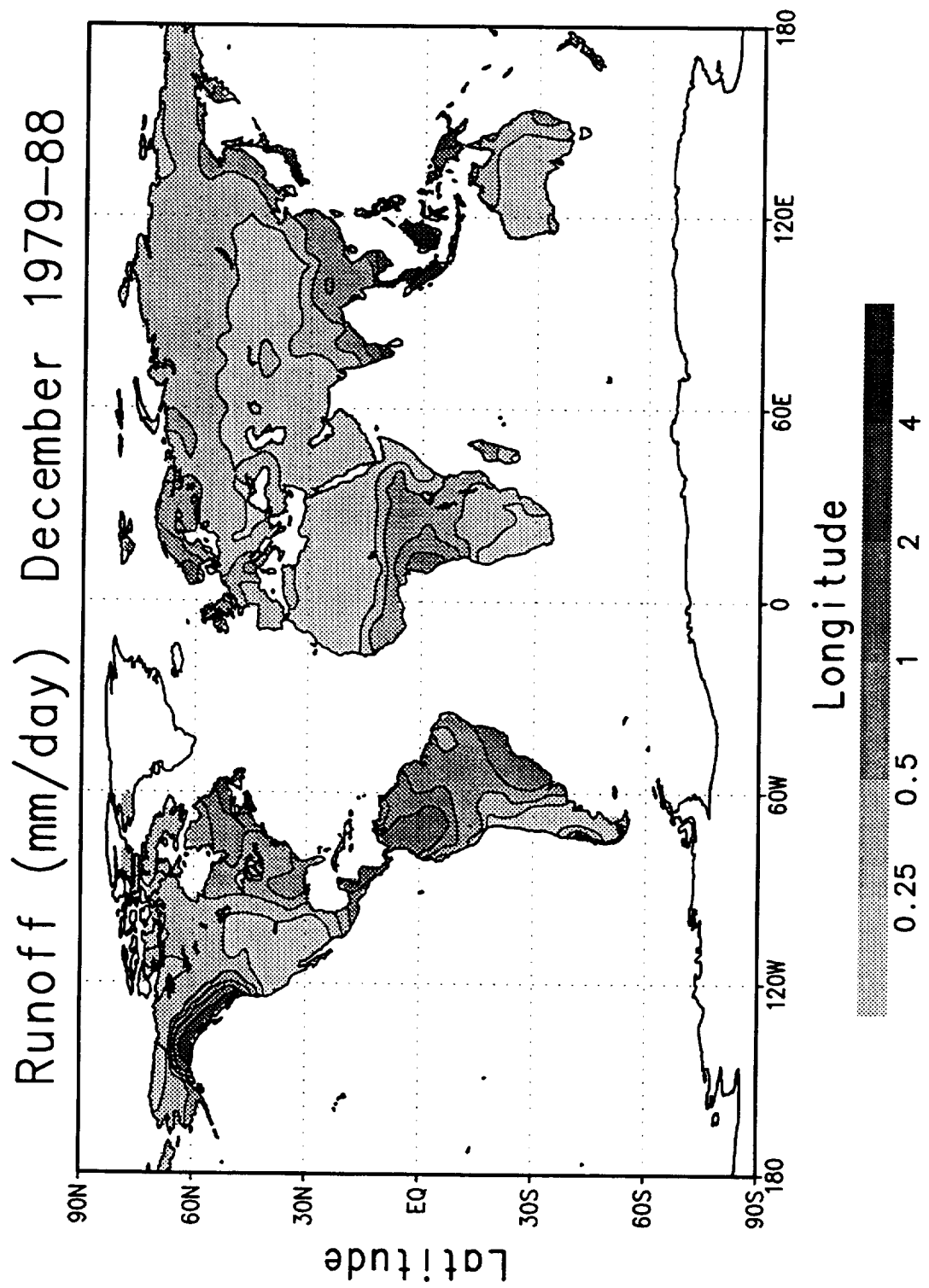
Runoff Standard Deviation (mm/day)
October 1979-88



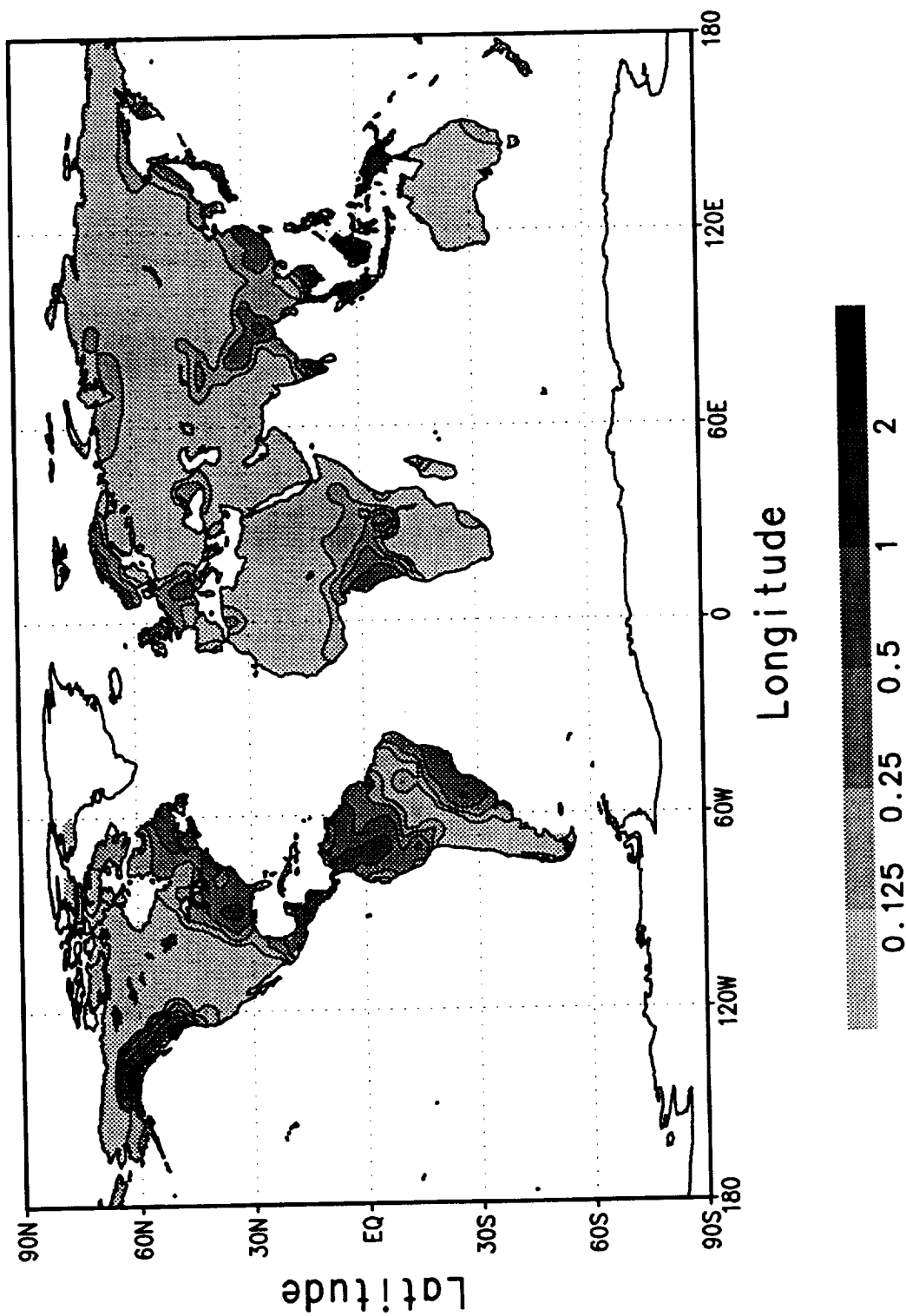


Runoff Standard Deviation (mm/day)
November 1979-88





Runoff Standard Deviation (mm/day)
December 1979-88



REPORT DOCUMENTATION PAGE

Form Approved
OMB No. 0704-0188

Public reporting burden for this collection of information is estimated to average 1 hour per response, including the time for reviewing instructions, searching existing data sources, gathering and maintaining the data needed, and completing and reviewing the collection of information. Send comments regarding this burden estimate or any other aspect of this collection of information, including suggestions for reducing this burden, to Washington Headquarters Services, Directorate for Information Operations and Reports, 1215 Jefferson Davis Highway, Suite 1204, Arlington, VA 22202-4302, and to the Office of Management and Budget, Paperwork Reduction Project (0704-0188), Washington, DC 20503.

1. AGENCY USE ONLY (Leave blank)		2. REPORT DATE August 1993	3. REPORT TYPE AND DATES COVERED Technical Memorandum	
4. TITLE AND SUBTITLE Design of a Global Soil Moisture Initialization Procedure for the Simple Biosphere Model			5. FUNDING NUMBERS JON-910-039-09-01-25	
6. AUTHOR(S) G. E. Liston, Y. C. Sud, and G. K. Walker				
7. PERFORMING ORGANIZATION NAME(S) AND ADDRESS (ES) Goddard Space Flight Center Greenbelt, Maryland 20771			8. PERFORMING ORGANIZATION REPORT NUMBER 93B00092	
9. SPONSORING / MONITORING AGENCY NAME(S) AND ADDRESS (ES) National Aeronautics and Space Administration Washington, DC 20546-0001			10. SPONSORING / MONITORING AGENCY REPORT NUMBER NASA TM-104590	
11. SUPPLEMENTARY NOTES G. E. Liston, Universities Space Research Association, Columbia, MD; Y. C. Sud, Goddard Space Flight Center, Greenbelt, MD; G. K. Walker, General Sciences Corporation, Laurel, MD				
12a. DISTRIBUTION / AVAILABILITY STATMENT Unclassified - Unlimited Subject Category 47			12b. DISTRIBUTION CODE	
13. ABSTRACT (Maximum 200 words) Global soil moisture and land-surface evapotranspiration fields are computed using an analysis scheme based on the Simple Biosphere (SiB) soil-vegetation-atmosphere interaction model. The scheme is driven with observed precipitation, and potential evapotranspiration, where the potential evapotranspiration is computed following the surface air temperature-potential evapotranspiration regression of Thornthwaite (1948). The observed surface air temperature is corrected to reflect potential (zero soil moisture stress) conditions by letting the ratio of actual transpiration to potential transpiration be a function of normalized difference vegetation index (NDVI). Soil moisture, evapotranspiration, and runoff data are generated on a daily basis for a 10-year period, January 1979 through December 1988, using observed precipitation gridded at a 4° by 5° resolution.				
14. SUBJECT TERMS Soil moisture, Precipitation, Evapotranspiration, Runoff, GCM initial conditions			15. NUMBER OF PAGES 138	
			16. PRICE CODE	
17. SECURITY CLASSIFICATION OF REPORT Unclassified	18. SECURITY CLASSIFICATION OF THIS PAGE Unclassified	19. SECURITY CLASSIFICATION OF ABSTRACT Unclassified	20. LIMITATION OF ABSTRACT UL	

National Aeronautics and
Space Administration

Goddard Space Flight Center
Greenbelt, Maryland 20771

Official Business
Penalty for Private Use, \$300

SPECIAL FOURTH-CLASS RATE
POSTAGE & FEES PAID
NASA
PERMIT No. G27



POSTMASTER: If Undeliverable (Section 158,
Postal Manual) Do Not Return
